ABC Imagem Cardiovascular

Volume 38 | Number 4

October/November/December 2025

Sociedade Brasileira de Cardiologia
ISSN-2675-312X

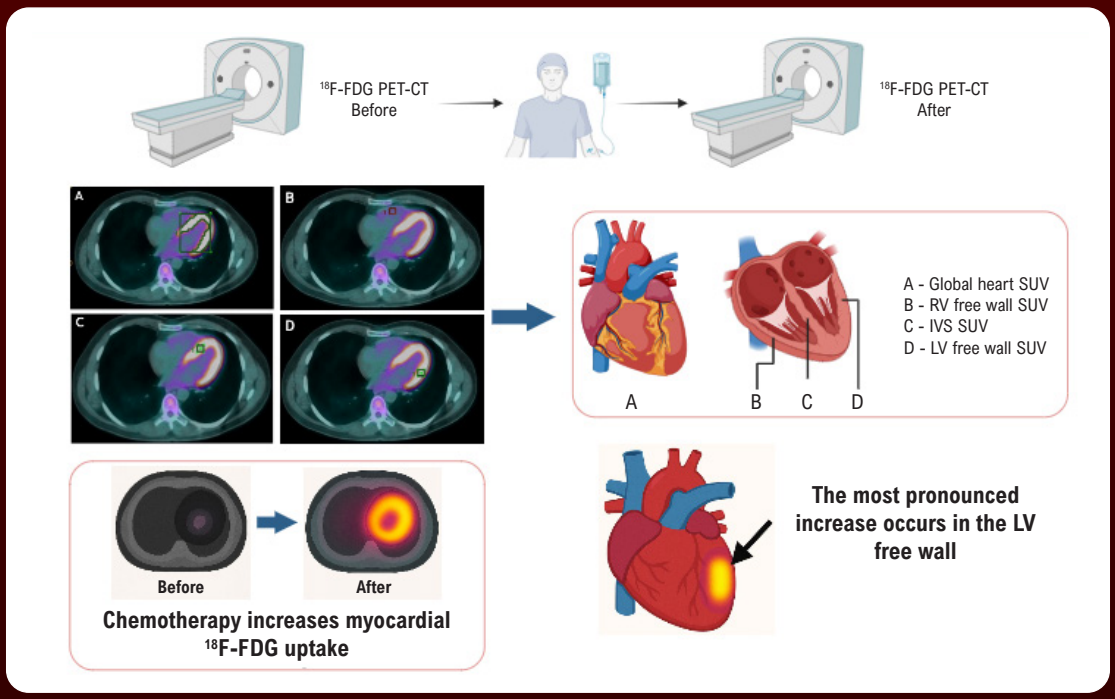

Central Illustration of the article: Monitoring Myocardial Metabolic Changes in Lymphoma Patients Undergoing Chemotherapy Using FDG PET/CT

ABC Imagem Cardiovascular

Contents

Click on the title to read the article

Case Report

Image

Departament of Cardiovascular Imaging

President
Silvio Henrique Barberato - PR

Vice President of Echocardiography
Daniela do Carmo Rassi Frota - GO

Vice President of Nuclear Cardiology
Cláudio Tinoco Mesquita – RJ

Vice President of Vascular Echography
Salomon Israel do Amaral – RJ

Vice President of Magnetic Resonance Imaging
Isabela Bispo Santos da Silva Costa – SP

Vice President of Computed Tomography
Jorge Andion Torreão – BA

Vice President of Congenital Heart Disease and Pediatric Cardiology
Andressa Mussi Soares – ES

Managing Director
Adenalva Lima de Souza Beck – DF

Financial Director
Gláucia Maria Penha Tavares - SP

Journal Editor
Marcelo Dantas Tavares de Melo – PB

Consulting Board

Members
André Luiz Cerqueira de Almeida - BA
Arnaldo Rabischoffsky - RJ
Carlos Eduardo Rochitte - SP
Marcelo Luiz Campos Vieira - SP
Samira Saady Morhy - SP

Scientific Committee

Coordinator
Daniela do Carmo Rassi Frota - GO

Members
Andressa Mussi Soares - ES
Cláudio Tinoco Mesquita - RJ
Isabela Bispo Santos da Silva Costa - SP
Jorge Andion Torreão - BA
Salomon Israel do Amaral - RJ

Echocardiography Certification Committee

Coordinator
Tatiane Mascarenhas Santiago Emerich - ES
Andrea de Andrade Vilela - SP

Adult Echo Members
Antonio Amador Calvilho JR. - SP
Antonio Tito Paladino Filho - SP
Eliza de Almeida Gripp - RJ
Jaime Paula Pessoa Linhares Filho - CE
João Carlos Moron Saes Braga - SP
Marcio Mendes Pereira - MA
Paulo Henrique Nunes Pereira - PA
Renato de Aguiar Hortegal - SP
Tiago Costa Bignoto - SP
Wanessa Nakamura Guimarães - DF

Congenital Echo Members
Barbara Neiva Tanaka - MA
Daniela Lago Kreuzig - SP
Danielle Lopes Rocha - ES
Halsted Alarcao Gomes Pereira da Silva - SP
Leandro Alves Freire - SP
Marcio Miranda Brito - TO
Maria Elisa Martini Albretch - SP

Seniors
Andrea de Andare Vilela - SP
Glaucia Maria Penha Tavares - SP
José Luiz Barros Pena - MG
Maria Estefania Bosco Otto - DF
Mohamed Hassan Saleh - SP
Solange Bernardes Tatani - SP

Social Media Committee

Coordinator
Alex dos Santos Félix - RJ
Antonio Carlos Leite de Barros Filho - SP

Members
Barbara Athayde Linhares Martins Vrandecic - MG
Cristiane Nunes Martins - MG
José Roberto Matos Souza - SP
Simone Cristina Soares Brandão - PE

Professional Defense and Institutional Relations Committee

Members
Fabio Cañellas Moreira - RS
Jorge Yussef Afiune - DF
Marcelo Haertel Miglioranza - RS
Mohamed Hassan Saleh - SP
Wagner Pires de Oliveira Júnior - DF

Committee of Education and Accreditation

Coordinator
Edgar Bezerra de Lira Filho - SP

Members
Andrea de Andare Vilela - SP
Sandra Nívea dos Reis Saraiva Falcão - CE

Intersociety Committee

Coordinator
Marcelo Luiz Campos Vieira - SP

Members
Ana Cristina de Almeida Camarozano - PR
José Luiz Barros Pena - MG
Marcelo Haertel Miglioranza - RS

DIC Youth Committee

Coordinator
Bruna Morhy Borges Leal Assunção - SP
Márcio Miranda Brito - TO

Adult Echo Members
Carolina da Costa Mendes - SP
Manoela Falsoni - SP
Talita Beithum Ribeiro Mialski - PR
Tauin Raoni Do Couto - PA

CR/MR Members
Maria Júlia Silveira Souto - SP

Vascular Ultrasound Member
Larissa Chaves Nunes de Carvalho - SP

Member Of Congenital Heart Diseases
Isabela de Sousa Lobo Silva - SP

Committee on Echocardiography, Congenital and Pediatric Cardiology

Coordinator
Andressa Mussi Soares - ES

Members
Cláudia Regina Pinheiro de Castro Grau - SP
Laura Mercer Rosa - USA
Márcia Ferreira Alves Barberato - PR

PORTAL DIC

Coordinator
Alex dos Santos Félix - RJ

ABC Imagem Cardiovascular

Volume 39, Nº 4, October/November/December 2025

Indexing: Scientific Electronic Library Online (SciELO), Lilacs (Latin American and Caribbean Health Sciences Literature), Latindex (Regional Cooperative Online Information System for Scholarly Journals from Latin America, the Caribbean, Spain and Portugal) and DOAJ (Directory of Open Access Journals)

Address: Av. Marechal Câmara, 160 – 3º andar – Sala 330
20020-907 • Centro • Rio de Janeiro, RJ • Brazil
Phone.: (21) 3478-2700
E-mail: abcimaging@cardiol.br
https://www.abcimaging.org/

Commercial Department
Phone: (11) 3411-5500
E-mail: comercialsp@cardiol.br

Editorial Production
SBC – Scientific Department

Graphic Design and Diagramming
SBC – Scientific Department

Tips and Pitfalls on the Role of Echocardiography in Percutaneous Intervention for Hypertrophic Cardiomyopathy

Claudio Henrique Fischer,[1,2] *Alessandra Joslin Oliveira*[2]
Universidade Federal de São Paulo,[1] *São Paulo, SP – Brazil*
Hospital Israelita Albert Einstein,[2] *São Paulo, SP – Brazil*

Hypertrophic cardiomyopathy (HCM) is the most prevalent genetic heart disease, affecting approximately 1 in 500 individuals in the general population,[1-3] with asymmetric septal hypertrophy as the most common phenotype. In obstructive HCM (oHCM), clinical relevance is greater due to its association with atrial fibrillation, heart failure, thromboembolic events, arrhythmias, and sudden cardiac death.[2,3] For patients who remain symptomatic despite optimized medical therapy, septal reduction has become an established strategy, with surgical septal myectomy as the gold standard.[4] Alcohol septal ablation is an alternative when surgical risk is prohibitive, there are contraindications to surgery, advanced age, or favorable coronary anatomy; it should be performed in experienced centers.[5-8] Other percutaneous approaches — such as radiofrequency septal ablation,[1] the use of coils, or liquid embolic agents — have also been described.

Echocardiography plays a central role throughout the management of oHCM undergoing percutaneous intervention. Beyond diagnosis, it is essential for periprocedural guidance and for postoperative assessment. Understanding its capabilities and recognizing potential pitfalls are critical to success. This editorial offers practical tips for echocardiographers and highlights key points that, if overlooked, may compromise outcomes.

The first challenge occurs before the procedure. In addition to measuring left-ventricular size and systolic/diastolic function, it is essential to confirm the location, distribution, and maximal wall thickness of hypertrophy; verify whether there is significant dynamic obstruction at the left ventricular outflow tract (LVOT) or at the mid-ventricular level; identify systolic anterior motion (SAM) of the mitral valve; and grade mitral regurgitation. Underestimation of the gradient is frequent when provocative maneuvers — such as the Valsalva maneuver or exercise — are not used.[2,3] In symptomatic patients whose peak LVOT gradient remains < 50 mm Hg after Valsalva, exercise stress echocardiography — preferably on a cycle ergometer — should be performed, as it allows continuous monitoring of obstruction progression and gradient rise.[2,3]

Overestimation is another common error, typically caused by inadvertently measuring the velocity of the mitral regurgitation jet instead of the LVOT jet. On apical continuous-wave Doppler, these envelopes often overlap, particularly when lateralization of the transducer is insufficient and the LVOT alignment passes near the origin of the regurgitant jet, causing contamination (Figure 1B). Careful interrogation of the continuous-wave Doppler — considering the onset, contour, and timing of the peak — is required to distinguish them.[2,3] Gradient magnitude also varies across the respiratory cycle, influenced by preload and afterload, which can further complicate interpretation. If uncertainty persists, a practical approach is to obtain the best mitral-regurgitation envelope on continuous-wave Doppler, measure the peak transmitral systolic gradient, and add the estimated left-atrial pressure (typically 10-15 mm Hg) to infer left-ventricular peak systolic pressure; the estimated dynamic gradient corresponds to the difference between ventricular and aortic systolic pressures (Figure 2). Finally, contractility, preload, and afterload should always be verified, as they determine the magnitude of the Venturi effect; abrupt volume depletion, for example, increases the gradient in any obstructive phenotype (Figure 1).

Once the diagnostic stage is complete, periprocedural planning becomes paramount. Echocardiographic guidance substantially increases procedural safety and efficacy and should be incorporated as a routine component of the protocol. Selection of the target septal branch for ablation depends on integrating coronary angiography with echocardiographic findings. Direct injection of radiographic contrast or, preferably, an ultrasound contrast agent (USCA) into the candidate septal branch is a mandatory step,[6,9] because it confirms perfusion of the region of interest and reveals inadvertent perfusion of off-target areas due to collateral flow between the septal artery and adjacent coronaries. It is essential to document perfusion of myocardial segments distant from the intended target — such as the anterolateral left-ventricular wall, the right-ventricular free wall, and the papillary muscles. In these situations, alcohol or other intravascular occlusive agents are contraindicated, and radiofrequency ablation is a viable alternative.[1] Use of USCA is associated with higher success rates, shorter procedure time, lower alcohol volumes, reduced risk of heart block, and smaller septal infarcts.[4,5,9] Transthoracic echocardiography is sufficient in most cases, but a transesophageal approach becomes

Keywords

Hypertrophic Cardiomyopathy; Echocardiography; Left Ventricular Outflow Obstruction

Mailing Address: Claudio Henrique Fischer •
R. Dr. Renato Paes de Barros, 188, ap. 61. Postal Code: 04530-000, São Paulo, SP – Brazil
E-mail: claudiohfischer@gmail.com
Manuscript received September 22, 2025; revised September 30, 2025; accepted September 30
Editor responsible for the review: Marcelo Dantas

DOI: https://doi.org/10.36660/abcimg.20250073i

CONTENTS

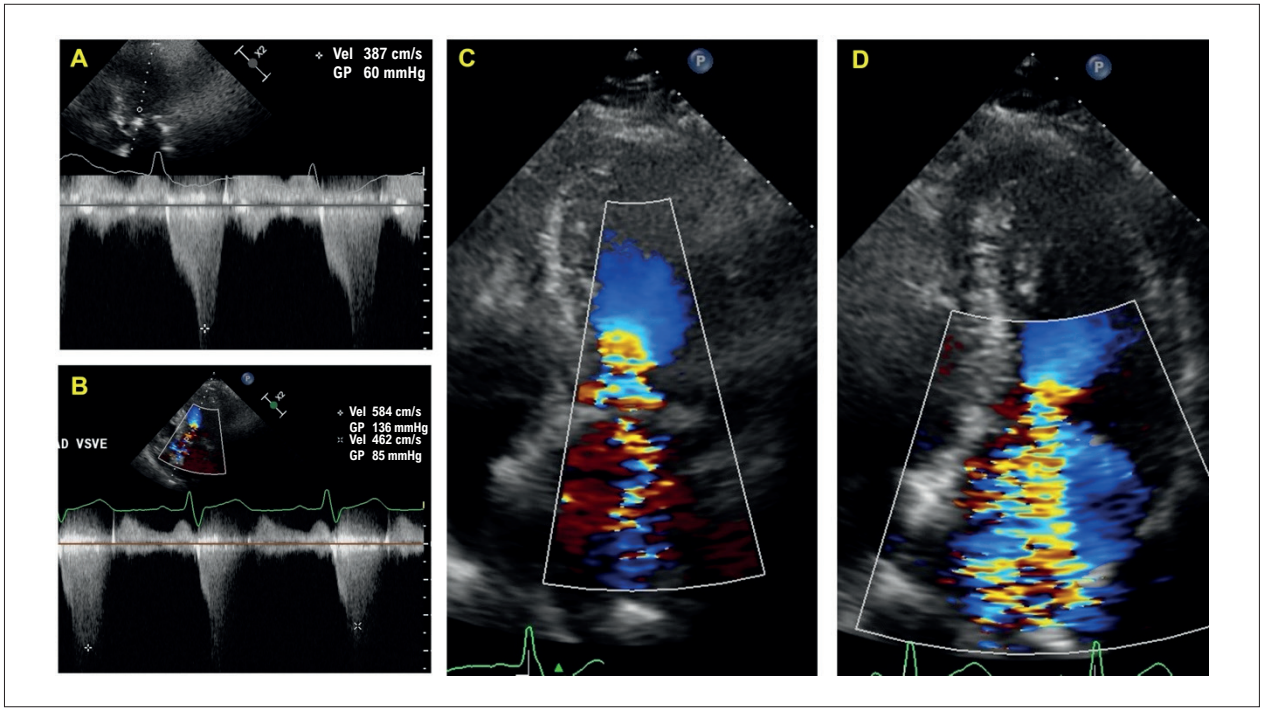

Figure 1 – *Increase in LVOT gradient from 60 mm Hg (A) to 136 mm Hg (B) and worsening mitral regurgitation (MR) from moderate (C) to severe (D) after dialysis with ultrafiltration. These findings indicate intensification of obstruction (greater Venturi effect) due to reduced preload. The post-ultrafiltration gradient curve suggests possible overlap of the mitral regurgitation signal. IM: mitral regurgitation; LVOT: left ventricular outflow tract; PG: pressure gradient; Vel: velocity.*

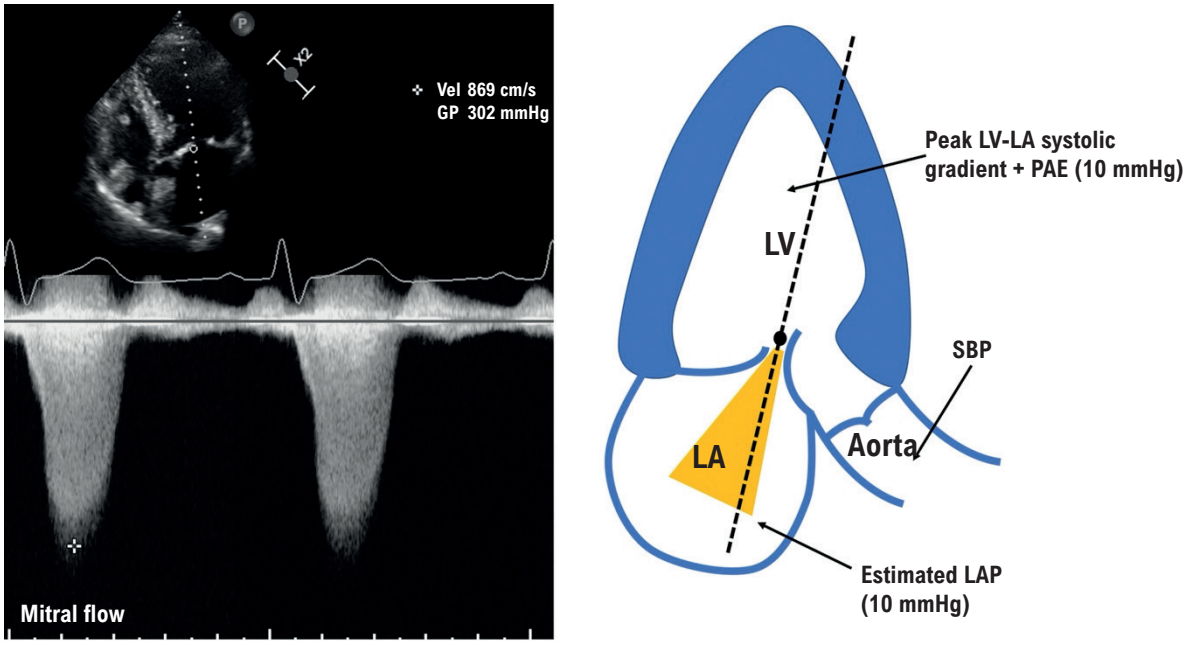

Figure 2 – *Cross-check of the post-ultrafiltration LVOT gradient by estimating left-ventricular systolic pressure from the peak systolic LV-LA transmitral gradient of the mitral-regurgitation jet. The difference between the estimated LV systolic pressure and brachial SBP matches the LVOT gradient estimated in Figure 1. LA: left atrium; LAP: left atrial pressure; LV: left ventricle; LVOT: left ventricular outflow tract; PG: pressure gradient; SBP: systolic blood pressure; Vel: velocity.*

mandatory when the transthoracic window is inadequate or when more detailed assessment of the interventricular septum and adjacent structures is required.

During the procedure, the echocardiographer's role becomes even more critical. An immediate gradient reduction indicates success — regardless of technique — and should be > 50% from baseline or leave a residual resting gradient < 30 mm Hg.[5,7] Interpretation, however, requires caution: transient changes driven by inflammatory mediators and acute hemodynamic fluctuations after the septal infarct can mask the final effect. At this stage, only akinesia of the alcoholized segment is observed; septal thinning from fibrotic scarring — and the resulting enlargement of the LVOT — develop later. Accordingly, additional parameters must be monitored with equal rigor, including reduction or resolution of SAM and the degree of mitral regurgitation, while ensuring proper Doppler alignment at every step.[2,3]

The most feared immediate complication is reflux of alcohol into the left anterior descending (LAD) artery, usually due to incomplete balloon occlusion of the septal branch, balloon rupture, or retrograde flow through collaterals. This risk can be prevented or mitigated by slow, judicious infusion of absolute alcohol by the interventionalist with vigilant, continuous echocardiographic monitoring.[6,9] When present, reflux almost invariably leads to distal LAD occlusion and an acute infarction of the anterior left-ventricular wall; therefore, global and regional systolic function of both ventricles should be continuously assessed and documented. Another rare complication that requires echocardiographic surveillance — from the acute phase through scar consolidation — is a ventricular septal defect.

In post-procedure follow-up, echocardiography remains indispensable. During the first weeks, the gradient may paradoxically increase because of edema in the infarcted septum, before fibrosis develops and consolidates durable remodeling.[8] Recognizing this temporal pattern is crucial to avoid a premature diagnosis of technical failure. Success should be documented with serial studies demonstrating a progressive decline in the gradient accompanied by clinical improvement.

Another essential point is the need for highly specialized training. There is a learning curve for echocardiographers in HCM, and misinterpretation can lead to inappropriate management. Consensus supports restricting these procedures to specialized centers where interventional cardiologists and echocardiographers work collaboratively with standardized protocols.[2,3]

In summary, echocardiography is indispensable at every stage of percutaneous intervention for oHCM: rigorous candidate selection, intraoperative strategy, procedural monitoring, and long-term follow-up. The chief pitfalls include under- or overestimation of the dynamic gradient, errors in selecting the target septal branch, and premature judgments of procedural success. These realities underscore the importance of operator experience, continuous training, and standardized protocols. In an era when percutaneous therapies are established as an effective alternative to surgery, the vigilant, judicious oversight of an experienced echocardiographer enhances both the safety and the efficacy of the procedure.

References

1. Zhou M, Ta S, Hahn RT, Hsi DH, Leon MB, Hu R, et al. Percutaneous Intramyocardial Septal Radiofrequency Ablation in Patients with Drug-Refractory Hypertrophic Obstructive Cardiomyopathy. JAMA Cardiol. 2022;7(5):529-38. doi: 10.1001/jamacardio.2022.0259.
2. Mitchell CC, Frye C, Jankowski M, Symanski J, Lester SJ, Woo A, et al. A Practical Approach to Echocardiographic Imaging in Patients with Hypertrophic Cardiomyopathy. J Am Soc Echocardiogr. 2023;36(9):913-32. doi: 10.1016/j.echo.2023.04.020.
3. Nagueh SF, Phelan D, Abraham T, Armour A, Desai MY, Dragulescu A, et al. Recommendations for Multimodality Cardiovascular Imaging of Patients with Hypertrophic Cardiomyopathy: An Update from the American Society of Echocardiography, in Collaboration with the American Society of Nuclear Cardiology, the Society for Cardiovascular Magnetic Resonance, and the Society of Cardiovascular Computed Tomography. J Am Soc Echocardiogr. 2022;35(6):533-69. doi: 10.1016/j.echo.2022.03.012.
4. Rigopoulos AG, Seggewiss H. Twenty Years of Alcohol Septal Ablation in Hypertrophic Obstructive Cardiomyopathy. Curr Cardiol Rev. 2016;12(4):285-96. doi: 10.2174/1573403x11666150107160344.
5. Spaziano M, Sawaya FJ, Lefèvre T. Alcohol Septal Ablation for Hypertrophic Obstructive Cardiomyopathy: Indications, Technical Aspects, and Clinical Outcomes. J Invasive Cardiol. 2017;29(12):404-10.
6. Faber L, Ziemssen P, Seggewiss H. Targeting Percutaneous Transluminal Septal Ablation for Hypertrophic Obstructive Cardiomyopathy by Intraprocedural Echocardiographic Monitoring. J Am Soc Echocardiogr. 2000;13(12):1074-9. doi: 10.1067/mje.2000.108250.
7. Lu M, Du H, Gao Z, Song L, Cheng H, Zhang Y, et al. Predictors of Outcome after Alcohol Septal Ablation for Hypertrophic Obstructive Cardiomyopathy: An Echocardiography and Cardiovascular Magnetic Resonance Imaging Study. Circ Cardiovasc Interv. 2016;9(3):e002675. doi: 10.1161/CIRCINTERVENTIONS.115.002675.
8. Lakkis NM, Nagueh SF, Kleiman NS, Killip D, He ZX, Verani MS, et al. Echocardiography-Guided Ethanol Septal Reduction for Hypertrophic Obstructive Cardiomyopathy. Circulation. 1998;98(17):1750-5. doi: 10.1161/01.cir.98.17.1750.
9. Urbano-Moral JA, Gonzalez-Gonzalez AM, Maldonado G, Gutierrez-Garcia-Moreno L, Vivancos-Delgado R, De Mora-Martin M, et al. Contrast-Enhanced Echocardiographic Measurement of Left Ventricular Wall Thickness in Hypertrophic Cardiomyopathy: Comparison with Standard Echocardiography and Cardiac Magnetic Resonance. J Am Soc Echocardiogr. 2020;33(9):1106-15. doi: 10.1016/j.echo.2020.04.009.

What Does Myocardial Work Offer Beyond Strain?

Luiz Otávio de Arruda Santos,[1,2] *Edgar Daminello,*[1] *Lucas Arraes de França*[1,3]

Hospital Israelita Albert Einstein,[1] *São Paulo, SP – Brazil*
Beneficencia Portuguesa de São Paulo,[2] *São Paulo, SP – Brazil*
Hospital Samaritano Paulista,[3] *São Paulo, SP – Brazil*

Introduction

In contemporary cardiovascular imaging, one of the methods that has gained significant relevance by adding diagnostic and prognostic information is speckle-tracking–derived Longitudinal Strain, particularly the assessment of left ventricular Global Longitudinal Strain (GLS). However, although GLS evaluates global myocardial deformation of the left ventricle, it is highly dependent on loading conditions, which may interfere with the accurate interpretation of its results. In this context, an emerging technique has been introduced, also derived from speckle tracking: Myocardial Work (MW). Compared with strain, MW offers the advantage of mitigating afterload bias by incorporating systemic arterial pressure into longitudinal strain analysis, generating Pressure–Strain Loops (PSL) throughout the cardiac cycle. Thus, MW quantifies not only the extent of longitudinal myocardial deformation but also the load under which this deformation occurs, providing refined diagnostic insight into ventricular function. The methodology is based on the work of Russell *et al*., who validated the PSL area as a noninvasive index of myocardial work and also introduced the concept of wasted work resulting from contractile discoordination.[1] In clinical practice, four global indices are derived: Global Work Index (GWI), Global Constructive Work (GCW), Global Wasted Work (GWW), and Global Work Efficiency (GWE = GCW / [GCW + GWW]) (Figure 1). Table 1 shows normal reference values for myocardial work and its indices derived from the Normal Reference Ranges for Echocardiography (NORRE) study of the European Association of Cardiovascular Imaging (EACVI).[2]

How Is Load Incorporated Into Strain?

In most cases, the Left Ventricular (LV) pressure curve is estimated using brachial systolic blood pressure measured by a cuff during the examination, synchronized with mitral and aortic valve opening and closing times. In conditions in which systemic systolic blood pressure does not reflect intraventricular pressure, such as Aortic Stenosis (AS), true afterload can be estimated by adding the mean transvalvular systolic aortic gradient to systemic systolic blood pressure, allowing noninvasive estimation of LV systolic pressure.[3-5] LV longitudinal strain is obtained by speckle tracking using apical three-, two-, and four-chamber views to estimate GLS. (Figura 2) By incorporating load into longitudinal myocardial deformation, MW helps determine whether reduced longitudinal strain values are due solely to increased afterload or reflect true intrinsic myocardial contractile dysfunction, which is something GLS alone cannot distinguish.[1,5]

Additional Diagnostic Value of Myocardial Work in Current Clinical Scenarios

1) Coronary Artery Disease (CAD)

In patients with preserved Left Ventricular Ejection Fraction (LVEF) and no resting regional wall motion abnormalities, GWI outperformed GLS in discriminating significant CAD. In the study by Edwards et al., the area under the ROC curve for global GWI was 0.786 versus 0.693 for GLS; a cutoff value of 1,810 mmHg% yielded a sensitivity of 92% and a specificity of 51% for detecting CAD, highlighting the greater sensitivity of MW in patients with single-vessel disease.[3] In such cases, GLS may be normal at rest, whereas MW demonstrates greater sensitivity for CAD screening by incorporating afterload.[3]

2) After ST-segment elevation myocardial infarction

Within the first 24–48 hours after Percutaneous Coronary Intervention (PCI) for anterior ST-segment elevation myocardial infarction (STEMI), myocardial segments exposed to high afterload may exhibit reduced strain values without a proportional loss of constructive work, which is a compensatory pattern that GLS alone cannot identify. Recent studies show that in this setting, myocardial constructive work (both segmental and global) was a better predictor of regional and global functional recovery compared with LVEF, GLS, and wall motion scores.[4] Additionally, patients with in-hospital complications exhibited lower absolute values of global GCW and GWI and higher N-terminal pro–B-type natriuretic peptide (NT-proBNP) levels, underscoring the prognostic role of MW.[4] Preserved global GCW in the Left Anterior Descending Artery (LAD) territory, despite reduced absolute strain values, suggests myocardial viability and a higher likelihood of contractile recovery. Conversely, markedly reduced GCW values indicate a higher risk of persistent contractile dysfunction and adverse outcomes[4] (Figure 3).

3) Aortic valve stenosis

In severe aortic valve stenosis, strain has major limitations in distinguishing reduced longitudinal myocardial deformation

Keywords

Echocardiography; Coronary Artery Disease; Aortic Valve Stenosis; Cardiac Resynchronization Therapy

Mailing Address: Lucas Arraes de França •
Hospital Israelita Albert Einstein. Av. Albert Einstein, 627/701. Postal Code: 05652-900. São Paulo, SP – Brazil
E-mail: lucas.franca81@gmail.com

DOI: https://doi.org/10.36660/abcimg.20250103i

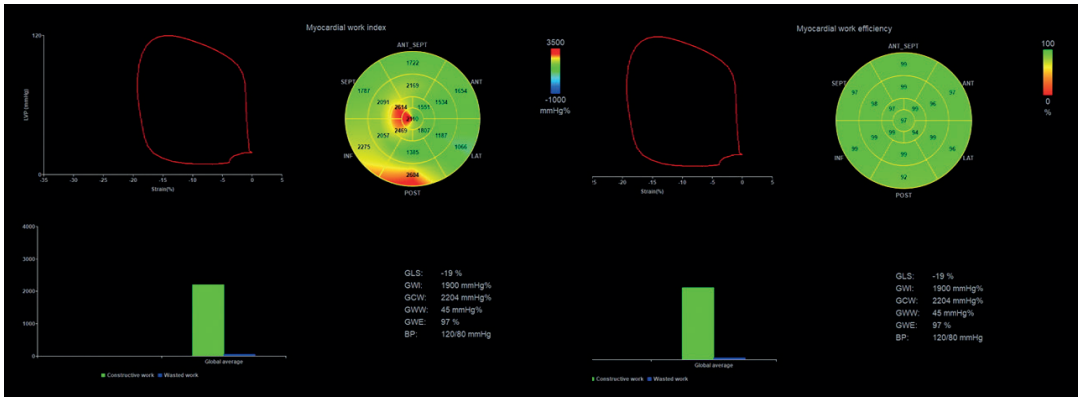

Figure 1 – *Polar map of myocardial work index displaying GLS, GWI, GCW, GWW, GWE, and systemic arterial pressure at the time of the examination.*

Table 1 – Normal reference values for myocardial work in men and women derived from the NORRE study of the EACVI.[2]

	Total	Male	Female
Number of patients	(n = 226)	(n = 85)	(n = 141)
GWI (mm Hg%)	1.896 ± 308	1.849 ± 295	1.924 ± 313
GCW (mm Hg%)	2.232 ± 331	2.228 ± 295	2.234 ± 352
GWW (mm Hg%)	78.5 (53 –122.2)	94 (61.5 –130.5)	74 (49.5 – 111)
GWE (%)	96 (94 – 97)	95 (94 – 97)	96 (94 – 97)

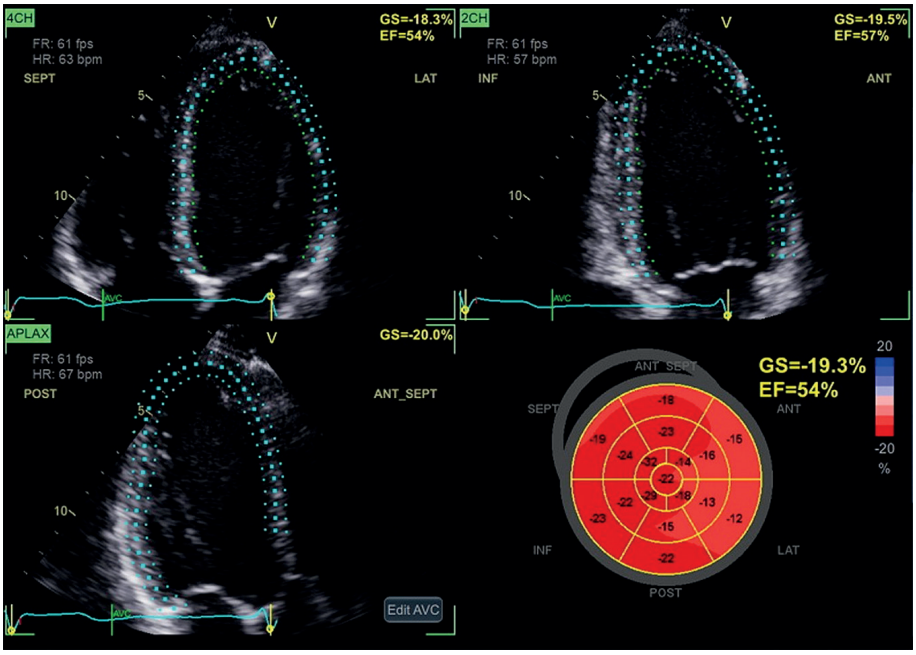

Figure 2 – *Apical four-, two-, and three-chamber views showing left ventricular longitudinal strain analysis derived from speckle tracking.*

Editorial

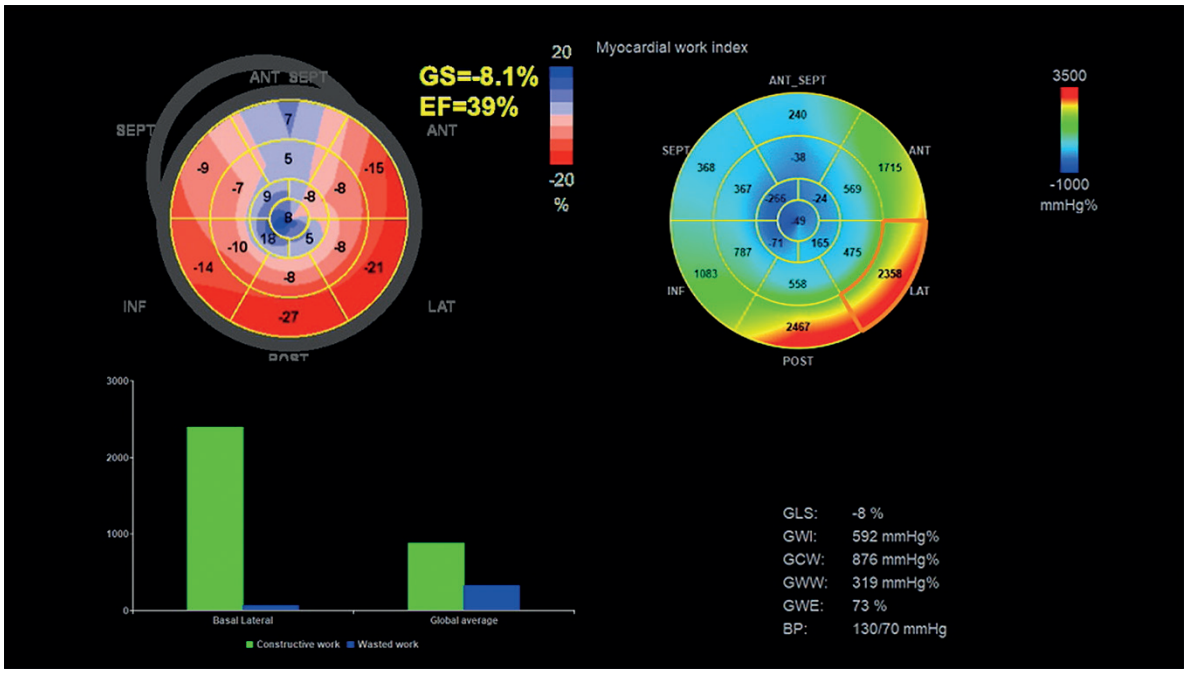

Figure 3 – *GLS and MW analysis in a patient with STEMI affecting the anteroseptal and apical segments of the left ventricle, showing significantly reduced GLS, LVEF, GCW, GWI, and GWE.*

due to adaptive response to increased afterload from deformation reduction caused by intrinsic myocardial dysfunction. MW provides incremental diagnostic value in this scenario. By appropriately estimating LV systolic pressure (adding the mean transvalvular systolic aortic gradient to systemic systolic blood pressure) and integrating it with LV longitudinal strain, GWI and GCW more accurately reflect the ventricle's ability to perform useful work under extremely high afterload. In a study of patients referred for Transcatheter Aortic Valve Implantation (TAVI), both GLS and MW were independently associated with heart failure symptoms (NYHA class III/IV); however, GLS showed weaker statistical correlation due to its load dependency. Clinically, this means that patients with similar GLS values may exhibit markedly different functional capacities. Patients with higher absolute GWI and GCW values tend to preserve mechanical efficiency despite elevated afterload and therefore present fewer symptoms, whereas lower values indicate incomplete adaptation and more pronounced symptoms. This more "physiological" interpretation supports a more refined discussion regarding optimal timing of intervention, particularly when LVEF remains preserved.[5]

4) Cardiac resynchronization therapy (CRT)

Response to CRT depends not only on correction of electromechanical delay but also on improvement in regional and global ventricular performance. In a retrospective cohort of 97 patients undergoing CRT, Total Constructive Work (CWtot), a global metric of constructive work, was an independent predictor of CRT response (left ventricular reverse remodeling at six months). A cutoff value of 1,057 mmHg% demonstrated good predictive performance, comparable to septal flash.[6] Additionally, the concept of wasted septal work (energy expended during paradoxical lengthening) correlated with mechanical inefficiency due to dyssynchrony. However, these are small, early studies that have not demonstrated clear superiority over pure strain-based metrics, highlighting the need for further investigation.[7] MW does not replace traditional criteria (QRS duration and morphology, presence of left bundle branch block, and scar burden) but may assist clinical decision-making in borderline cases.[8]

Interpreting MW as a Complement to GLS

MW and GLS are complementary tools that enable a more comprehensive assessment of myocardial deformation. GLS is an excellent technique for detecting subclinical systolic dysfunction, monitoring cardiotoxicity, tracking disease progression across multiple conditions, and providing prognostic information. MW emerges as an additional tool when loading conditions limit isolated GLS interpretation or when deformation needs to be translated into effective myocardial work. In hypertensive patients and those with aortic valve stenosis, MW mitigates afterload bias and prevents underestimation of systolic function. In suspected Coronary Arterial Disease (CAD) with normal conventional echocardiographic parameters of LV systolic function, reduced global MW values at rest increase suspicion of ischemia and support further diagnostic investigation.

After an anterior myocardial infarction, constructive work has prognostic value in predicting recovery of LV systolic function. In CRT candidates, higher absolute pre-implant constructive work values suggest preserved contractile reserve and a greater likelihood of reverse ventricular remodeling. Echocardiographic reports should ideally include both GLS and MW values, along with systemic blood pressure and heart rate at the time of examination, to enable more accurate interpretation of results.[9]

Myocardial Work and Its Limitations

Like speckle-tracking–derived longitudinal strain, MW measurement depends on adequate image quality for reliable speckle tracking. Furthermore, MW relies on noninvasive estimation of systemic blood pressure, requiring careful consideration in specific clinical contexts. As discussed, in patients with aortic valve stenosis, LV systolic pressure estimation must incorporate the mean transvalvular systolic aortic gradient. In other scenarios, such as fixed or dynamic obstructions, interpretation should be cautious. Logistical limitations also exist, as analysis is currently restricted to a single proprietary software platform, limiting broader dissemination across echocardiography laboratories. Finally, although studies demonstrate incremental value across multiple clinical settings, available evidence originates from a limited number of centers with relatively small sample sizes and short follow-up periods.[9]

Conclusion

Myocardial work provides incremental information beyond strain, with a fundamental role in assessing myocardial deformation under varying loading conditions. By integrating longitudinal myocardial deformation with systemic arterial pressure, MW delivers valuable insights into the effective work performed by the left ventricle throughout the cardiac cycle. In high afterload states, MW helps distinguish whether reduced absolute GLS values reflect intrinsic myocardial dysfunction. It also aids in predicting recovery of LV systolic function in STEMI patients treated with PCI and in identifying patients more likely to respond to CRT. Although broader standardization and multicenter validation are still needed, MW already offers meaningful incremental diagnostic and prognostic information.

References

1. Russell K, Eriksen M, Aaberge L, Wilhelmsen N, Skulstad H, Remme EW, et al. A Novel Clinical Method for Quantification of Regional Left Ventricular Pressure-Strain Loop Area: A Non-Invasive Index of Myocardial Work. Eur Heart J. 2012;33(6):724-33. doi: 10.1093/eurheartj/ehs016.
2. Manganaro R, Marchetta S, Dulgheru R, Ilardi F, Sugimoto T, Robinet S, et al. Echocardiographic Reference Ranges for Normal Non-Invasive Myocardial Work Indices: Results from the EACVI NORRE Study. Eur Heart J Cardiovasc Imaging. 2019;20(5):582-90. doi: 10.1093/ehjci/jey188.
3. Edwards NFA, Scalia GM, Shiino K, Sabapathy S, Anderson B, Chamberlain R, et al. Global Myocardial Work is Superior to Global Longitudinal Strain to Predict Significant Coronary Artery Disease in Patients with Normal Left Ventricular Function and Wall Motion. J Am Soc Echocardiogr. 2019;32(8):947-57. doi: 10.1016/j.echo.2019.02.014.
4. Meimoun P, Abdani S, Stracchi V, Elmkies F, Boulanger J, Botoro T, et al. Usefulness of Noninvasive Myocardial Work to Predict Left Ventricular Recovery and Acute Complications after Acute Anterior Myocardial Infarction Treated by Percutaneous Coronary Intervention. J Am Soc Echocardiogr. 2020;33(10):1180-90. doi: 10.1016/j.echo.2020.07.008.
5. Fortuni F, Butcher SC, van der Kley F, Lustosa RP, Karalis I, de Weger A, et al. Left Ventricular Myocardial Work in Patients with Severe Aortic Stenosis. J Am Soc Echocardiogr. 2021;34(3):257-66. doi: 10.1016/j.echo.2020.10.014.
6. Galli E, Leclercq C, Fournet M, Hubert A, Bernard A, Smiseth OA, et al. Value of Myocardial Work Estimation in the Prediction of Response to Cardiac Resynchronization Therapy. J Am Soc Echocardiogr. 2018;31(2):220-30. doi: 10.1016/j.echo.2017.10.009.
7. Vecera J, Penicka M, Eriksen M, Russell K, Bartunek J, Vanderheyden M, et al. Wasted Septal Work in Left Ventricular Dyssynchrony: A Novel Principle to Predict Response to Cardiac Resynchronization Therapy. Eur Heart J Cardiovasc Imaging. 2016;17(6):624-32. doi: 10.1093/ehjci/jew019.
8. Galli E, Leclercq C, Hubert A, Bernard A, Smiseth OA, Mabo P, et al. Role of Myocardial Constructive Work in the Identification of Responders to CRT. Eur Heart J Cardiovasc Imaging. 2018;19(9):1010-8. doi: 10.1093/ehjci/jex191.
9. Roemer S, Jaglan A, Santos D, Umland M, Jain R, Tajik AJ, et al. The Utility of Myocardial Work in Clinical Practice. J Am Soc Echocardiogr. 2021;34(8):807-18. doi: 10.1016/j.echo.2021.04.013.

Emerging Topics in Pediatric Echocardiography: A Review by the Associate Editors of the Pediatric Section

Karen Saori Shiraishi Sawamura,[1,2] *Márcio Miranda Brito*[3]
Universidade de São Paulo, Instituto da Criança,[1] *São Paulo, SP – Brazil*
Einstein Hospital Israelita,[2] *São Paulo, SP – Brazil*
Universidade Federal do Norte do Tocantins,[3] *Araguaina, TO – Brazil*

In this review, we selected five recently published studies addressing structural, functional, and methodological aspects of echocardiographic assessment in pediatrics (Table 1). The studies provide new perspectives on the embryological basis of ventricular septation, the quality and applicability of echocardiographic nomograms, the accuracy of right ventricular (RV) diastolic function assessment, and the use of RV and left ventricular (LV) strain as early markers of dysfunction. The objective of this review is to offer readers of *ABC Imagem Cardiovascular* a critical synthesis of emerging topics with potential applicability in both clinical practice and research in pediatric echocardiography.

We wish all readers an engaging and informative reading experience.

Ventricular septal morphology and cardiac development

Anderson et al.[1] convened international experts to propose a unified morphofunctional classification of ventricular septal defects, with emphasis on embryological features and ventriculoarterial connections. The authors critically examine the nomenclature currently in use and suggest that defect descriptions should encompass both their anatomical location and the borders involved. This approach integrates principles of cardiac development and allows, for example, differentiation between perimembranous defects in hearts with double outlet right ventricle and those with concordant ventriculoarterial connections. The article provides a clear and didactic review of cardiac embryological development, supported by illustrations that facilitate a more precise diagnostic and surgical approach.

Echocardiographic nomograms: advances and gaps

In their review, Cantinotti et al.[2] critically analyze approximately 2 decades of scientific production related to nomograms in pediatric echocardiography. The study highlights important advances, including greater methodological robustness, larger sample sizes, improved standardization, and the use of more rigorous statistical models. Nevertheless, significant limitations persist, such as underrepresentation of diverse ethnic groups, limited data in preterm infants and low-birth-weight neonates, and inconsistencies in the normalization of diastolic parameters. The authors also advocate for the integration of nomograms into echocardiographic reporting systems and emphasize the need for further studies with greater population diversity and multicenter validation of emerging metrics, including strain and three-dimensional volumes.

Assessment of RV diastolic function: technical challenges and innovative approaches

Henry and Mertens[3] address the current state of RV diastolic function assessment, an area that has traditionally received less attention than LV evaluation. The article highlights the limitations of conventional parameters, such as the tricuspid E/A ratio and e′ velocity, particularly in children, in whom age-related variability, heart rate, and hemodynamic loading conditions are substantial. As alternative approaches, the authors propose the use of right atrial reservoir strain and RV global longitudinal strain (RVGLS). In addition, emerging techniques are discussed, including ultrafast ultrasound imaging, with potential applications in assessing intraventricular pressure gradients and shear wave velocity for the analysis of myocardial stiffness. These methods are described as promising, although they remain largely experimental.

RV maturation in preterm infants with pulmonary disease

Within the context of RV functional assessment, Sawamura et al.[4] conducted a longitudinal study to evaluate the maturation of RV function in preterm infants during the first year of life. The results demonstrated that the presence of bronchopulmonary dysplasia impairs the expected trajectory of cardiac maturation, an effect detectable through RV strain analysis. The study also identified a significant impact of mechanical ventilation strategies on long-term cardiac function. High-frequency oscillatory ventilation was associated with better RVGLS performance at 1 year of age, whereas prolonged invasive ventilation and oxygen dependency were predictors of poorer ventricular function. These findings suggest that ventilatory strategies may directly influence cardiac maturation in this population.

Keywords

Echocardiography; Child; Pediatrics

Mailing Address: Karen Saori Shiraishi Sawamura •
Hospital das Clínicas, Faculdade de Medicina, Universidade de São Paulo. Av. Dr. Enéas Carvalho de Aguiar, 647. Postal code: 05403-000. São Paulo, SP – Brazil
E-mail: kasaori@gmail.com
Manuscript received November 6, 2025; revised November 11, 2025; accepted November 12, 2025.
Editor responsible for the review: Marcelo Dantas

DOI: https://doi.org/10.36660/abcimg.20250093i

CONTENTS

Table 1 – Recently published studies addressing structural, functional, and methodological aspects of pediatric echocardiographic assessment

Study ID	Reference	Study summary
1	Anderson et al., 2025[1]	Proposal of a unified morphofunctional nomenclature for ventricular septal defects, grounded in embryological development, with direct implications for diagnosis and surgical planning.
2	Cantinotti et al., 2025[2]	Review of advances in pediatric echocardiographic nomograms, highlighting methodological improvements while emphasizing limitations related to ethnic diversity and representation across different age groups.
3	Henry e Mertens, 2025[3]	Critical analysis of current limitations in assessing RV diastolic function in children, with the proposal of emerging methods, including ultrafast ultrasound imaging and strain parameters.
4	Sawamura et al., 2025[4]	Longitudinal study in preterm infants demonstrating an association between bronchopulmonary dysplasia and reduced RV functional gain, and identifying a positive impact of high-frequency oscillatory ventilation on RVGLS.
5	Melo et al., 2024[5]	Study evaluating pre-CPB LVGLS by transesophageal echocardiography, demonstrating prognostic associations with mortality and postoperative complications.

CPB: cardiopulmonary bypass; LVGLS: left ventricular global longitudinal strain; RV: right ventricle; RVGLS: right ventricular global longitudinal strain.

LV global longitudinal strain (LVGLS) in pediatric cardiac surgery

Melo et al.[5] evaluated the association between LVGLS, measured by transesophageal echocardiography, and postoperative outcomes in children undergoing congenital cardiac surgery with cardiopulmonary bypass (CPB). LVGLS proved to be a feasible, reproducible measure for assessing ventricular function. Both pre-CPB and post-CPB values demonstrated effective discriminatory capacity for predicting 30-day mortality, with pre-CPB LVGLS showing the greatest predictive power. Pre-CPB LVGLS values $\leq -12\%$ were significantly associated with higher vasoactive–inotropic scores and longer durations of mechanical ventilation. The authors suggest that LVGLS may represent a relevant prognostic tool for predicting mortality and postoperative complications in this population.

References

1. Anderson RH, Houyel L, Lopez L, Pandey NN, Spicer DE, Cook AC, et al. Reaching Consensus as to How Knowledge of Development Underscores our Understanding of Deficient Ventricular Septation. Cardiol Young. 2025;35(8):1617-30. doi: 10.1017/S104795112510139X.
2. Cantinotti M, Marchese P, Capponi G, Franchi E, Santoro G, Pizzuto A, et al. Pediatric Echocardiographic Nomograms: Twenty Years of Advances-do We Now Have a Complete and Reliable Tool, or are Gaps Still Present? An Up-to-Date Review. J Clin Med. 2025;14(15):5215. doi: 10.3390/jcm14155215.
3. Henry M, Mertens L. Echocardiographic Assessment of Right Ventricular Diastolic Function in Children and Adults: Present State and Future Directions. Can J Cardiol. 2025;41(6):1142-51. doi: 10.1016/j.cjca.2025.03.024.
4. Sawamura KSS, Sadeck LSR, Assunção NA Jr, Kushikawa NYY, Lianza AC, Diniz MFR, et al. The Impact of Bronchopulmonary Dysplasia on the Maturation of Preterm Infants' Right Ventricular Mechanics Over the First Year of Life: A Prospective Strain-Echocardiography Cohort. Pediatr Cardiol. 2025. doi: 10.1007/s00246-025-04043-9.
5. Melo S, Alzate-Ricaurte S, Pedroza S, Moreno M, Largo J, Rivera R, et al. Optimal Global Longitudinal Strain Thresholds for Pediatric Heart Surgery: Insights from a University Hospital. Pediatr Cardiol. 2024;45(4):780-6. doi: 10.1007/s00246-024-03437-5.

Original Article

Monitoring Myocardial Metabolic Changes in Lymphoma Patients Undergoing Chemotherapy Using FDG PET/CT

Diego Rafael Freitas Berenguer,[1,2] Gustavo Freitas Alves de Arruda,[1] Monica de Moraes Chaves Becker,[1] Mayara Lais Coelho Dourado,[2] Roberto de Oliveira Buril,[1] Felipe Alves Mourato,[2] Paulo José de Almeida Filho,[3] Brivaldo Markman-Filho,[1] Simone Cristina Soares Brandão[1,4]

Universidade Federal de Pernambuco,[1] Recife, PE – Brazil
Hospital das Clínicas da Universidade Federal de Pernambuco,[2] Recife, PE – Brazil
Real Hospital Português de Beneficência em Pernambuco,[3] Recife, PE – Brazil
Brigham and Women's Hospital,[4] Boston, Massachusetts – USA

Abstract

Background: Cardiotoxicity is a serious adverse effect of chemotherapy, often identified only after irreversible myocardial damage has occurred. Positron emission tomography/computed tomography (PET/CT) using fluorine-18 fluorodeoxyglucose (^{18}F-FDG) allows for the evaluation of myocardial glucose metabolism and may help detect early metabolic changes related to chemotherapy.

Objective: To assess changes in ^{18}F-FDG standardized uptake values (SUVs) across different cardiac regions before and after chemotherapy in patients with lymphoma, and to identify which region exhibits the greatest increase.

Methods: This retrospective cohort study included 62 lymphoma patients who underwent ^{18}F-FDG PET/CT before and after chemotherapy. SUV measurements were obtained in the left ventricular (LV) free wall, interventricular septum (IVS), right ventricular (RV) free wall, and global myocardium. Control regions included the liver and aorta. Pre- and post-treatment SUV values were compared to evaluate metabolic changes related to chemotherapy.

Results: Myocardial ^{18}F-FDG uptake increased significantly after chemotherapy across all cardiac regions, with the most pronounced rise observed in the LV free wall (maximum SUV increase of 73%, $p<0.001$). The RV free wall showed a non-significant increase in SUV, and no significant changes were observed in the liver or aorta.

Conclusions: Chemotherapy was associated with a global increase in myocardial ^{18}F-FDG uptake, with the most pronounced elevation observed in the LV free wall. This regional predominance highlights the LV free wall as the most sensitive site for detecting early metabolic changes potentially related to cardiotoxicity.

Keywords: Cardiotoxicity; Chemotherapy; ^{18}F-FDG PET/CT; Myocardial metabolism; Lymphoma.

Introduction

Cardiotoxicity (CTX) is one of the most severe long-term adverse effects of cancer treatment, potentially leading to heart failure with reduced ejection fraction (HFrEF) and other cardiovascular complications.[1] Although initially defined as a reduction in left ventricular ejection fraction (LVEF), CTX has been expanded in recent guidelines to include a broader range of cardiovascular conditions.[2,3] Among chemotherapy drugs, anthracyclines remain one of the leading causes of CTX due to their well-documented association with HFrEF, which is often irreversible and carries high morbidity and mortality.[4-8]

The clinical manifestations of CTX often appear months or years after initial chemotherapy, limiting the utility of traditional methods like LVEF assessment, which detects systolic dysfunction only after substantial myocardial injury has occurred.[3,9,10] Positron emission tomography/computed tomography (PET/CT) with fluorine-18 fluorodeoxyglucose (^{18}F-FDG) offers a promising alternative by providing insights into myocardial metabolism and detecting subtle metabolic changes preceding overt contractile dysfunction.[11] Studies suggest that ^{18}F-FDG uptake alterations in cardiomyocytes during or after chemotherapy may reflect early mitochondrial and metabolic stress, potentially serving as an early marker of CTX.[9-15]

Interestingly, ^{18}F-FDG uptake varies physiologically between different cardiac regions. The left ventricle, due to its higher myocyte density and energy demand, exhibits greater glucose consumption than the right ventricle.[16,17] This disparity may be further influenced by oxidative stress induced by chemotherapy, which could preferentially affect certain myocardial regions. Understanding these regional differences in ^{18}F-FDG uptake may provide deeper insights into the mechanisms of CTX and its early detection.

This study aimed to evaluate changes in ^{18}F-FDG standardized uptake values (SUV) in different myocardial regions before and

Mailing Address: Diego Rafael Freitas Berenguer •
Hospital das Clínicas da Universidade Federal de Pernambuco. Av. Professor Moraes do Rego, Cidade Universitária. Postal Code: 50670-901, Recife, PE – Brazil
E-mail: diegoberenguer@gmail.com
Manuscript received September 19, 2025; revised September 30, 2025; accepted September 30, 2025
Editor responsible for the review: Marcelo Dantas

DOI: https://doi.org/10.36660/abcimg.20250067i

CONTENTS

Central Illustration: Monitoring Myocardial Metabolic Changes in Lymphoma Patients Undergoing Chemotherapy Using FDG PET/CT

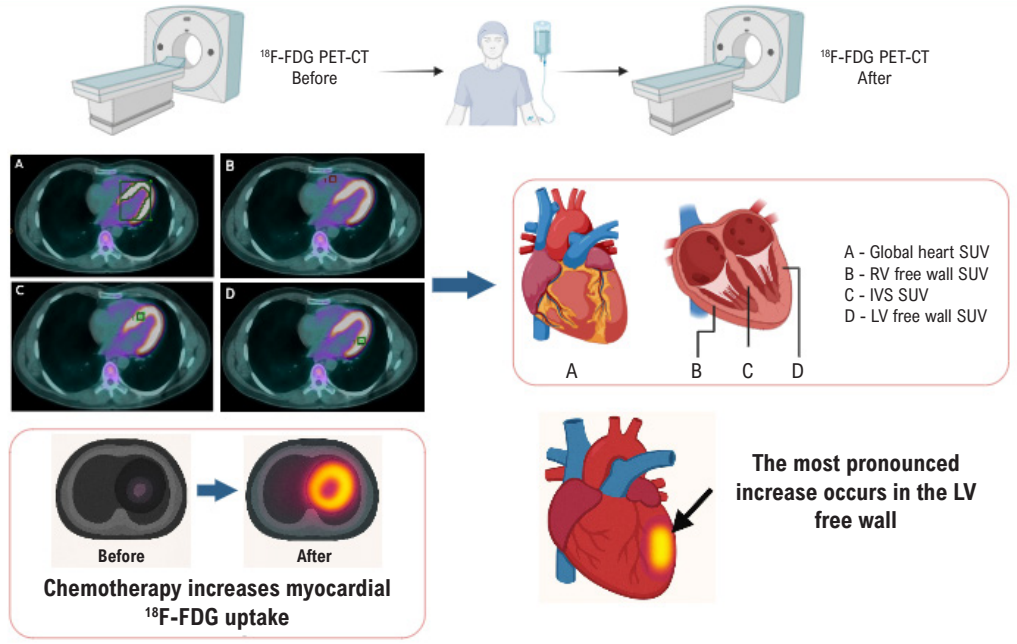

Arq Bras Cardiol: Imagem cardiovasc. 2025;38(4):e20250067

Monitoring myocardial metabolic changes after chemotherapy. ^{18}F-FDG PET-CT: Positron emission tomography/computed tomography with fluorine-18 fluorodeoxyglucose; IVS: Interventricular septum. LV: left ventricle. RV: right ventricle. SUV: standardized uptake values. Created with BioRender.com.

after chemotherapy, offering a novel perspective on metabolic markers of CTX during cancer treatment monitoring.

Materials and Methods

This is a retrospective cohort study that reexamined the medical records and imaging exams of 70 patients who participated in a previous study conducted by the Nuclear Medicine Department of a private hospital between January 1, 2012, and August 28, 2017.

The inclusion criteria were age 18 years or older; diagnosis of lymphoma; and having undergone at least two ^{18}F-FDG PET/CT scans – one prior to chemotherapy and another during or after treatment, as illustrated in the Central Illustration.

Patients were excluded due to insufficient data in their medical records, unavailability or inability to evaluate the ^{18}F-FDG PET/CT images, prior mediastinal chemotherapy or radiotherapy (before the baseline PET/CT of this study), or insulin therapy administered on the day of any ^{18}F-FDG PET/CT exam. After reviewing the exams, eight patients were excluded due to the inability to assess the images.

Clinical data and personal history were retrieved from the medical records attached to the initial assessment form, which was completed by the patient prior to each PET scan. For PET/CT analysis, we collected the following parameters: ^{18}F-FDG injected dose, activation time, and both maximum and mean SUV of the descending aorta, liver, and heart. We measured ^{18}F-FDG SUV in various cardiac regions: the whole heart, the mid-region of the septal wall, the left ventricular (LV) free wall, and the right ventricular (RV) free wall (see Central Illustration; Figure 1).

The evolution of SUVs was analyzed based on the numerical measurements in the different cardiac segments evaluated, as well as in the control organs (aorta and liver). A comparison between the final and baseline maximum SUV values was also performed.

^{18}F-FDG PET/CT Protocol

Patients were instructed to fast for six hours prior to the exam, continue taking their usual medications, and avoid physical activity for 24 hours beforehand. To proceed with the exam, blood glucose levels had to be below 180 mg/dL. The radiopharmaceutical ^{18}F-FDG was administered at a dose of 3.7 to 4.8 MBq/kg, and patients were instructed to rest for 60 minutes (corresponding to the uptake period). After this interval, they were taken to the imaging room for acquisition.

All exams were performed using the same PET/CT scanner (Biograph 16, Siemens Healthcare, USA). Images were acquired from the skull base to the proximal middle third of the lower limbs (femur) in three-dimensional mode, with a scan time of

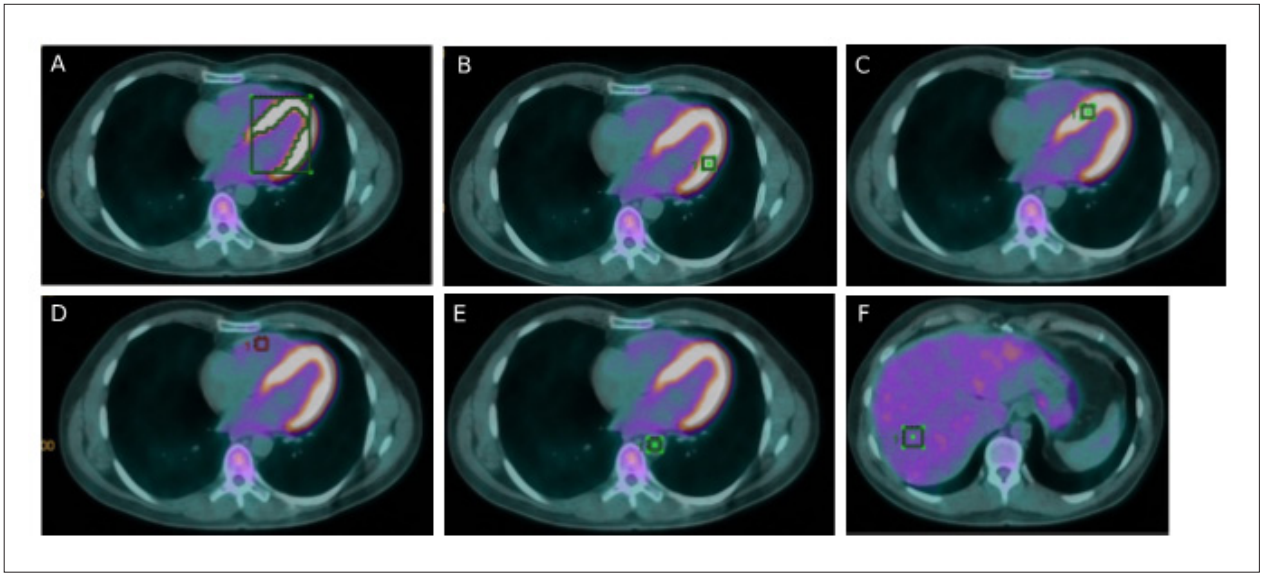

Figure 1 – *Regions of interest (ROIs) for SUV acquisition in various cardiac sites and in control regions (aorta and liver) (A), global heart SUV; (B), LV free wall SUV; (C), IVS SUV; (D), RV free wall; (E), Aorta SUV; (F), Liver SUV. SUV: standardized uptake value, LV: left ventricle, IVS: interventricular septum, RV: right ventricle*

three minutes per bed position (each body segment). The images were processed using iterative reconstruction (2 iterations with 8 subsets and a Gaussian filter).

Computed tomography (CT) acquisition parameters included a 5 mm slice thickness, 120 kV voltage, and no intravenous contrast administration. Additionally, the exam was complemented by a chest helical acquisition performed during maximum inspiration.

Statistical Analysis

Data were analyzed using R software version 4.0.0 (R Foundation for Statistical Computing, Vienna, Austria). Numerical data are presented as median and interquartile range, as they do not follow a normal distribution, while categorical data are expressed as n (%). The Bayesian Repeated Measures Profile Modeling (BRPM) method was used to compare SUV values between baseline and final PET groups. SUV analysis was performed across all cardiac regions as well as in the liver and aorta. A significance level of 5% was adopted to reject the null hypothesis.

Results

General Descriptive Analysis

A total of 62 patients were included in this study. The sample characteristics are further detailed according to socio-demographic and clinical criteria (Table 1). The mean age was 49 ± 15 years, and the average weight was 73 ± 9 kg. Clinical characteristics and patient data at the time of the exams are also presented (Table 2).

Evolution of the SUV During Cancer Therapy

Both maximum and mean SUV values increased significantly during cancer treatment across all assessed cardiac regions (see Central Illustration). The most prominent elevations were observed in the global cardiac SUV and the LV free wall SUV. In contrast, the aortic and hepatic SUVs (both mean and maximum) showed no statistically significant differences between the baseline and final PET scans (Table 2). Figure 2 illustrates the progression of maximum and mean SUVs across all cardiac segments and control regions (aorta and liver).

Discussion

This study demonstrated a statistically significant increase in cardiac ^{18}F-FDG uptake across all left ventricular regions during chemotherapy. The most pronounced uptake was observed in the lateral wall of the LV. Although an increase in SUV uptake was also noted in the lateral wall of the RV, this change did not reach statistical significance.

Baucknet et al.[18] reported that cardiac ^{18}F-FDG uptake is directly proportional to the oxidative stress induced by anthracycline use. Therefore, the increased myocardial ^{18}F-FDG uptake in these segments may suggest a greater rise in oxidative stress within the LV regions compared to other sites.

The more noticeable changes in the left heart segments may be due to the higher density of cardiac muscle cells in the left ventricle. Since the left ventricle has a larger muscle mass, it contains more cells that have been affected by oxidative damage caused by chemotherapy.[16] Another possible explanation is that the fibers on the left side of the heart have a greater energy demand. Under oxidative stress, these cells can no longer produce enough energy to function properly, leading to cell death (apoptosis). Because the fibers in the LV require more energy, this process of cell damage occurs more frequently in these fibers, resulting in greater ^{18}F-FDG uptake in the myocardium.[17]

Bulten et al.[19] observed that only some cardiomyocytes are susceptible to anthracycline-induced injury and that this damage

Table 1 – Sociodemographic and clinical characteristics of patients undergoing ^{18}F-FDG PET/CT in the assessment of myocardial uptake during chemotherapy treatment.

Variable (N=62)	N (%)
Female	31 (50%)
Hypertension	13 (20.9%)
Dyslipidemia	9 (14.5%)
Diabetes mellitus	8 (12.9%)
Coronary artery disease	3 (4.8%)
Smoke	
Smoker	2 (3.2%)
Not smoker	44 (70.9%)
Ex-smoker	16 (25.8%)
Type of Lymphoma	
Hodgkin	23 (37%)
Não Hodgkin	39 (62.9%)
Chemoterapy used[a]	
ABVD	12 (37.5%)
ABVD + alternative scheme	1 (3.1%)
R-CHOP	14 (43.9%)
R-CHOP + alternative scheme	2 (6.2%)
BEACOPP	1 (3.1%)
DA-EPOCH-R	1 (3.1%)
Imunotherapy	1 (3.1%)
Mediastinal radiotherapy	9 (14%)
Use of medication	
No	4 (6.4%)
Yes (Cardioprotective)[b]	15 (24.1%)
Sim (Non-cardioprotective)[b]	43 (69.3%)

[a]Available for 32 patients. [b]Cardioprotective medication: angiotensin II receptor blocker, beta-blocker, angiotensin-converting enzyme inhibitor. ABVD: Adriamycin or Doxorubicin + Bleomycin + Vinblastine + Dacarbazine, BEACOPP: Bleomycin + Etoposide + Doxorubicin + Cyclophosphamide + Vincristine + Procarbazine + Prednisone, DA-EPOCH-R: Etoposide + Prednisone + Vincristine + Cyclophosphamide + Doxorubicin + Rituximab Dose adjusted, R-

occurs even with low doses of doxorubicin. A greater ^{18}F-FDG uptake in the different cardiac segments may be a consequence of the greater presence of these susceptible cells in those segments.

It is possible that PET/CT provides a diagnosis of this process in which the oxidative stress increases until the cell starts its apoptosis. It is known that the apoptosis process can be reversed until the moment immediately prior to the cell membrane lysis.[20] If there is a possibility of suppression of this oxidative stress, the cardiomyocytes death could be avoided. Hence the importance of diagnosing this cellular damage as early as possible.

When analyzing the SUV changes, a notable rise in all cardiac segments examined was observed. This finding aligns with the results from the study by Dourado et al.,[21] where they reported an average increase of 66.5% in the maximum global cardiac SUV when comparing baseline PET/CT to PET/CT after chemotherapy.

Baucknehet al.[22] performed ^{18}F-FDG PET/CT scans on 69 patients with Hodgkin's lymphoma undergoing doxorubicin therapy. Four scans were conducted: one at baseline, one during treatment, another four to six weeks after chemotherapy, and a final scan six months post-treatment. The study revealed a significant increase in LV SUV following chemotherapy. Moreover, the LV SUV was notably low prior to treatment and was identified as a potential predictive marker for the development of CTX.

Kim et al.[13] evaluated not only the increase in myocardial ^{18}F-FDG uptake but also the uptake pattern. In their study, among 121 patients monitored, 15 developed CTX, diagnosed via echocardiography one week after treatment with anthracyclines (doxorubicin and epirubicin) or trastuzumab. A diffuse uptake pattern and increased LV ^{18}F-FDG uptake were more frequently observed in patients who developed CTX.[12]

Another key finding was that an increase of 0.4 in the RV maximum SUV, as well as an RV maximum SUV greater than 1.8, were statistically significant indicators of CTX.[12] In the present study, although less pronounced, both the maximum and mean RV SUV values increased during cancer therapy, partially corroborating the findings of Kim et al.[13] These results highlight the need for more targeted studies to better understand the role of the RV and its association with the development of CTX.

While this study offers valuable insights, several limitations should be acknowledged. First, its retrospective design limits control over confounding factors, such as pre-existing cardiac conditions or concurrent medications, which may have influenced the results. Future prospective studies with stricter controls could help mitigate these biases. The small sample size also restricts the generalizability of the findings; expanding the cohort in future research would enhance statistical power and enable subgroup analyses.

Additionally, the lack of functional data – such as echocardiography or cardiac magnetic resonance imaging (MRI) – makes it challenging to correlate metabolic changes with functional outcomes. Including these assessments in future studies would provide a more comprehensive understanding of the relationship between metabolic alterations and CTX. Finally, although the follow-up period was short and the study was conducted at a single center without standardized dietary preparation, larger multi-center studies with extended follow-up and consistent protocols would help overcome these limitations.

Still, the results help to further clarify the behavior of ^{18}F-FDG myocardial uptake before and after chemotherapy. Moreover, this investigation offers an innovative perspective, given the limited number of studies in this field and the fact that CTX diagnosis remains delayed.

Conclusion

This study demonstrated an increased ^{18}F-FDG uptake in various cardiac regions in patients with lymphoma undergoing chemotherapy. Among the evaluated cardiac sites, the maximum

Table 2 – Evolution of standardized uptake value, body weight, and test characteristics in patients undergoing ^{18}F-FDG PET/CT for myocardial uptake assessment during chemotherapy

Variable	Basal[1] (N = 62)	Final[1] (N = 62)	P[2]	Final vs Baseline Dif. (95%CI)[3]
Weight (kg)	73 (66 - 82)	74 (65 - 83)		
Activation time (min)	67 (60 - 76)	65 (60 - 76)		
Dose injected (MBq)	344 (303 - 394)	333 (296 - 392)		
Mean heart SUV	1.80 (1.40 – 2.73)	2.55 (1.61 – 3.77)	< 0.001	0.75 (0.35 – 1.37)
Maximum heart SUV	2.96 (2.29 – 5.47)	5.12 (3.16 – 8.77)	< 0.001	2.23 (1.04 – 3.43)
Mean interventricular septum SUV	1.87 (1.42 – 2.74)	2.62 (1.64 – 4.39)	0.024	0.75 (0.15 – 2.05)
Maximum interventricular septum SUV	2.16 (1.67 – 2.49)	3.00 (1.96 – 5.61)	0.020	0.83 (0.10 – 2.62)
Mean right ventricular SUV	1.33 (1.16 – 1.54)	1.49 (1.31 – 1.72)	0.059	0.16 (-0.01 – 0.31)
Maximum right ventricular SUV	1.69 (1.43 – 1.96)	1.83 (1.60 – 2.10)	0.068	0.14 (-0.01 – 0.36)
Mean left ventricular SUV	2.03 (1.54 – 3.66)	3.62 (1.86 – 5.64)	< 0.001	1.60 (0.68 – 2.66)
Maximum left ventricular SUV	2.43 (1.87 – 4.58)	4.51 (2.28 – 7.18)	< 0.001	2.08 (0.87 – 3.07)
Mean aorta SUV	1.48 (1.28 – 1.67)	1.44 (1.22 – 1.68)	0.766	-0.03 (-0.16 – 0.12)
Maximum aorta SUV	1.80 (1.51 – 2.11)	1.67 (1.45 – 2.02)	0.405	-0.12 (-0.28 – 0.105)
Mean liver SUV	2.20 (1.86 – 2.50)	2.29 (2.04 – 2.63)	0.125	0.09 (-0.05 – 0.24)
Maximum liver SUV	2.57 (2.18 – 2.98)	2.63 (2.38 – 2.99)	0.331	0.06 (-0.10 – 0.22)

[1]Median (interquartile range). Kg: kilograms. min: minutes. MBq: megabecquerel. [2]BRPM Method [3]Difference between medians and their respective 95% confidence interval.

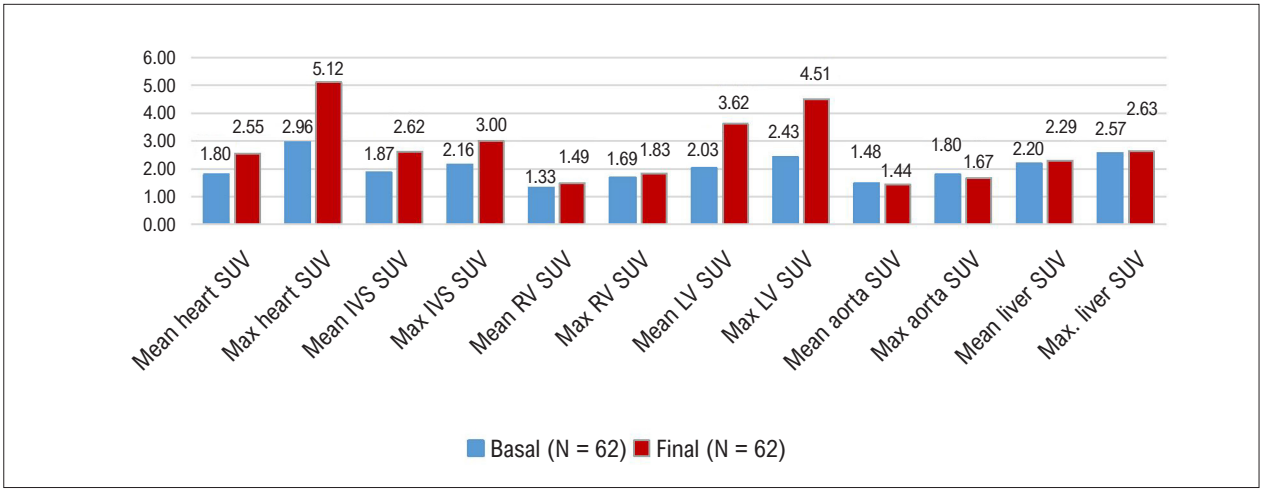

Figure 2 – *Evolution of maximum and mean SUVs (median values) across different cardiac regions and control sites (aorta and liver) at baseline and at the end of chemotherapy treatment. [1]median (interquartile range). IVS: Interventricular septum. LV: left ventricle. RV: right ventricle. AO: aorta. Created with Microsoft Excel.*

SUV in the LV free wall showed the most significant increase during treatment.

Author Contributions

Conception and design of the research: Becker MMC, Markman-Filho B, Brandão SCS. Acquisition of data: Berenguer DRF, Arruda GFA, Dourado MLC, Almeida-Filho PJ, Mourato FA. Analysis and interpretation of the data: Berenguer DRF, Arruda GFA, Becker MMC, Dourado MLC, Buril RO, Almeida-Filho PJ, Mourato FA, Markman-Filho B, Brandão SCS. Statistical analysis: Berenguer DRF, Brandão SCS. Writing of the manuscript: Berenguer DRF, Becker MMC, Markman-Filho B, Brandão SCS. Critical revision of the manuscript for intellectual content:

Berenguer DRF, Becker MMC, Buril RO, Markman-Filho B, Brandão SCS.

Potential Conflict of Interest

No potential conflict of interest relevant to this article was reported.

Sources of Funding

This study was partially funded by FACEPE (Fundação de Apoio a Ciência e Tecnologia de Pernambuco).

Study Association

This article is part of the thesis of master submitted by Diego Rafael Freitas Berenguer, from Graduate Program in Translational Health at the Universidade Federal de Pernambuco (UFPE).

Ethics Approval and Consent to Participate

This study was approved by the Ethics Committee of the Hospital das Clínicas of UFPE under the protocol number 4.052.412. All the procedures in this study were in accordance with the 1975 Helsinki Declaration, updated in 2013. Informed consent was obtained from all participants included in the study.

Use of Artificial Intelligence

The authors did not use any artificial intelligence tools in the development of this work.

Availability of Research Data

The data cannot be made publicly available because it comes from the database of the Real Hospital Português de Beneficência in Pernambuco, containing clinical information on patients and subject to the institution's confidentiality and secrecy rules. Interested researchers may contact the management committee of the Real Hospital Português de Beneficência in Pernambuco for any formal access requests, which will be analyzed on a case-by-case basis.

Reference

1. Kalil R Filho, Hajjar LA, Bacal F, Hoff PM, Diz MP, Galas FR, et al. I Brazilian Guideline for Cardio-Oncology from Sociedade Brasileira de Cardiologia. Arq Bras Cardiol. 2011;96(2 Suppl 1):1-52.
2. Hajjar LA, Costa IBSDSD, Lopes MACQ, Hoff PMG, Diz MDPE, Fonseca SMR, et al. Brazilian Cardio-Oncology Guideline - 2020. Arq Bras Cardiol. 2020;115(5):1006-43. doi: 10.36660/abc.20201006.
3. Zamorano JL, Lancellotti P, Muñoz DR, Aboyans V, Asteggiano R, Galderisi M, et al. 2016 ESC Position Paper on Cancer Treatments and Cardiovascular Toxicity Developed Under the Auspices of the ESC Committee for Practice Guidelines: The Task Force for Cancer Treatments and Cardiovascular Toxicity of the European Society of Cardiology (ESC). Eur Heart J. 2016;37(36):2768-801. doi: 10.1093/eurheartj/ehw211.
4. Giordano SH, Lin YL, Kuo YF, Hortobagyi GN, Goodwin JS. Decline in the Use of Anthracyclines for Breast Cancer. J Clin Oncol. 2012;30(18):2232-9. doi: 10.1200/JCO.2011.40.1273.
5. Nabhan C, Byrtek M, Rai A, Dawson K, Zhou X, Link BK, et al. Disease Characteristics, Treatment Patterns, Prognosis, Outcomes and Lymphoma-Related Mortality in Elderly Follicular Lymphoma in the United States. Br J Haematol. 2015;170(1):85-95. doi: 10.1111/bjh.13399.
6. Chihara D, Westin JR, Oki Y, Ahmed MA, Do B, Fayad LE, et al. Management Strategies and Outcomes for Very Elderly Patients with Diffuse Large B-Cell Lymphoma. Cancer. 2016;122(20):3145-51. doi: 10.1002/cncr.30173.
7. Ainger LE, Bushore J, Johnson WW, Ito J. Daunomycin: A Cardiotoxic Agent. J Natl Med Assoc. 1971;63(4):261-7.
8. Felker GM, Thompson RE, Hare JM, Hruban RH, Clemetson DE, Howard DL, et al. Underlying Causes and Long-Term Survival in Patients with Initially Unexplained Cardiomyopathy. N Engl J Med. 2000;342(15):1077-84. doi: 10.1056/NEJM200004133421502.
9. Curigliano G, Cardinale D, Suter T, Plataniotis G, Azambuja E, Sandri MT, et al. Cardiovascular Toxicity Induced by Chemotherapy, Targeted Agents and Radiotherapy: ESMO Clinical Practice Guidelines. Ann Oncol. 2012;23(Suppl 7):vii155-66. doi: 10.1093/annonc/mds293.
10. Negishi K, Negishi T, Haluska BA, Hare JL, Plana JC, Marwick TH. Use of Speckle Strain to Assess Left Ventricular Responses to Cardiotoxic Chemotherapy and Cardioprotection. Eur Heart J Cardiovasc Imaging. 2014;15(3):324-31. doi: 10.1093/ehjci/jet159.
11. Berenguer DRF, Becker MMC, Buril RO, Bertão PA, Markman B Filho, Brandão SCS. Progression of Myocardial 18F-FDG Uptake in a Patient with Cardiotoxicity. Arq Bras Cardiol. 2024;121(2):e20230276. doi: 10.36660/abc.20230276.
12. Sarocchi M, Bauckneht M, Arboscello E, Capitanio S, Marini C, Morbelli S, et al. An Increase in Myocardial 18-Fluorodeoxyglucose Uptake is Associated with Left Ventricular Ejection Fraction Decline in Hodgkin Lymphoma Patients Treated with Anthracycline. J Transl Med. 2018;16(1):295. doi: 10.1186/s12967-018-1670-9.
13. Kim J, Cho SG, Kang SR, Yoo SW, Kwon SY, Min JJ, et al. Association between FDG Uptake in the Right Ventricular Myocardium and Cancer Therapy-Induced Cardiotoxicity. J Nucl Cardiol. 2020;27(6):2154-63. doi: 10.1007/s12350-019-01617-y.
14. Becker MMC, Arruda GFA, Berenguer DRF, Buril RO, Cardinale D, Brandão SCS. Anthracycline Cardiotoxicity: Current Methods of Diagnosis and Possible Role of 18F-FDG PET/CT as a New Biomarker. Cardiooncology. 2023;9(1):17. doi: 10.1186/s40959-023-00161-6.
15. Hirata K, Kamagata K, Ueda D, Yanagawa M, Kawamura M, Nakaura T, et al. From FDG and Beyond: The Evolving Potential of Nuclear Medicine. Ann Nucl Med. 2023;37(11):583-95. doi: 10.1007/s12149-023-01865-6.
16. Bengel FM, Higuchi T, Javadi MS, Lautamäki R. Cardiac Positron Emission Tomography. J Am Coll Cardiol. 2009;54(1):1-15. doi: 10.1016/j.jacc.2009.02.065.
17. Pinker K, Riedl C, Weber WA. Evaluating Tumor Response with FDG PET: Updates on PERCIST, Comparison with EORTC Criteria and Clues to Future Developments. Eur J Nucl Med Mol Imaging. 2017;44(Suppl 1):55-66. doi: 10.1007/s00259-017-3687-3.
18. Bauckneht M, Pastorino F, Castellani P, Cossu V, Orengo AM, Piccioli P, et al. Increased Myocardial 18F-FDG Uptake as a Marker of Doxorubicin-Induced Oxidative Stress. J Nucl Cardiol. 2020;27(6):2183-94. doi: 10.1007/s12350-019-01618-x.

19. Bulten BF, Sollini M, Boni R, Massri K, de Geus-Oei LF, van Laarhoven HWM, et al. Cardiac Molecular Pathways Influenced by Doxorubicin Treatment in Mice. Sci Rep. 2019;9(1):2514. doi: 10.1038/s41598-019-38986-w.

20. Okada DR, Liu Z, Johnson G 3rd, Beju D, Khaw BA, Okada RD. 99mTc-Glucarate Kinetics Differentiate Normal, Stunned, Hibernating, and Nonviable Myocardium in a Perfused Rat Heart Model. Eur J Nucl Med Mol Imaging. 2010;37(10):1909-17. doi: 10.1007/s00259-010-1495-0.

21. Dourado MLC, Dompieri LT, Leitão GM, Mourato FA, Santos RGG, Almeida PJ Filho, et al. Chemotherapy-Induced Cardiac18F-FDG Uptake in Patients with Lymphoma: An Early Metabolic Index of Cardiotoxicity? Arq Bras Cardiol. 2022;118(6):1049-58. doi: 10.36660/abc.20210463.

22. Baucknehtt M, Ferrarazzo G, Fiz F, Morbelli S, Sarocchi M, Pastorino F, et al. Doxorubicin Effect on Myocardial Metabolism as a Prerequisite for Subsequent Development of Cardiac Toxicity: A Translational 18F-FDG PET/CT Observation. J Nucl Med. 2017;58(10):1638-45. doi: 10.2967/jnumed.117.191122.

Infective Endocarditis in Brazil: A Narrative Review and Critical Analysis of Population and Hospital Case Data

Diego Augusto Medeiros Santos,[1] Flávio Tarasoutchi,[1] João Ricardo Cordeiro Fernandes,[1] Milena Ribeiro Paixão,[1] Tânia Mara Varejão Strabelli,[1] Karen Francine Köohler,[2] Alfredo José Mansur,[1] Rinaldo Focaccia Siciliano[1]

Universidade de São Paulo, Instituto do Coração,[1] São Paulo, SP – Brazil

Hospital Israelita Albert Einstein,[2] São Paulo, SP – Brazil

Central Illustration: Infective Endocarditis in Brazil: A Narrative Review and Critical Analysis of Population and Hospital Case Data

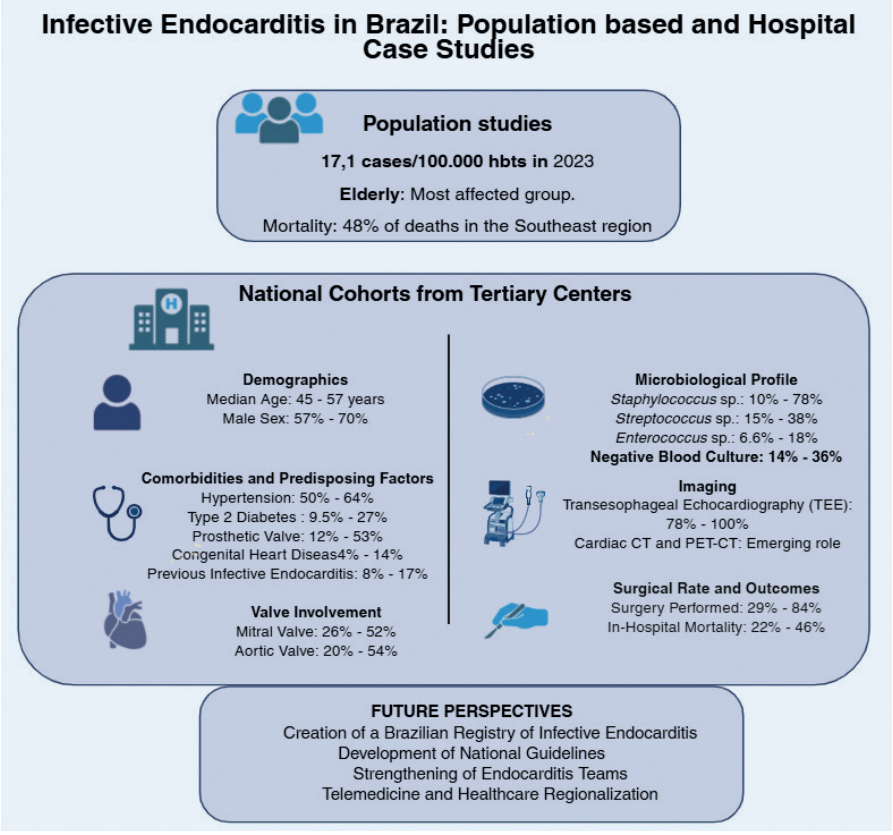

Arq Bras Cardiol: Imagem cardiovasc. 2025;38(4):e20250098

Overview of Infective Endocarditis in Brazil: Epidemiology, Challenges, and Future Perspectives

Keywords

Endocarditis; Unified Health System; Heart Valve Diseases; Diagnostic Imaging.

Mailing Address: Diego Augusto Medeiros Santos •
Universidade de São Paulo, Instituto do Coração. Av. Dr. Enéas Carvalho de Aguiar, 44. Postal code: 05403-000. São Paulo, SP – Brazil
E-mail: diego_ams90@hotmail.com
Manuscript received December 4, 2025; revised December 15, 2025; accepted December 15, 2025
Editor responsible for the review: Marcelo Tavares

DOI: https://doi.org/10.36660/abcimg.20250098i

Abstract

Infective endocarditis remains a serious condition with high morbidity and mortality rates despite advances in diagnostic and therapy. While the Global North has seen a shift toward older patients with prosthetic valve infections, Brazil's understanding of the disease is hindered by reliance on fragmented, hospital-based data, primarily from the Southeast region. This narrative review synthesizes recent evidence to outline the national panorama. Population studies indicate an increase in incidence and mortality, primarily

affecting men and the elderly, but with marked regional heterogeneity. Analyses of hospital case series reveal an epidemiological profile characterized by patients younger than international averages, with a high prevalence of comorbidities, underlying structural heart disease, and prosthetic valves. The microbiological landscape is diverse, with no consistent predominance between staphylococci and streptococci. Nevertheless, a particularly concerning finding is the high incidence of negative blood cultures. Severe complications are frequent, and variability exists in surgical intervention rates and in-hospital mortality across studies. In light of this scenario, the authors propose a set of strategic actions to guide future advances: the creation of a Brazilian Registry of Infective Endocarditis, the development of Contextualized National Guidelines, the strengthening of multidisciplinary teams (Endocarditis Teams), and the implementation of measures with the potential to reduce regional disparities, such as telemedicine and the regionalization of care. The consolidation of these initiatives has the potential to transform the current landscape by enhancing epidemiological knowledge, standardizing care practices, and ultimately improving clinical outcomes nationwide.

Introduction

Infective endocarditis (IE) is a severe systemic disease of high clinical complexity, presenting significant challenges for management.[1,2] It predominantly affects individuals with pre-existing valvular heart disease and, despite scientific advances, remains associated with a high risk of complications and mortality.[3-6]

In recent decades, the epidemiological profile of endocarditis has undergone a significant transformation, primarily described in the Global North. It has evolved into a condition that predominantly affects elderly individuals, those with multiple comorbidities, with an increasing number of cases related to cardiac device use.[2] This epidemiological shift has been driven mainly by the greater availability of cardiac procedures, including prosthetic valves, pacemakers, and the use of intravascular catheters. Consequently, the disease has assumed a more acute character, affecting older individuals with comorbidities, who constitute a group at higher risk for complications and mortality.[2]

In contrast, studies from the Global South indicate that the disease affects younger patients, often associated with valvular sequelae of rheumatic fever and streptococcal infections.[6,7] However, some case series describe a different profile, with many cases occurring in individuals with congenital heart disease,[8] and the epidemiological transition observed in the Global North appears to be underway in other parts of the world as well.[9]

In 2019, an estimated 1,090,530 cases of the disease and 66,320 deaths occurred globally.[8] Population-based studies indicate that the incidence of IE has been increasing in recent decades,[8] along with its lethality. On a global scale, the incidence of IE also demonstrates considerable heterogeneity, with reported rates ranging from 4.9 to 10.2 cases per 100,000 inhabitants.[10,11]

This epidemiological variability is further reflected in risk factors, microbiology, surgical indications, and disease outcomes. For example, marked differences are observed in the proportion of cases associated with intravenous drug use,[12] the percentage of negative blood cultures,[7,11] rates of surgical indication,[13,14] the spectrum of complications, and lethality, which can range from 14.9% to 45.8%.[11,15] These indicators vary widely across regions and populations, underscoring the complexity of the disease.

Brazil likely exhibits marked particularities, as distinct epidemiological realities coexist within the same territory, ranging from large, developed urban centers to regions with limited access to healthcare.

Given this scenario, the objective of this narrative review is to integrate global data, population estimates, and recent Brazilian hospital case series, providing a critical analysis of the national landscape of IE and proposing practical recommendations to improve disease management in Brazil.

Methodology

For the development of this narrative review, a comprehensive bibliographic search was conducted in major national and international scientific databases, including PubMed, MEDLINE, the Virtual Health Library (BVS), LILACS, and Google Scholar. The search strategy utilized the descriptors “infective endocarditis,” “endocarditis,” “bacterial endocarditis,” “Brazil,” and “Duke criteria,” combined using the Boolean operators AND and OR.

The search focused on publications from the last six years (2020-2025) in Portuguese or English, including original articles, reviews, cohort studies, meta-analyses, and other relevant documents. Classic Brazilian studies were intentionally included to complement the initial search results. The selection process involved identification, screening of titles and abstracts, and assessment for eligibility through full-text reading.

To avoid duplication of case series, a single publication per cohort was selected based on the most comprehensive study. Case series restricted to specific subgroups were excluded to maintain a broad overview of the disease within the national context.

As this is a narrative review, no meta-analysis was conducted, nor was a standardized risk-of-bias assessment tool applied. Evidence extracted from the selected studies was synthesized descriptively and comparatively, with the aim of highlighting consistent trends, knowledge gaps, and the particularities of IE in the Brazilian context.

Thirteen Brazilian publications reporting hospital-based case series of IE from January 2020 to November 2025 were identified. Of these, seven cohorts containing clinical, microbiological, and outcome data were selected for tabular synthesis (Tables 1–3).

Results and Discussion

To synthesize the key interrelationships between epidemiology, clinical presentation, care challenges, and proposed solutions discussed in this review, the Central Figure provides a comprehensive visual overview. The following sections will provide a detailed critical analysis of each of these components, beginning with population-based data.

Table 1 – Baseline characteristics and comorbidities in Brazilian infective endocarditis cohorts

Year	Location	N	Age (median)	Male sex	Community acquired	Rheumatic valve disease	Congenital heart disease	Prosthetic valve	Previous endocarditis	SAH	T2DM
2025	São Paulo[45]	530	56	63.6%	-	35.1%	4.1%	53%	16.9%	52%	18%
2024	Minas Gerais[46]	263	52	60.5%	-	30%	9%	26%	8.5%	-	14%
2024	São Paulo[47]	204	53	57%	37.7%	9%	-	12%	9.3%	64%	27%
2024	Rio de Janeiro[48]	502	48	65%	64.7%	30.7%	13.9	31%	12.6%	50%	15%
2023	Rio de Janeiro[15]	240	55	57%	46%	-	-	22%	8%	-	21%
2023	Rio Grande do Sul[49]	179	57	70%	-	-	-	12%	-	51%	20%
2021	Minas Gerais[50]	211	48	70.6%	-	-		30%		-	-

** Subtitle - SAH - Systemic arterial hypertension; T2DM - Type 2 diabetes mellitus; (-) - Data not reported.*

Table 2 – Microbiological profile in Brazilian Infective Endocarditis Cohorts

Location	*Staphylococcus sp*	*Streptococcus sp*	*Enterococcus sp*	HACEK *	Culture negative
São Paulo[45]	11.5%	26%	7.7%	1.1%	21%
Minas Gerais[46]	35%	14%	7.6%	0.4%	33.8%
São Paulo[47]	78%	14.6%	7%	0%	18%
Rio de Janeiro[48]	10%	15%	12.8%	<5%	33%
Rio de Janeiro[15]	37%	38%	18%	0.8%	19%
Rio Grande do Sul[49]	22%	15%	-	-	14%
Minas Gerais[50]	19%	14.7%	6.6%	-	33.3%

** HACEK - Haemophilus, Aggregatibacter, Cardiobacterium, Eikenella, and Kingella; (-) - Data not reported.*

Table 3 – Valve Involvement, Echocardiographic Findings, Complications, and In-Hospital Outcomes in Brazilian Infective Endocarditis Cohorts

Location	Mitral valve	Aortic valve	TEE	HF	Perivalvular Abscess	Surgical Treatment	In-Hospital Mortality
São Paulo[45]	52%	54%	-	40%	12.9%	56%	30.2%
Minas Gerais[46]	-	-	-	-	28%	57.5%	34.2%
São Paulo[47]	44%	20%	100%	29.1%	30%	34%	44.6%
Rio de Janeiro[48]	44%	38%	78%	58%	21%	83.6%	25%
Rio de Janeiro[15]	43.8%	22%	-	-	-	29%	45.8%
Rio Grande do Sul[49]	33%	38%	81%	54%	10%	38%	22.3%
Minas Gerais[50]	41%	26%	-	-	-	-	22.3%

**Abbreviations: TEE - Transesophageal Echocardiography; HF - Heart Failure; (-) - Data not reported.*

Population-Based Studies

The understanding of IE in Brazil is largely derived from hospital-based cohorts in tertiary centers, with a notable concentration in the Southeast region. Robust population-based studies on incidence and prevalence are lacking nationwide. To address this gap, large hospital databases, such as the DATASUS systems, including the Mortality Information System (SIM) and the Hospital Information System (SIH), have been employed.[16,17]

Among the available epidemiological surveys, the Global Burden of Disease (GBD) study is the most comprehensive. Although it does not provide a publication dedicated exclusively to Brazil, data from this source[8] indicate that the incidence rate of the disease increased from 9.15 to 17.14 cases per 100,000 inhabitants between 1993 and 2023. Additionally, mortality associated with the disease reached 2,958 recorded deaths in 2023.

This apparent growth in incidence may not solely reflect a true increase in cases. Factors such as improved access to healthcare services, advances in diagnostic methods (like the wider availability of echocardiography), the adoption of electronic medical records, and potential changes in disease coding may have significantly contributed to enhanced detection and reporting, thereby inflating the observed rates.

According to SIM data,[16] a total of 52,055 deaths from IE were reported between 2000 and 2019. The mortality profile was predominantly male, within the 60–79-year age group, and concentrated in the Southeast region. Cluster analysis identified three distinct mortality profiles: (a) women aged 80 years or older, with endocrine and circulatory diseases, concentrated in the South and Southeast; (b) men aged between 30 and 79 years, with infectious and genitourinary diseases, also predominant in the South and Southeast; and (c) individuals aged 0 to 29 years of both sexes, with respiratory diseases, showing a higher proportion of deaths in the North, Northeast, and Central-West regions.[16]

Brazilian Hospital Case Series

While population-based studies help to frame the problem on a large scale, a detailed understanding of the clinical presentation, microbiological profile, and outcomes of IE in Brazil relies predominantly on case series and cohorts conducted in tertiary reference hospitals. Tables 1, 2, and 3 summarize the selected Brazilian studies.

The following section provides a synthesis of these publications. The analysis is organized according to the main risk factors and predisposing conditions, followed by the characterization of etiological agents, specifics of valve involvement, and associated complications. In addition, surgical rates and in-hospital mortality are evaluated.

It is important to note that most studies were conducted in tertiary centers with access to cardiac surgery. Considerable heterogeneity is observed in the study periods, as well as in the number of cases from each center.

The selected studies encompass a broad temporal spectrum, with inclusion periods ranging from 2000 to 2023, and most reported follow-up periods exceeding ten years. Nevertheless, heterogeneity in recruitment windows and the absence of systematic overlap between study periods limit the ability to perform a consistent temporal analysis of the evolution of IE in Brazil.

The studies also differ in their methodological objectives. These include publications aimed at validating predictive risk scores, assessing long-term neurological outcomes, and conducting descriptive analyses of individual case series.

Diagnostic Criteria and Presenting Symptoms

All analyzed studies employed the Modified Duke Criteria[18] for the case definition of IE. Beginning in 2024, the incorporation of the new Duke-ISCVID criteria[19] was observed in two publications, reflecting the recent update in international guidelines.

The reporting of signs and symptoms related to endocarditis was not always consistent across studies. Fever upon admission was documented in 67.5% to 90.6% of cases, and a new cardiac murmur was reported in 50.7% to 74.8% of patients.

Demographic Profile of Patients

The aggregate analysis of the seven published studies from Brazilian tertiary centers (Tables 1, 2, and 3) revealed a median age ranging from 45 to 57 years. These values are generally lower than those documented in case series from the Global North, where median ages frequently exceed 60 years.[3-5,10,13,20,21]

The predominance of male sex (57% to 70%) is consistent with the international literature.[10,13,20-22] Despite a lower incidence of the disease, women present with a higher risk of death and lower rates of cardiac surgery.[23-25]

Presence of Comorbidities

Systemic arterial hypertension stands out as the most prevalent comorbidity, present in 50-64% of patients across the centers that reported this data. Diabetes mellitus shows a prevalence ranging from 9.5% to 27% among the different cohorts.

The prevalence of systemic arterial hypertension is close to 50% in various international case series,[5,11,26] and the Brazilian studies are consistent with this finding. Regarding the prevalence of diabetes mellitus, approximately 20-30% of patients in Global North countries present with this condition,[5,11] values slightly higher than those observed in the Brazilian studies.

Valve Involvement and Predisposing Factors

The analysis of risk factors reveals a diverse profile of predisposing conditions. Prosthetic valve endocarditis was described in 12-53% of cases, cases related to cardiac electronic devices in 6.9-29.3%, and congenital heart disease in 4.1-13.9%. A personal history of a previous episode of IE was documented in 8% to 16.9% of cases.

Cases related to illicit intravenous drug use were infrequent. This scenario contrasts with some countries where the condition constitutes a public health challenge,[27] and accounts

for up to 23.5% of IE cases, as observed in the study by Jordal et al.[28] This is a complex problem with impacts on individual health and psychosocial well-being, requiring multidisciplinary care.[27]

Structural valvular disease due to rheumatic fever was documented in only four studies, with a variable frequency of 9% to 35%. This heterogeneity likely reflects differences in the referral profile and specialization of the services, as some centers are references for patients with pre-existing valvular disease or those who have undergone cardiac surgery.

Regarding the most frequently affected valve, data varies between the aortic (20-54%) and mitral (26-52%) valves. Globally, these are the most commonly affected valves, with discrepancies among studies as to which is predominant.[26,29-31] Tricuspid valve endocarditis appears in third place in frequency, and its involvement is considered a factor related to socioeconomic vulnerability, also due to its correlation with intravenous drug use.[32]

Population-based studies indicate that rheumatic heart disease has shown a reduction in its incidence in Brazil in recent decades, although with a trend towards stabilization of its prevalence. This contrasts with the increase in prevalence estimates and crude mortality for non-rheumatic valvular heart diseases, especially in older ages, driven by degenerative conditions.[33]

Microbiological Profile

Most Frequently Involved Microorganisms

The microbiological analysis of Brazilian cohorts reveals a disparity in the predominance between staphylococcal (10% to 37%) and streptococcal (14.7% to 38%) infections, as described in Table 2. One center reported an atypical prevalence of 78% for *Staphylococcus* sp., constituting an outlier value, possibly related to specific characteristics of the served population or methodological particularities.

More recent case series show a preponderance of *S. aureus* infections globally,[5,6,26,34-36] and some temporal series indicate that staphylococcal infections have been increasing in recent decades,[5] with additional concern for the rise in infections caused by methicillin-resistant *Staphylococcus aureus*.[37]

In third place are infections by *Enterococcus* sp., a pathogen typically associated with infections in older individuals with comorbidities and linked to worse clinical outcomes.[1,5] A Brazilian study that specifically evaluated the elderly population identified enterococci as the most frequently isolated pathogens.[38]

Culture-Negative Endocarditis

A particularly relevant finding is the high proportion of negative blood cultures, which ranged from 14% to 36% across different centers. The absence of microbial growth in blood cultures primarily reflects the prior use of antimicrobials and infections caused by fastidious microorganisms or those that do not grow in conventional culture media.[39] Its occurrence is related to therapeutic challenges and worse clinical outcomes.[40]

The rates of negative blood cultures in IE vary widely worldwide, from 7.5% to 50% of cases,[7,28] reflecting population heterogeneity and disparities in access to healthcare services across regions.

In addition to optimizing the diagnostic workup by encouraging blood culture collection *prior* to antimicrobial administration, the investigation of fastidious pathogens such as *Bartonella* sp., *Coxiella burnetii*, and *Brucella* sp. is essential. National publications have previously discussed these infections individually.[40,41]

Although there are no systematic Brazilian studies documenting these disparities at a national level, clinical experience, combined with the wide variation observed in the published data, indicates that this is a relevant challenge in clinical practice.

Imaging Exams: Access and Application in the National Scenario

Imaging evaluation plays a central role in the diagnosis and management of IE. International guidelines systematically recommend performing a transthoracic echocardiogram (TTE) in all patients with suspected endocarditis, followed by a transesophageal echocardiogram (TEE) when the TTE is inconclusive, in patients with prosthetic valves or intracardiac devices, and whenever the clinical probability of the disease remains high.[1]

In the Brazilian cohorts analyzed in this article, the use of TEE is frequent but not uniform, ranging from 78% to 100%. On the other hand, in some large cohorts, the use of TEE was not reported or could not be quantified in a standardized manner, suggesting heterogeneity both in practice and in the systematic recording of exams.

This scenario is compatible with the perception that, in large tertiary services, access to echocardiography – including TEE – is usually broad and relatively agile, allowing for integrated diagnostic confirmation, risk stratification, and surgical planning. In contrast, in smaller hospitals and regions with a lower density of specialists, the evaluation is often likely restricted to TTE, with greater difficulty in documenting small vegetations, abscesses, and prosthetic dehiscence, although there is a lack of published systematic data quantifying these disparities.

Additional modalities, such as cardiac computed tomography (CT) and 18F-FDG PET-CT, are being incorporated as complementary tools for detecting perivalvular complications, assessing prosthetic endocarditis, and investigating extracardiac embolic foci.[42,43]

In Brazil, despite the wide availability of cardiac CT in tertiary centers and the recognized utility of PET-CT in specific scenarios, these exams remain poorly incorporated into the routine care of IE. This limitation stems from structural, logistical, and professional training factors, directly impacting the early detection of perivalvular complications and diagnostic confirmation in prosthetic valves.

The Brazilian case series analyzed here do not describe, in a standardized way, the routine use of these imaging exams. Practical experience suggests that these exams remain concentrated in high-complexity centers and private services, with limited supply and unequal access in the public network.

This restriction may contribute to the underdiagnosis of structural complications, delays in surgical indication, and a reduced ability to identify distant embolic foci, especially in contexts where TEE is inconclusive or technically limited.

Cardiac CT is an additional tool for detecting perivalvular complications, including abscesses, pseudoaneurysms, fistulas, and valve dehiscence. According to the ESC 2023 guidelines,[1] its role is complementary to echocardiography, being particularly valuable when TEE is inconclusive or limited – whether due to prosthetic artifacts, unfavorable anatomy, or persistent clinical suspicion without definitive echocardiographic documentation.

CT is useful in both native and prosthetic valves, although its contribution is even greater in prostheses due to the acoustic limitations of TEE. Despite its wide availability and more accessible cost compared to PET-CT, the use of CT in the national context can still be expanded. Some factors that may influence its utilization include the clinical request in the initial management, the definition of institutional routines, and the refinement of specific imaging protocols for endocarditis. When not considered early, there is a possibility that significant structural complications are identified in more advanced stages of management, sometimes during the surgical procedure.

18F-FDG PET-CT, in contrast, plays a role in demonstrating active inflammation, with high accuracy in patients with prosthetic valves. According to the ESC 2023 guidelines,[1] it is considered a Class I recommendation for the assessment of prosthetic endocarditis more than three months after implantation, especially when clinical suspicion persists despite a negative or inconclusive TEE. In these scenarios, PET-CT provides significant diagnostic value, and contributes to the identification of distant embolic foci.

Its use, however, remains limited in Brazil due to cost, restricted availability in the public healthcare system, and the need for specialized training of nuclear medicine teams. Nevertheless, national data, including experience from a tertiary center, demonstrate relevant clinical impact in prosthetic valves and other complex scenarios.[43]

Thus, CT and PET-CT are complementary methods, each with strengths in different diagnostic dimensions:

- CT: is especially effective in identifying structural complications and is usually more accessible, although it depends on early request and radiological expertise.
- PET-CT: is extremely useful in cases involving prosthetic valves, especially when clinical suspicion persists. However, its use is limited by high cost and lower availability.

Expanding the appropriate use of these modalities requires institutional care pathways, training of imaging teams, and systematic integration of these exams into Endocarditis Team discussions, ensuring faster, more precise, and evidence-based decisions.

Complications and Outcomes

Heart Failure and Perivalvular Abscess

The Brazilian cohorts analyzed in this study demonstrate a high frequency of severe complications from IE. Decompensated heart failure was a common presentation, affecting 29.1% to 58% of patients in the centers that reported this data. The formation of perivalvular abscesses, a serious local complication, was documented in up to 30% of patients in one center, with other records indicating prevalences between 10% and 28%.

Parallel to international registries,[26,30] which report heart failure in 14.1% to 31.9% and embolic events/stroke in 17.5% to 20.6%, the Brazilian cohorts demonstrate a particularly severe disease burden. Embolic complications were also widely reported in the national cohorts, although heterogeneity in definitions prevents direct comparison with international rates. Finally, the formation of perivalvular abscesses showed similar rates, ranging from 13% to 16% in international registries.[26,30]

Surgical Intervention and In-Hospital mortality

The rate of surgical intervention for IE differed substantially among Brazilian centers (29% to 83.6%). This variation reflects potential differences in patient profiles and the surgical indications established by each service. In comparison, large international registries, such as EURO-ENDO and ICE, describe rates of surgical approach of 51% and 52%.[26,30]

In-hospital mortality in the analyzed Brazilian cohorts showed heterogeneity, with rates between 22.3% and 45.8%. This variability falls within the global spectrum reported in the literature, where mortality rates also fluctuate significantly: ranging from 14.9% to 25.1% in European and Latin American registries,[11,14,26,30] and reaching up to 37.1% in specific series.[25]

Multidisciplinary Approach: Endocarditis Teams

According to the most recent international guidelines (ESC 2023), the management of IE by specialized multidisciplinary teams – Endocarditis Teams – is a central recommendation and a standard of quality care.[1] These teams should preferably integrate cardiologists, cardiovascular surgeons, infectious disease specialists, imaging experts, microbiologists, and palliative care specialists.

Observational evidence suggests a positive association between the operation of Endocarditis Teams and improved clinical outcomes, including reduced short-term mortality.[44]

Beyond the core Endocarditis Team, responsible for coordinating and integrating care, more complex cases often require support from other medical specialties such as neurosurgery, vascular surgery, nephrology, and intensive care medicine, as well as the involvement of professionals from dentistry, psychology, physiotherapy, and social work.

The lack of a formal assessment of this implementation in Brazil constitutes a relevant research gap. Consequently, the creation, structuring, and consolidation of Endocarditis Teams, adapted to the reality of the Brazilian Unified Health System (SUS) and supplementary healthcare, emerge as a priority for improving the quality of IE care in the country.

Final Considerations, Limitations, and Future Perspectives

The analysis of evidence on IE in Brazil, although marked by fragmentation and methodological limitations, reveals a

complex scenario. The available findings indicate a distinctive epidemiological profile, characterized by younger patients than those described in international case series, but with a significant burden of comorbidities. Most cases were left-sided endocarditis, and a heterogeneous percentage of cases occurred in patients with cardiac prostheses.

The microbiological profile is diverse, with concerning rates of negative blood cultures, reflecting both regional particularities and opportunities for improvement in diagnostic workup. Similarly, the wide variation in surgical intervention rates and in-hospital mortality across different centers may indicate disparities in the structure and organization of care throughout the country.

These conclusions, however, must be interpreted considering some limitations. The use of secondary databases is subject to underreporting and coding errors, just as the modeled estimates from the GBD lack individual-level clinical validation. Furthermore, the predominance of publications originating from tertiary services in the Southeast and some state capitals results in the underrepresentation of other Brazilian regions, limiting the generalizability of the findings. Additionally, the heterogeneity in study objectives, definitions of events, complications, and surgical indications among services prevents more robust comparisons.

Given this scenario, several enhancement opportunities can be considered to strengthen the epidemiological understanding and care organization for IE in Brazil. These proposals should not be interpreted as prescriptive models, but as potential pathways, conditioned on technical feasibility and the country's regional differences.

Brazilian Registry of Infective Endocarditis: The creation of a collaborative, multicenter, and progressively expanded registry could reduce the current fragmentation of information and generate more representative data. Implementation would depend on coordination between centers, resource availability, and institutional interest.

Contextualized National Guidelines: The development of recommendations adapted to the epidemiological and structural realities of the diverse regions, including protocols for investigating negative cultures, could contribute to greater standardization of practices. Such an initiative requires broad technical consensus and participation from scientific societies.

Strengthening Multidisciplinary Teams: International experience suggests benefits from the operation of Endocarditis Teams. In the Brazilian context, models adapted to local conditions—not necessarily uniform—could improve integration between cardiology, surgery, infectious diseases, imaging, and palliative care.

Multidisciplinary and inter-institutional collaboration represents a promising path for advancing patient care. The formation of research networks, hospital consortia, and partnerships between academia and health services has the potential to accelerate the translation of knowledge into more effective care practices and, consequently, better clinical outcomes.

Author Contributions

Conception and design of the research, acquisition of data, analysis and interpretation of the data, statistical analysis, writing of the manuscript and critical revision of the manuscript for intellectual content: Santos DAM, Tarasoutchi F, Fernandes JRC, Paixão MR, Strabelli TMV, Köohler KF, Mansur AJ, Siciliano RF.

Potential Conflict of Interest

No potential conflict of interest relevant to this article was reported.

Sources of Funding

There were no external funding sources for this study.

Study Association

This study is not associated with any thesis or dissertation work.

Ethics Approval and Consent to Participate

This article does not contain any studies with human participants or animals performed by any of the authors.

Use of Artificial Intelligence

During the preparation of this work, the author(s) used Deep Seek to refine the academic language, ensure terminological precision in medical English, and enhance the overall clarity and coherence of the manuscript. After using this tool/service, the author(s) reviewed and edited the content as needed and take full responsibility for the content of the published article.

Availability of Research Data

All datasets supporting the results of this study are available upon request from the corresponding author.

References

1. Delgado V, Marsan NA, Waha S, Bonaros N, Brida M, Burri H, et al. 2023 ESC Guidelines for the Management of Endocarditis. Eur Heart J. 2023;44(39):3948-4042. doi: 10.1093/eurheartj/ehad193.
2. Li M, Kim JB, Sastry BKS, Chen M. Infective Endocarditis. Lancet. 2024;404(10450):377-92. doi: 10.1016/S0140-6736(24)01098-5.
3. Shah ASV, McAllister DA, Gallacher P, Astengo F, Rodríguez Pérez JA, Hall J, et al. Incidence, Microbiology, and Outcomes in Patients Hospitalized with Infective Endocarditis. Circulation. 2020;141(25):2067-77. doi: 10.1161/CIRCULATIONAHA.119.044913.
4. Zulet P, Olmos C, Fernández-Pérez C, Del Prado N, Rosillo N, Bernal JL, et al. Regional Differences in Infective Endocarditis Epidemiology

and Outcomes in Spain. A Contemporary Population-Based Study. Rev Esp Cardiol. 2024;77(9):737-46. doi: 10.1016/j.rec.2024.01.003.

5. Buergler H, Gregoriano C, Laager R, Mueller B, Schuetz P, Conen A, et al. Microbiological Trends, In-Hospital Outcomes, and Mortality in Infective Endocarditis: A Swiss Nationwide Cohort Study. Clin Infect Dis. 2025;80(4):784-94. doi: 10.1093/cid/ciae582.

6. Saricaoglu EM, Basaran S, Seyman D, Arslan M, Ozkan-Ozturk S, Tezer-Tekce Y, et al. Epidemiological, Clinical and Microbiological Aspects of Infective Endocarditis in Türkiye. Eur J Clin Microbiol Infect Dis. 2025;44(6):1325-33. doi: 10.1007/s10096-025-05095-8.

7. Noubiap JJ, Nkeck JR, Kwondom BS, Nyaga UF. Epidemiology of Infective Endocarditis in Africa: A Systematic Review and Meta-Analysis. Lancet Glob Health. 2022;10(1):e77-e86. doi: 10.1016/S2214-109X(21)00400-9.

8. Chen H, Zhan Y, Zhang K, Gao Y, Chen L, Zhan J, et al. The Global, Regional, and National Burden and Trends of Infective Endocarditis from 1990 to 2019: Results from the Global Burden of Disease Study 2019. Front Med. 2022;9:774224. doi: 10.3389/fmed.2022.774224.

9. Mutagaywa RK, Vroon JC, Fundikira L, Wind AM, Kunambi P, Manyahi J, et al. Infective Endocarditis in Developing Countries: An Update. Front Cardiovasc Med. 2022;9:1007118. doi: 10.3389/fcvm.2022.1007118.

10. Li HL, Tromp J, Teramoto K, Tse YK, Yu SY, Lam LY, et al. Temporal Trends and Patterns of Infective Endocarditis in a Chinese Population: A Territory-Wide Study in Hong Kong (2002-2019). Lancet Reg Health West Pac. 2022;22:100417. doi: 10.1016/j.lanwpc.2022.100417.

11. Becher PM, Goßling A, Fluschnik N, Schrage B, Seiffert M, Schofer N, et al. Temporal Trends in Incidence, Patient Characteristics, Microbiology and in-Hospital Mortality in Patients with Infective Endocarditis: A Contemporary Analysis of 86,469 Cases between 2007 and 2019. Clin Res Cardiol. 2024;113(2):205-15. doi: 10.1007/s00392-022-02100-4.

12. Wurcel AG, Anderson JE, Chui KK, Skinner S, Knox TA, Snydman DR, et al. Increasing Infectious Endocarditis Admissions among Young People who Inject Drugs. Open Forum Infect Dis. 2016;3(3):ofw157. doi: 10.1093/ofid/ofw157.

13. Sousa C, Nogueira P, Pinto FJ. Insight Into the Epidemiology of Infective Endocarditis in Portugal: A Contemporary Nationwide Study from 2010 to 2018. BMC Cardiovasc Disord. 2021;21(1):138. doi: 10.1186/s12872-021-01937-3.

14. Urina-Jassir M, Jaimes-Reyes MA, Martinez-Vernaza S, Quiroga-Vergara C, Urina-Triana M. Clinical, Microbiological, and Imaging Characteristics of Infective Endocarditis in Latin America: A Systematic Review. Int J Infect Dis. 2022;117:312-21. doi: 10.1016/j.ijid.2022.02.022.

15. Damasco PV, Solórzano VEF, Fortes NRQ, Setta DXB, Fonseca AGD, Perez MCA, et al. Trends of Infective Endocarditis at Two Teaching Hospitals: A 12-Year Retrospective Cohort Study in Rio de Janeiro, Brazil. Trop Med Infect Dis. 2023;8(12):516. doi: 10.3390/tropicalmed8120516.

16. Cordeiro JVFA, Raposo LM, Godoy PH. Mortality Profile of Deaths Related to Infective Endocarditis in Brazil and Regions: A Population-Based Analysis of Death Records. Trop Med Infect Dis. 2024;9(12):291. doi: 10.3390/tropicalmed9120291.

17. Melo SN, Torres BRS, Nascimento MMG, Xavier AFS Jr, Rodrigues WG, Lima RBS, et al. Caracterização do Perfil Epidemiológico da Mortalidade por Endocardite Infecciosa na Região Nordeste de 2010-2019. Rev Eletrônica Acervo Saúde. 2021;13(9):e8828. doi: 10.25248/reas.e8828.2021.

18. Li JS, Sexton DJ, Mick N, Nettles R, Fowler VG Jr, Ryan T, et al. Proposed Modifications to the Duke Criteria for the Diagnosis of Infective Endocarditis. Clin Infect Dis. 2000;30(4):633-8. doi: 10.1086/313753.

19. Fowler VG, Durack DT, Selton-Suty C, Athan E, Bayer AS, Chamis AL, et al. The 2023 Duke-International Society for Cardiovascular Infectious Diseases Criteria for Infective Endocarditis: Updating the Modified Duke Criteria. Clin Infect Dis. 2023;77(4):518-26. doi: 10.1093/cid/ciad271.

20. Jensen AD, Bundgaard H, Butt JH, Bruun NE, Voldstedlund M, Torp-Pedersen C, et al. Temporal Changes in the Incidence of Infective Endocarditis in Denmark 1997-2017: A Nationwide Study. Int J Cardiol. 2021;326:145-52. doi: 10.1016/j.ijcard.2020.10.029.

21. DeSimone DC, Lahr BD, Anavekar NS, Sohail MR, Tleyjeh IM, Wilson WR, et al. Temporal Trends of Infective Endocarditis in Olmsted County, Minnesota, between 1970 and 2018: A Population-Based Analysis. Open Forum Infect Dis. 2021;8(3):ofab038. doi: 10.1093/ofid/ofab038.

22. Miguel-Yanes JM, Jimenez-Garcia R, Miguel-Diez J, Hernández-Barrera V, Carabantes-Alarcon D, Zamorano-Leon JJ, et al. Differences in Sex and the Incidence and in-Hospital Mortality among People Admitted for Infective Endocarditis in Spain, 2016-2020. J Clin Med. 2022;11(22):6847. doi: 10.3390/jcm11226847.

23. Grillo S, Isler B, Bonet-Basiero A, Roselló-Díez E, Escolà-Vergé L; Study Group for Bloodstream Infections, Endocarditis, and Sepsis (ESGBIES). Does Biological Sex Determine the Natural History and Management of Infective Endocarditis? Can J Cardiol. 2025:S0828-282X(25)01300-5. doi: 10.1016/j.cjca.2025.10.041.

24. Barca LV, López-Menéndez J, Elorza EN, Mur JLM, Hernéndez TC, Palacios AR, et al. Long-Term Prognosis after Surgery for Infective Endocarditis: Distinction between Predictors of Early and Late Survival. Enferm Infecc Microbiol Clin. 2019;37(7):435-40. doi: 10.1016/j.eimc.2018.10.017.

25. van den Brink FS, Swaans MJ, Hoogendijk MG, Alipour A, Kelder JC, Jaarsma W, et al. Increased Incidence of Infective Endocarditis after the 2009 European Society of Cardiology Guideline Update: A Nationwide Study in the Netherlands. Eur Heart J Qual Care Clin Outcomes. 2017;3(2):141-7. doi: 10.1093/ehjqcco/qcw039.

26. Habib G, Erba PA, Iung B, Donal E, Cosyns B, Laroche C, et al. Clinical Presentation, Aetiology and Outcome of Infective Endocarditis. Results of the ESC-EORP EURO-ENDO (European Infective Endocarditis) Registry: A Prospective Cohort Study. Eur Heart J. 2019;40(39):3222-32. doi: 10.1093/eurheartj/ehz620.

27. Baddour LM, Weimer MB, Wurcel AG, McElhinney DB, Marks LR, Fanucchi LC, et al. Management of Infective Endocarditis in People who Inject Drugs: A Scientific Statement from the American Heart Association. Circulation. 2022;146(14):e187-e201. doi: 10.1161/CIR.0000000000001090.

28. Jordal S, Kittang BR, Salminen PR, Eide GE, Kommedal Ø, Wendelbo Ø, et al. Infective Endocarditis in Western Norway: A 20-Year Retrospective Survey. Infect Dis. 2018;50(10):757-63. doi: 10.1080/23744235.2018.1482419.

29. Murdoch DR, Corey GR, Hoen B, Miró JM, Fowler VG Jr, Bayer AS, et al. Clinical Presentation, Etiology, and Outcome of Infective Endocarditis in the 21st Century: The International Collaboration on Endocarditis-Prospective Cohort Study. Arch Intern Med. 2009;169(5):463-73. doi: 10.1001/archinternmed.2008.603.

30. Ambrosioni J, Hernández-Meneses M, Durante-Mangoni E, Tattevin P, Olaison L, Freiberger T, et al. Epidemiological Changes and Improvement in Outcomes of Infective Endocarditis in Europe in the Twenty-First Century: An International Collaboration on Endocarditis (ICE) Prospective Cohort Study (2000-2012). Infect Dis Ther. 2023;12(4):1083-101. doi: 10.1007/s40121-023-00763-8.

31. Erdem H, Puca E, Ruch Y, Santos L, Ghanem-Zoubi N, Argemi X, et al. Portraying Infective Endocarditis: Results of Multinational ID-IRI Study. Eur J Clin Microbiol Infect Dis. 2019;38(9):1753-63. doi: 10.1007/s10096-019-03607-x.

32. Badiee B, Sakowitz S, Mallick S, Le N, Chaturvedi A, Tabibian K, et al. Association of Socioeconomic Disadvantage with Operative Outcomes for Infective Endocarditis. PLoS One. 2025;20(11):e0333221. doi: 10.1371/journal.pone.0333221.

33. Nascimento B, Sampaio RO, Caldeira Brant LC, Oliveira GMM, Teixeira RA, Malta DC, et al. Changes in the Pattern of Valvular Heart Disease Following the Epidemiological Transition in Brazil from 1990 to 2019: Data From the Global Burden of Disease 2019 study. Eur Heart J. 2021;42(Suppl 1):ehab724.1583. doi: 10.1093/eurheartj/ehab724.1583.

34. Dobreva-Yatseva B, Nikolov F, Raycheva R, Uchikov P, Tokmakova M. Trend in Infective Endocarditis in Bulgaria: Characteristics and Outcome, 17-Years, Single Center Experience. Microorganisms. 2024;12(8):1631. doi: 10.3390/microorganisms12081631.

35. Ruiz-Beltran AM, Barron-Magdaleno C, Ruiz-Beltran SM, Sánchez-Villa JD, Orihuela-Sandoval C, Oseguera-Moguel J, et al. Infective Endocarditis: 10-Year Experience in a Non-Cardiovascular Center. Arch Cardiol Mex. 2022;92(1):5-10. doi: 10.24875/ACM.20000467.

36. Giannitsioti E, Pefanis A, Gogos C, Lekkou A, Dalekos GN, Gatselis N, et al. Evolution of Epidemiological Characteristics of Infective Endocarditis in Greece. Int J Infect Dis. 2021;106:213-20. doi: 10.1016/j.ijid.2021.03.009.

37. Toyoda N, Chikwe J, Itagaki S, Gelijns AC, Adams DH, Egorova NN. Trends in Infective Endocarditis in California and New York State, 1998-2013. JAMA. 2017;317(16):1652-60. doi: 10.1001/jama.2017.4287.

38. Lemos LHB, Silva LRD, Correa MG, Golebiovski W, Weksler C, Garrido RQ, et al. Infective Endocarditis in the Elderly: Distinct Characteristics. Arq Bras Cardiol. 2021;117(4):775-81. doi: 10.36660/abc.20201134.

39. DeSimone DC, Garrigos ZE, Marx GE, Tattevin P, Hasse B, McCormick DW, et al. Blood Culture-Negative Endocarditis: A Scientific Statement from the American Heart Association: Endorsed by the International Society for Cardiovascular Infectious Diseases. J Am Heart Assoc. 2025;14(8):e040218. doi: 10.1161/JAHA.124.040218.

40. Lamas CC, Fournier PE, Zappa M, Brandão TJ, Januário-da-Silva CA, Correia MG, et al. Diagnosis of Blood Culture-Negative Endocarditis and Clinical Comparison between Blood Culture-Negative and Blood Culture-Positive Cases. Infection. 2016;44(4):459-66. doi: 10.1007/s15010-015-0863-x.

41. Siciliano RF, Castelli JB, Mansur AJ, Santos FP, Colombo S, Nascimento EM, et al. Bartonella spp. and Coxiella Burnetii Associated with Community-Acquired, Culture-Negative Endocarditis, Brazil. Emerg Infect Dis. 2015;21(8):1429-32. doi: 10.3201/eid2108.140343.

42. Sammartino AM, Bonfioli GB, Dondi F, Riccardi M, Bertagna F, Metra M, et al. Contemporary Role of Positron Emission Tomography (PET) in Endocarditis: A Narrative Review. J Clin Med. 2024;13(14):4124. doi: 10.3390/jcm13144124.

43. Camargo RA, Bitencourt MS, Meneghetti JC, Soares J, Gonçalves LFT, Buchpiguel CA, et al. The Role of 18F-Fluorodeoxyglucose Positron Emission Tomography/Computed Tomography in the Diagnosis of Left-Sided Endocarditis: Native vs Prosthetic Valves Endocarditis. Clin Infect Dis. 2020;70(4):583-94. doi: 10.1093/cid/ciz267.

44. Roy AS, Hagh-Doust H, Azim AA, Caceres J, Denholm JT, Dong MQD, et al. Multidisciplinary Teams for the Management of Infective Endocarditis: A Systematic Review and Meta-Analysis. Open Forum Infect Dis. 2023;10(9):ofad444. doi: 10.1093/ofid/ofad444.

45. Paixão MR, Besen BAMP, Felicio MF, Pocebon LZ, Furtado RHM, Silva PGMB, et al. Prediction of Hospital Mortality in Patients with Left-Sided Infective Endocarditis Using a Score in the First Hours of Admission. Sci Rep. 2025;15(1):28566. doi: 10.1038/s41598-025-13592-1.

46. Pinto PHOM, Fae IG, Oliveira GB, Duque RAS, Oliveira MVM, Barbalho LSM, et al. Impact of Neurological Complications on Long-Term Outcomes in Patients with Infective Endocarditis. Trop Med Infect Dis. 2024;9(6):132. doi: 10.3390/tropicalmed9060132.

47. Becker JB, Moisés VA, Guerra-Martín MD, Barbosa DA. Epidemiological Differences, Clinical Aspects, and Short-Term Prognosis of Patients with Healthcare-Associated and Community-Acquired Infective Endocarditis. Infect Prev Pract. 2024;6(1):100343. doi: 10.1016/j.infpip.2024.100343.

48. Carvalho MGB, Almeida TVPA, Feijóo NAP, Garrido RQ, Barbosa GLF, Golebiovski WF, et al. Contemporary Cohort Study in Adult Patients with Infective Endocarditis. Braz J Infect Dis. 2025;29(3):104521. doi: 10.1016/j.bjid.2025.104521.

49. Alves SG, Pivatto F Jr, Filippini FB, Dannenhauer GP, Seroiska G, Bischoff HM, et al. Performance of the SHARPEN Score and the Charlson Comorbidity Index for in-Hospital and Post-Discharge Mortality Prediction in Infective Endocarditis. Arq Bras Cardiol. 2024;120(12):e20230441. doi: 10.36660/abc.20230441.

50. Bezerra RL, Salgado LS, Silva YM, Figueiredo GGR, Bezerra RM Filho, Machado ELG, et al. Epidemiological Profile of Patients with Infective Endocarditis at Three Tertiary Centers in Brazil from 2003 to 2017. Int J Cardiovasc Sci. 2021;35(4):467-75. doi: 10.36660/ijcs.20210181.

My Approach to Wilkins-Block score in rheumatic mitral stenosis

Nayana Flamini Arantes Gomes,[1] *Fernanda de Azevedo Figueiredo,*[1,2] *Estela Fófano Rodrigues,*[1] *Carolina Kuchenbecker Soares,*[1] *Maria Carmo Pereira Nunes*[1]

Hospital das Clínicas da Universidade Federal de Minas Gerais,[1] *Belo Horizonte, MG – Brazil*

Universidade Federal de Lavras,[2] *Lavras, MG – Brazil*

Abstract

Mitral stenosis (MS) is the main clinical expression of chronic rheumatic heart disease. In symptomatic patients with severe MS and favorable anatomy, percutaneous mitral balloon valvuloplasty (PMBV) is the first-line therapeutic strategy. For the proper selection of candidates, the Wilkins-Block echocardiographic score was developed to characterize mitral valve morphology and predict eligibility for the procedure. This score includes four structural domains: leaflet mobility, valve thickening, degree of calcification, and subvalvular apparatus involvement, grading each parameter from 1 to 4 points, resulting in an overall range of 4 to 16 points, in increasing order of anatomical severity. The Wilkins score has become a widely validated tool, showing a consistent correlation with the immediate and long-term outcomes of PMBV.

Among the limitations of the score, the absence of commissural anatomy assessment stands out, a variable recognized as a relevant prognostic determinant due to its strong association with the occurrence of post-procedure mitral regurgitation, considered the most frequent and clinically significant complication of PMBV. With the accumulation of clinical and technical experience, the indications for PMBV have been progressively extended to include patients with less favorable anatomical profiles. In these contexts, selection must be particularly rigorous, incorporating not only morphological criteria derived from echocardiographic evaluation, but also clinical aspects, in order to ensure satisfactory results and minimize the risk of complications.

Introduction

Rheumatic fever is a disease resulting from pharyngotonsillitis caused by the bacterium *Streptococcus pyogenes* in susceptible individuals[1]. Chronic rheumatic heart disease (CRHD) is the most important consequence of rheumatic fever and constitutes a significant public health problem, especially in low- and middle-income countries, where it continues to be associated with high morbidity and mortality.[1,2] The mitral valve (MV) is the most frequently affected in CRHD, with mitral stenosis (MS) being its main chronic manifestation.

Pathophysiology of mitral stenosis

Rheumatic mitral stenosis (RMS) results from thickening and calcification of the cusps, shortening of the chordae tendineae, and commissural fusion, progressively reducing the valve area. The consequent atrioventricular diastolic gradient leads to pulmonary venocapillary congestion, pulmonary hypertension, and right ventricular dysfunction.[3] Left atrial pressure overload promotes structural remodeling, predisposing to arrhythmias, especially atrial fibrillation (AF), which precipitates symptoms and increases the risk of thromboembolic events. It is estimated that 80% of strokes in patients with rheumatic stenosis occur in the MS-AF association, with a substantial impact on quality of life.[2,4]

Echocardiography in the evaluation of the mitral valve

The MV is a complex anatomical structure that includes the fibromuscular ring, two cusps (anterior and posterior), chordae tendineae, and papillary muscles, and has a close structural relationship with the underlying ventricular myocardium.[5] The anterior cusp is longer and semicircular, while the posterior cusp is shorter and segmented; the posterior cusp is subdivided into three segments (P1-lateral, P2-central, P3-medial), corresponding to A1, A2, and A3 of the anterior cusp.[5]

Echocardiographic evaluation of the mitral valve requires a multimodal approach, in which two-dimensional transthoracic echocardiography (2D TTE) represents the initial and fundamental method for morphological and functional analysis of the valve. This modality enables an accurate analysis of the thickness and mobility of the cusps, the presence and extent of calcifications, and the integrity and impairment of the subvalvular apparatus.[6] Doppler ultrasound allows for the quantification of the severity of mitral valve lesions by measuring transvalvular gradients, effective orifice areas in cases of stenosis, and regurgitation parameters, such as volume and regurgitant fraction. Color Doppler analysis complements this assessment, allowing for the visualization of the regurgitant jet, estimation of the vena contracta, and application of the Proximal Isovelocity Surface Area (PISA) technique for a more accurate quantification of mitral regurgitation.[6] The Transesophageal echocardiography (TEE) is recommended when greater anatomical detail is needed, particularly in the characterization of mitral regurgitation mechanisms, the evaluation of infective endocarditis, and the planning of percutaneous or surgical therapies.[5] Three-dimensional (3D) echocardiography, especially via TEE, improves the spatial analysis of the valve, enabling multiplanar reconstructions with

Keywords

Mitral Valve Stenosis; Echocardiography; Rheumatic Heart Disease

Mailing Address: Maria Carmo Pereira Nunes •
Faculdade de Medicina, Departamento de Clinica Médica, Universidade Federal de Minas Gerais. Professor Alfredo Balena, 190. Postal code: 30130-100. Belo Horizonte, MG – Brazil
E-mail: mcarmo@waymail.com.br
Manuscript received October 29, 2025; revised October 29, 2025; accepted November 17, 2025
Editor responsible for the review: Marcelo Tavares

DOI: https://doi.org/10.36660/abcimg.20250083i

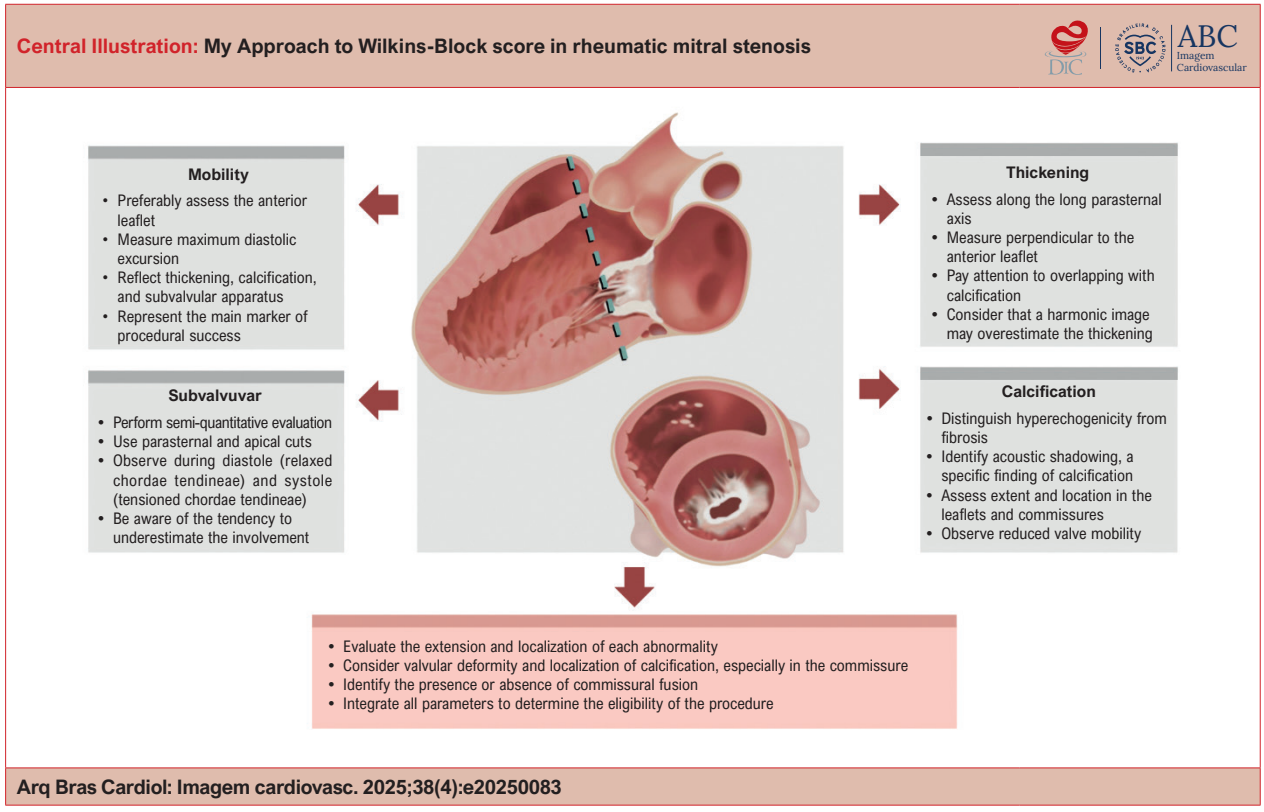

Practical recommendations for echocardiographic evaluation of rheumatic mitral stenosis (RMS) in the selection of candidates for percutaneous mitral balloon valvuloplasty (PMBV).

direct anatomical correlation, a more precise measurement of the valve area, a dynamic evaluation of the annulus, and the segmental characterization of the cusps.[6]

Percutaneous mitral balloon valvuloplasty

The PMBV. introduced in 1984 by Inoue et al., is the treatment of choice for severe mitral stenosis with favorable anatomy.[7] It is an invasive procedure, with efficacy comparable to surgical commissurotomy.[8] Balloon inflation promotes mitral valve opening, primarily through commissural separation of fibrotic adhesions.[9] When inflated inside the valve orifice, the balloon generates radial forces that concentrate in the commissural regions, promoting tension redistribution and favoring symmetrical orifice opening.[9]

Prior echocardiographic evaluation is mandatory to determine if the MV anatomy is adequate for commissural opening and if it will allow for an increased valve area without inducing significant mitral regurgitation. Several scores have been developed for this purpose.[10] Obtaining good results depends particularly on the appropriate selection of patients. Several outcome predictors have been described, including age, functional class, previous commissurotomy, valve area, valve anatomy, and balloon size. Among these, mitral valve morphology is the single most determinant factor, reinforcing the need for the systematic use of echocardiographic scores. Unfavorable results are frequently related to adverse morphological changes, especially cusp calcification and subvalvular involvement.[11] To estimate the probability of successful dilation, the Wilkins-Block score was developed, based on the 2D assessment of valve morphology.

Wilkins-Block Score

Wilkins et al., in 1988,[12] proposed an echocardiographic score for the structural evaluation of RMS, which demonstrated a significant correlation with valve opening capacity after percutaneous valvuloplasty. In the original score, success was defined dichotomously by obtaining a mitral valve area > 1.0 cm^2, without considering the development of mitral regurgitation. This score is obtained through a systematic and relatively simple analysis of valve morphology as viewed through a TTE, using the conventional cuts employed in the evaluation of the mitral valve. In certain situations, modified cuts may be necessary for better anatomical characterization, especially of the subvalvular apparatus (Central Figure).

The evaluation of each parameter is performed subjectively through a semi-quantitative score that covers leaflet mobility, valve thickening, degree of calcification, and involvement of the subvalvular apparatus. Each item receives a score from 1 to 4 points, resulting in a total score ranging from 4 to 16 points, in ascending order of structural severity. In general, patients with a score ≤ 8 have favorable anatomy and are the best candidates for PMBV, with high rates of immediate success and maintenance of long-term results.[13] Patients with intermediate scores, between 9 and 11, may still be considered

for the procedure, especially when a detailed evaluation of the commissures suggests a favorable morphology. Scores ≥ 12 reflect extensively affected and calcified valves, in which the probability of significant hemodynamic gain is reduced and the chance of complications increases, making surgical valve replacement more appropriate.

Leaflet mobility is graded according to the degree of restriction of the anterior leaflet during the diastole (Figure 1A). Increased restriction corresponds to progressively higher scores. Thus, when the limitation is restricted to the ends of the leaflets, 1 point is assigned. In cases where mobility is preserved in the medial and basal regions, the value is 2 points. Restriction of mobility limited only to the basal region corresponds to 3 points. Finally, complete immobility of the leaflets is scored with 4 points. Table 1 presents a practical checklist for the systematic application of the Wilkins score.

Subvalvular involvement refers to the involvement of the chordae tendineae and papillary muscles (Figure 1B). One point is assigned when the thickening is minimal and restricted to the region immediately below the leaflets. Thickening that extends beyond this level, but that is limited to the proximal third of the chordae tendineae, corresponds to 2 points. When there is involvement that reaches the distal third of the chordae tendineae, 3 points are assigned. Finally, diffuse thickening associated with the shortening of all chordae tendineae, extending to the level of the papillary muscles, receives 4 points.

The thickness of the leaflets is measured in the parasternal section at maximum diastole (Figure 1C). Leaflets with thickness close to normal (≈4–5 mm) receive 1 point. Thickening restricted to the extremities, preserving the middle region, with measurements between 5–8 mm, corresponds to 2 points. Diffuse thickening involving all portions of the leaflet, still within the range of 5–8 mm, receives 3 points. When there is significant thickening of the entire leaflet, with measurements greater than 8–10 mm, 4 points are assigned.

Valvular calcification is determined by the presence and extent of hyperechogenic areas (Figure 1D). The isolated presence of a small area receives 1 point. Minimal areas confined to the extremities correspond to 2 points. When calcification extends to the middle region of the leaflets, 3 points are assigned. Diffuse calcification, extending beyond the limits of the leaflets, is scored with 4 points.

Although each component of the score is evaluated individually, the parameter that best reflects the overall morphology of the valve is the sum of the scores assigned to each item, translating the degree of structural involvement. Leaflet mobility, in turn, constitutes an integrating parameter, as it reflects the combined impact of thickening, calcification, and subvalvular involvement, all contributing to the restriction of valve movement. Figure 2 illustrates a case of mitral stenosis with thin leaflets, restriction limited to the extremities, absence of calcification, and no evidence of subvalvular involvement. By contrast, Figure 3 demonstrates calcification affecting the medial and distal portions of the leaflets, with a preservation of the basal region and no involvement of the commissures, which would not contraindicate the percutaneous procedure.

Experience accumulated over the years

Since its introduction, the Wilkins score continues to be the most widely used tool for selecting suitable candidates for PMBV, due to its simplicity and practicality.[14] The main valvular heart disease guidelines of the AHA/ACC and ESC[7,15] use the Wilkins score as an eligibility criterion for patients with rheumatic MS for the percutaneous procedure.

In addition to its usefulness in morphological characterization, the Wilkins score is an important predictor of long-term outcomes after PMBV.[16] However, this score does not include the assessment of commissural anatomy, currently recognized as a relevant prognostic determinant due to its association with the development of post-procedure mitral regurgitation (MR).[17] Figure 4 illustrates the wide spectrum of commissural involvement patterns in RMS. In patients with marked commissural asymmetry, balloon inflation tends to exert disproportionate force on the contralateral commissure, predisposing to the onset of MR. Similarly, when there is significant commissural calcification, the balloon's inability to adequately separate the commissures results in excessive force transmission to the valve tissue, favoring rupture or laceration of the leaflets.[18,19]

With the advancement of experience, the indications for PMBV have been progressively expanded to include less favorable conditions, demonstrating that it is a safe and effective procedure in certain patients with an intermediate Wilkins score.[16] The selection of these cases, however, must be judicious and individualized, considering not only echocardiographic parameters, but also clinical and hemodynamic aspects, such as age, history of previous commissurotomy, NYHA functional class, presence of atrial fibrillation and pulmonary hypertension.[14] Among the echocardiographic criteria, intense calcification of the leaflets, severe or asymmetric commissural calcification or fusion, and the presence of extensive subvalvular disease stand out as major risk factors for complications.[20]

Limitations of the Wilkins-Block score

Despite its widespread use in clinical practice, the Wilkins score has important limitations. The analysis of the components is semi-quantitative and subject to interobserver variability, in addition to assigning identical weight to variables that have different predictive capacities for the post-PMBV outcome. The score also does not assess commissural anatomy, a fundamental aspect in predicting post-PMBV MR, and frequently underestimates subvalvular involvement. Added to this are the difficulty in distinguishing nodular fibrosis from calcification, the disregard for the heterogeneous distribution of lesions, and the lack of integration of information provided by transesophageal or 3D echocardiography.[10,11,17]

In view of these limitations, new models, such as the Nunes score,[17] have been proposed. Unlike the Wilkins score, the Nunes score assigns different weights to variables, incorporates commissural parameters, and allows one to predict the risk of post-procedure MR, in addition to identifying good candidates for PMBV even among patients with borderline Wilkins scores (9 to 11 points), traditionally considered to be at a higher risk.[17] Table 2 presents the main studies that described new

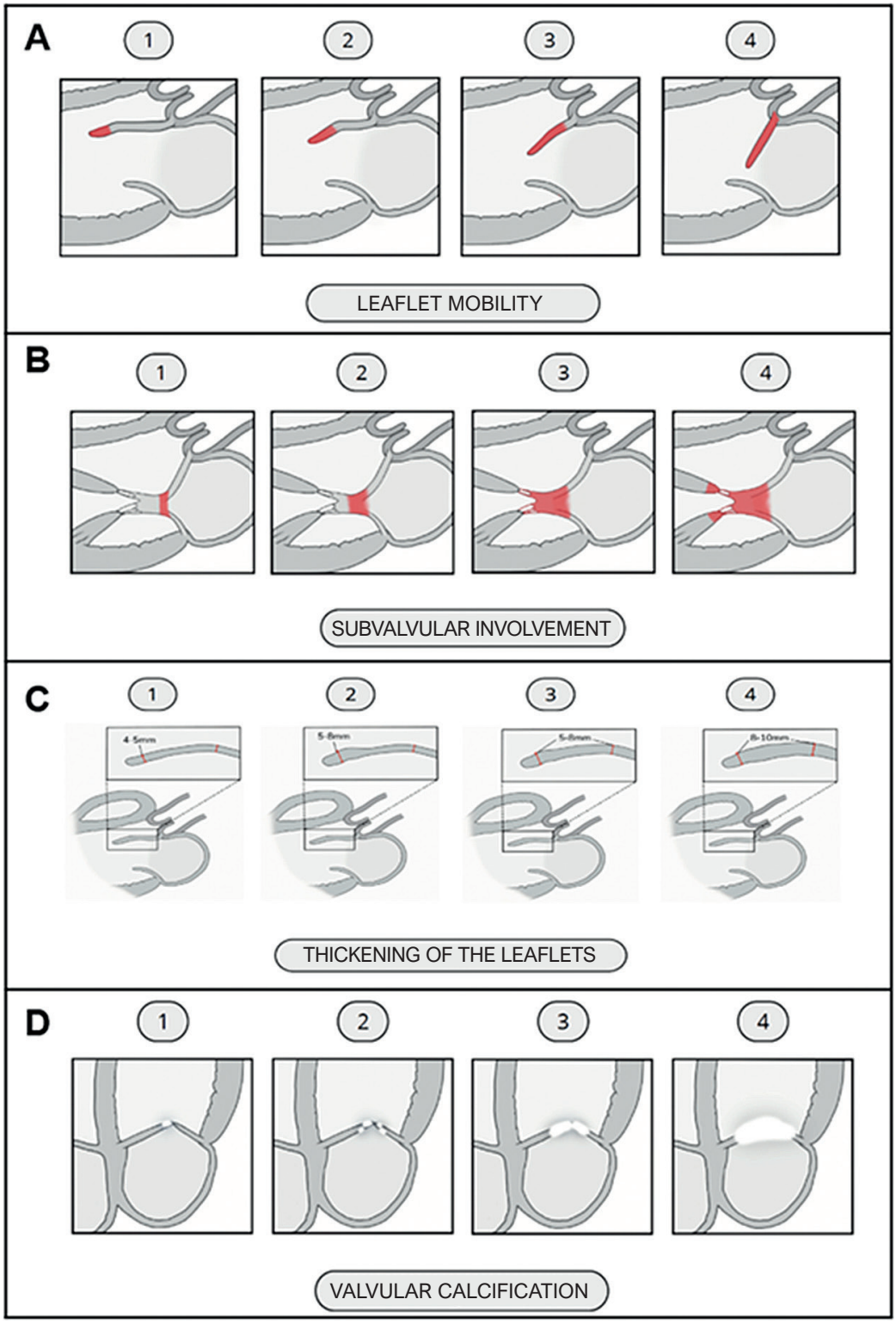

Figure 1 – *Schematic representation of the Wilkins score. A: Leaflet mobility (red marking indicates progression of reduced mobility). B: Subvalvular involvement (red marking indicates progression of thickening and shortening of the chordae tendineae). C: Anterior leaflet thickening (the detailed image shows the values that determine each score). D: Valvular calcification (white dots progress in quantity and extent across the leaflets).*

Table 1 – Wilkins Score – Practical Checklist

Parameters		Score			
		1	2	3	4
Leaflets	Mobility	Restriction only at the edges. Thin, almost normal leaflets.	Restriction of distal third	Restriction of more than half of the leaflet	Minimal or no mobility
	Thickening	Restriction only at the edges. Thin, almost normal leaflets.	Thickening restricted to the extremity	Thickening involving the extremity and medial third	Diffuse thickening
	Calcification	Absent	Points at the extremity	Extensive at the extremity and medial	Diffuse and extensive in both
Subvalular		No significant changes	Thickening near the leaflets	Thickening reaching the middle region of the strands	Thickening up to the distal third or extensive fusion

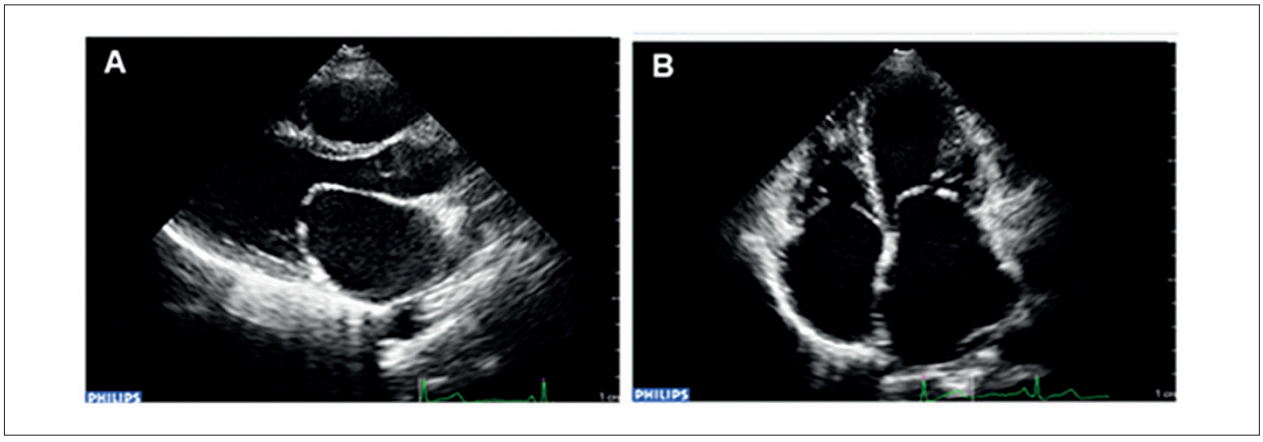

Figure 2 – *Rheumatic mitral stenosis (RMS) with favorable anatomy. 2D transthoracic echocardiogram (TTE): parasternal long-axis view (A) and apical four-chamber view (B), showing mitral valve with thin, mobile leaflets without calcification, consistent with anatomy favorable to PMBV.*

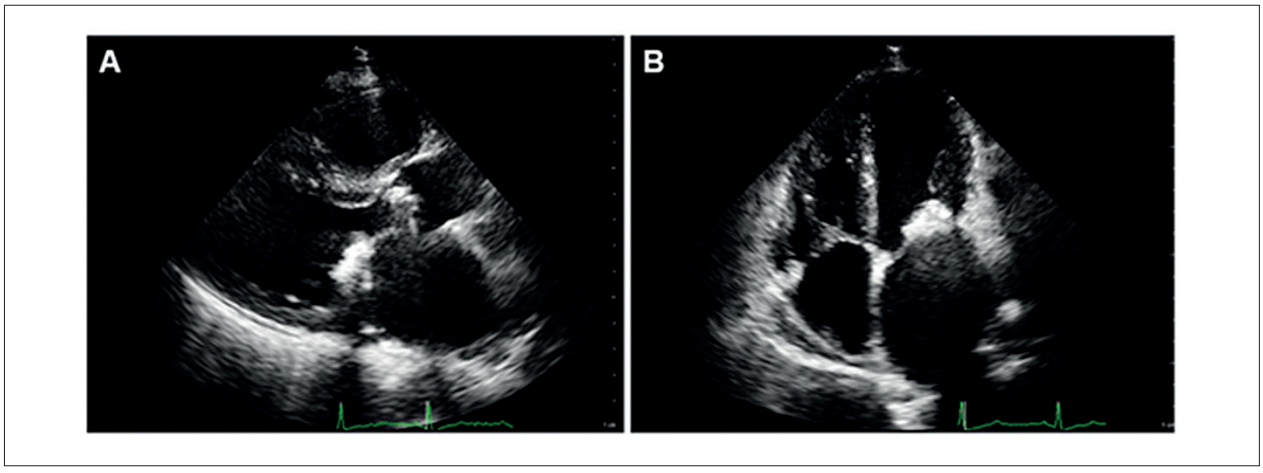

Figure 3 – *Valvular calcification. Echocardiographic images show the calcification of the mitral valve leaflets, affecting their medial and distal portions, with preservation of the base, demonstrated in the parasternal long-axis view (A) and in the apical four-chamber view (B). It is important to note that, in this case, the calcification is restricted to the leaflets, without commissure involvement, which does not constitute a contraindication to PMBV.*

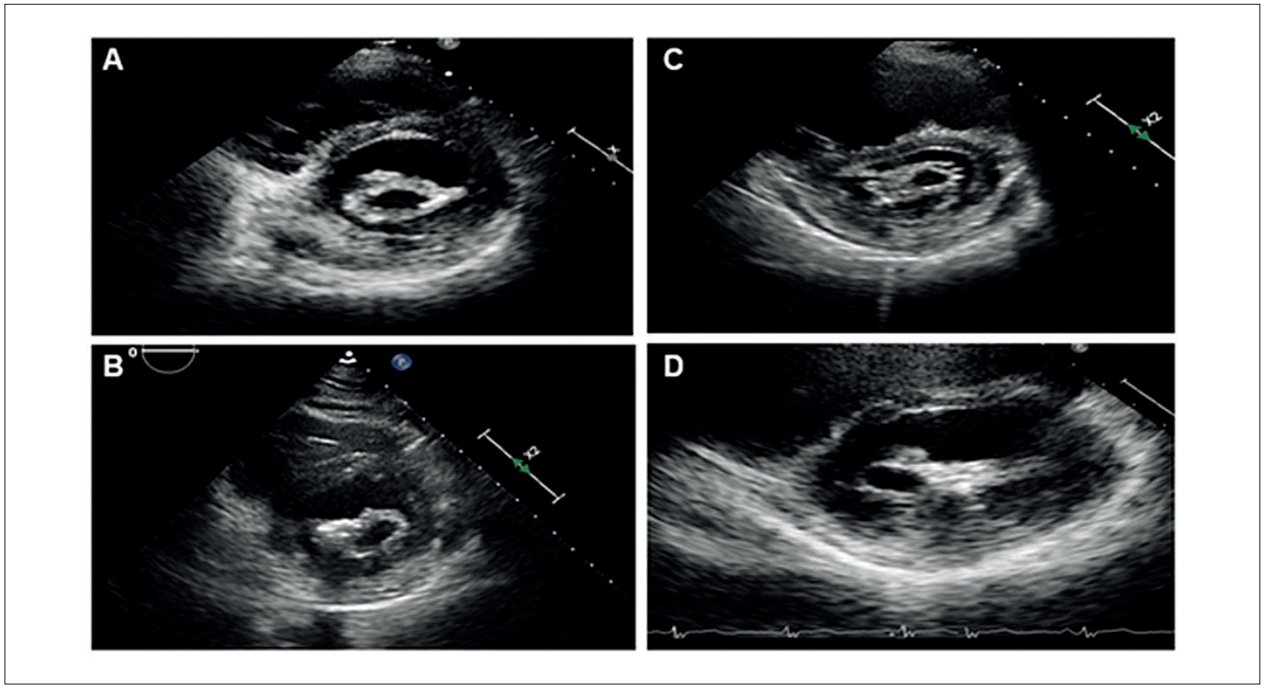

Figure 4 – *Patterns of commissural involvement (parasternal short axis view). A: symmetrical commissural involvement. B/C: commissural asymmetry with predominance of thickening and calcification of the posteromedial commissure. D: large valvular deformity and commissural asymmetry with predominance of thickening and calcification of the anterolateral commissure.*

models for evaluating MV morphology, when compared to the Wilkins score. With the evolution of PMBV, several studies have also identified additional valve morphology variables associated with post-PMBV outcomes, highlighting the inherent limitations of the Wilkins score.

Conclusions and future perspectives

The Wilkins score has become an international benchmark for selecting patients for PMBV, due to its simplicity and broad clinical applicability. However, the evidence accumulated over the last few decades demonstrates that its limitations reduce the ability to predict post-procedure outcomes in certain scenarios, especially due to the lack of assessment of commissural anatomy and the uniform weighting assigned to variables with unequal prognostic impact. Other scores, including the Nunes score, emerge as promising alternatives, incorporating additional parameters and a greater ability to discriminate outcomes, especially in the subgroup of patients with intermediate Wilkins scores. These advances contribute to reducing complications, such as post-procedure mitral regurgitation, and increasing the safety of PMBV recommendations within more heterogeneous populations.

In the future, the integration of new imaging technologies, including 3D echocardiography, TEE, and quantitative morphological analysis techniques, should further refine the structural assessment of the MV. Furthermore, algorithms based on artificial intelligence and machine learning can offer more robust predictive models, capable of accurately combining anatomical, clinical, and hemodynamic parameters. Such strategies would not only be able to improve the selection of candidates for PMBV, but they could also guide therapeutic decisions in cases of unfavorable anatomy, expanding the role of echocardiography in the contemporary management of RMS.

Author Contributions

PConception and design of the research: Gomes NFA, Nunes MCP; Writing of the manuscript and critical revision of the manuscript for intellectual content: Gomes NFA, Figueiredo FA, Rodrigues EF, Soares CK, Nunes MCP.

Potential conflict of interest

No potential conflict of interest relevant to this article was reported.

Sources of funding

Maria Carmo Pereira Nunes receives a research grant from CNPq, in the PQ-1A category.

Study association

The authors of this article are affiliated with the Postgraduate Program in Health Sciences: Infectious Diseases and Tropical Medicine at UFMG.

Ethics approval and consent to participate

This article does not contain any studies with human participants or animals performed by any of the authors.

Table 2 – Data from the main articles that described new models for evaluating rheumatic mitral valve, as compared to the Wilkins score for selecting patients eligible for PMBV

Authors	Year	Patients (n)	Evaluated variables	Comparison with Wilkins Score	Conclusion
Cannan *et al.*[21]	1997	149	Commissural calcification.	Best predictor of intermediate-term outcomes.	The presence of commissural calcification is a predictor of outcome after PMBV*.
Padial *et al.*[22]	1999	117	Thickness and calcification of the leaflets, degree and symmetry of commissural involvement, severity of subvalvular involvement.	Identifies patients at a higher risk of developing MI† post-VMP.	Predictor of MR development post-PMBV.
Palacios *et al.*[23]	2002	879	Mitral valve area, history of previous commissurotomy, MR.	Identifies patients more favorable to PMBV among patients with a low or intermediate Wilkins score.	Clinical and morphological predictors associated with the Wilkins score identify patients most favorable to PMBV.
Cruz-Gonzales *et al.*[24]	2009	1085	Age < 55 years, NYHA‡ I or II, AVM§ pre-PMBV < 1.0cm^2, MR pre-PMBV ≤2\, Wilkins score ≤8, Male sex.	Greater sensitivity and specificity.	Clinical, anatomical, and hemodynamic variables predict the success of PMBV and clinical outcomes.
Rifaie *et al.*[25]	2009	50	Calcification (mainly commissural) and subvalvular involvement.	Greater sensitivity, specificity, and positive and negative predictive values.	Best predictor of MR post-PMBV.
Anwar *et al.*[26]	2010	91	Thickness, mobility, calcification and subvalvular apparatus through 3D TTE//	Improved the morphological assessment of the mitral valve, particularly for the detection of calcification and commissural anatomy.	Adds prognostic information to the Wilkins score.
Babu *et al.*[27]	2013	100	Commissural morphology through TEE¶.	Predictor of good outcomes in patients with a Wilkins score > 8.	Should be evaluated together with the Wilkins score to adequately select patients for PMBV.
Nunes *et al.*[17]	2014	325	AVM ≤1cm2, maximum leaflet displacement ≤12mm, commissural area ratio ≥1.25, subvalvular involvement.	Improved risk classification.	Quantitative echocardiographic parameters with greater accuracy in predicting outcomes after PMBV.

** percutaneous mitral balloon valvuloplasty; † mitral regurgitation; ‡ New York Heart Association functional class; § mitral valve area; // 3D transthoracic echocardiogram (TTE); ¶ transesophageal echocardiogram (TEE).*

Use of Artificial Intelligence

During the preparation of this work, the author(s) used Chat GPT 5.2 for grammatical correction of the manuscript. After using this tool, the author(s) reviewed and edited the content as needed and take full responsibility for the content of the published article.

Data Availability Statement

The underlying content of the research text is contained within the manuscript.

References

1. Cunningham MW, Kirvan CA. Post-Streptococcal Autoimmune Sequelae, Rheumatic Fever and Beyond: A New Perspective. In: Ferretti JJ, Stevens DL, Fischetti VA, editors. Streptococcus pyogenes: Basic Biology to Clinical Manifestations. 2nd ed. Oklahoma City: University of Oklahoma Health Sciences Center; 2022.
2. Figueiredo FA, Esteves WAM, Hung J, Gomes NFA, Taconeli CA, Pantaleão AN, et al. Left Atrial Function in Patients with Rheumatic Mitral Stenosis: Addressing Prognostic Insights Beyond Atrial Fibrillation Prediction. Eur Heart J Imaging Methods Pract. 2024;2(2):qyae067. doi: 10.1093/ehjimp/qyae067.
3. Jain S, Mankad SV. Echocardiographic Assessment of Mitral Stenosis: Echocardiographic Features of Rheumatic Mitral Stenosis. Cardiol Clin. 2013;31(2):177-91. doi: 10.1016/j.ccl.2013.03.006.
4. Vasconcelos M, Vasconcelos L, Ribeiro V, Campos C, Di-Flora F, Abreu L, et al. Incidence and Predictors of Stroke in Patients with Rheumatic Heart Disease. Heart. 2021;107(9):748-54. doi: 10.1136/heartjnl-2020-318054.
5. Robinson S, Ring L, Augustine DX, Rekhraj S, Oxborough D, Harkness A, et al. The Assessment of Mitral Valve Disease: A Guideline from the British Society of Echocardiography. Echo Res Pract. 2021;8(1):G87-G136. doi: 10.1530/ERP-20-0034.
6. Nishimura RA, Otto CM, Bonow RO, Carabello BA, Erwin JP 3rd, Fleisher LA, et al. 2017 AHA/ACC Focused Update of the 2014 AHA/ACC Guideline for the Management of Patients with Valvular Heart Disease: A Report of the American College of Cardiology/American Heart Association Task Force on Clinical Practice Guidelines. Circulation. 2017;135(25):e1159-95. doi: 10.1161/CIR.0000000000000503.
7. Otto CM, Nishimura RA, Bonow RO, Carabello BA, Erwin JP 3rd, Gentile F, et al. 2020 ACC/AHA Guideline for the Management of Patients with Valvular Heart Disease: Executive Summary: A Report of the American College of Cardiology/American Heart Association Joint Committee on Clinical Practice Guidelines. J Am Coll Cardiol. 2021;77(4):450-500. doi: 10.1016/j.jacc.2020.11.035.
8. Turi ZG, Reyes VP, Raju BS, Raju AR, Kumar DN, Rajagopal P, et al. Percutaneous Balloon versus Surgical Closed Commissurotomy for Mitral Stenosis. A Prospective, Randomized Trial. Circulation. 1991;83(4):1179-85. doi: 10.1161/01.cir.83.4.1179.
9. Palacios I, Block PC, Brandi S, Blanco P, Casal H, Pulido JI, et al. Percutaneous Balloon Valvotomy for Patients with Severe Mitral Stenosis. Circulation. 1987;75(4):778-84. doi: 10.1161/01.cir.75.4.778.
10. Silbiger JJ. Advances in Rheumatic Mitral Stenosis: Echocardiographic, Pathophysiologic, and Hemodynamic Considerations. J Am Soc Echocardiogr. 2021;34(7):709-722.e1. doi: 10.1016/j.echo.2021.02.015.
11. Soliman OI, Anwar AM, Metawei AK, McGhie JS, Geleijnse ML, Ten Cate FJ. New Scores for the Assessment of Mitral Stenosis Using Real-Time Three-Dimensional Echocardiography. Curr Cardiovasc Imaging Rep. 2011;4(5):370-7. doi: 10.1007/s12410-011-9099-z.
12. Wilkins GT, Weyman AE, Abascal VM, Block PC, Palacios IF. Percutaneous Balloon Dilatation of the Mitral Valve: An Analysis of Echocardiographic Variables Related to Outcome and the Mechanism of Dilatation. Br Heart J. 1988;60(4):299-308. doi: 10.1136/hrt.60.4.299.
13. Palacios IF. Percutaneous Mitral Balloon Valvuloplasty - State of the Art. Mini-Invasive Surg. 2020;4:73. doi: 10.20517/2574-1225.2020.72.
14. Prota-Filho LEB, Meneguz-Moreno RA, Queiroz CCV, Wohnrath FC, Carboni FAC, Silva GRC, et al. Novel Prognostic Score for Immediate and Late Success after Percutaneous Mitral Balloon Commissurotomy in Patients with Mitral Stenosis. J Invasive Cardiol. 2020;32(6):211-7. doi: 10.25270/jic/19.00363.
15. Vahanian A, Beyersdorf F, Praz F, Milojevic M, Baldus S, Bauersachs J, et al. 2021 ESC/EACTS Guidelines for the Management of Valvular Heart Disease: Developed by the Task Force for the Management of Valvular Heart Disease of the European Society of Cardiology (ESC) and the European Association for Cardio-Thoracic Surgery (EACTS). Rev Esp Cardiol. 2022;75(6):524. doi: 10.1016/j.rec.2022.05.006.
16. Paiva M, Correia AS, Lopes R, Gonçalves A, Almeida R, Almeida PB, et al. Selection of Patients for Percutaneous Balloon Mitral Valvotomy: Is there a Definitive Limit for the Wilkins Score? Rev Port Cardiol. 2013;32(11):873-8. doi: 10.1016/j.repc.2013.02.017.
17. Nunes MC, Tan TC, Elmariah S, Lago R, Margey R, Cruz-Gonzalez I, et al. The Echo Score Revisited: Impact of Incorporating Commissural Morphology and Leaflet Displacement to the Prediction of Outcome for Patients Undergoing Percutaneous Mitral Valvuloplasty. Circulation. 2014;129(8):886-95. doi: 10.1161/CIRCULATIONAHA.113.001252.
18. Nunes MCP, Levine RA, Braulio R, Pascoal-Xavier MA, Elmariah S, Gomes NFA, et al. Mitral Regurgitation after Percutaneous Mitral Valvuloplasty: Insights into Mechanisms and Impact on Clinical Outcomes. JACC Cardiovasc Imaging. 2020;13(12):2513-26. doi: 10.1016/j.jcmg.2020.07.020.
19. Passos LSA, Becker-Greene D, Braulio R, Le TD, Gelape CL, Almeida LFR, et al. Proinflammatory Matrix Metalloproteinase-1 Associates with Mitral Valve Leaflet Disruption Following Percutaneous Mitral Valvuloplasty. Front Cardiovasc Med. 2022;8:804111. doi: 10.3389/fcvm.2021.804111.
20. Abdelghani M, Nunes MCP, Anwar AM, Prendergast B. Assessment of Suitability for Percutaneous Mitral Commissurotomy: A Contemporary Review of Key Anatomical Criteria and Predictive Models. Eur Heart J Cardiovasc Imaging. 2024;25(6):739-53. doi: 10.1093/ehjci/jeae052.
21. Cannan CR, Nishimura RA, Reeder GS, Ilstrup DR, Larson DR, Holmes DR, et al. Echocardiographic Assessment of Commissural Calcium: A Simple Predictor of Outcome after Percutaneous Mitral Balloon Valvotomy. J Am Coll Cardiol. 1997;29(1):175-80. doi: 10.1016/s0735-1097(96)00422-6.
22. Padial LR, Abascal VM, Moreno PR, Weyman AE, Levine RA, Palacios IF. Echocardiography can Predict the Development of Severe Mitral Regurgitation after Percutaneous Mitral Valvuloplasty by the Inoue Technique. Am J Cardiol. 1999;83(8):1210-3. doi: 10.1016/s0002-9149(99)00061-2.
23. Palacios IF, Sanchez PL, Harrell LC, Weyman AE, Block PC. Which Patients Benefit from Percutaneous Mitral Balloon Valvuloplasty? Prevalvuloplasty and Postvalvuloplasty Variables that Predict Long-Term Outcome. Circulation. 2002;105(12):1465-71. doi: 10.1161/01.cir.0000012143.27196.f4.
24. Cruz-Gonzalez I, Sanchez-Ledesma M, Sanchez PL, Martin-Moreiras J, Jneid H, Rengifo-Moreno P, et al. Predicting Success and Long-Term Outcomes of Percutaneous Mitral Valvuloplasty: A Multifactorial Score. Am J Med. 2009;122(6):581.e11-9. doi: 10.1016/j.amjmed.2008.10.038.
25. Rifaie O, Esmat I, Abdel-Rahman M, Nammas W. Can a Novel Echocardiographic Score Better Predict Outcome after Percutaneous Balloon Mitral Valvuloplasty? Echocardiography. 2009;26(2):119-27. doi: 10.1111/j.1540-8175.2008.00774.x.
26. Anwar AM, Attia WM, Nosir YF, Soliman OI, Mosad MA, Othman M, et al. Validation of a New Score for the Assessment of Mitral Stenosis Using Real-Time Three-Dimensional Echocardiography. J Am Soc Echocardiogr. 2010;23(1):13-22. doi: 10.1016/j.echo.2009.09.022.
27. Babu DS, Ranganayakulu KP, Rajasekhar D, Vanajakshamma V, Kumar TP. Assessment of Mitral Valve Commissural Morphology by Transoesophageal Echocardiography Predicts Outcome after Balloon Mitral Valvotomy. Indian Heart J. 2013;65(3):269-75. doi: 10.1016/j.ihj.2013.04.022.

Review Article

How I Assess Left Ventricular Systolic Function

Ana Clara Tude Rodrigues[1,2]

INRAD – Instituto de Radiologia do Hospital das Clínicas da Faculdade de Medicina da Universidade de São Paulo (HCFMUSP),[1] *São Paulo, SP – Brazil*
Hospital Israelita Albert Einstein,[2] *São Paulo, SP – Brazil*

Abstract

Assessment of left ventricular systolic function is central to transthoracic echocardiography and remains essential in clinical practice and research. Although left ventricular ejection fraction is still the most widely used parameter, advances in echocardiographic techniques have broadened diagnostic assessment. This review summarizes key methods for evaluating systolic function, from traditional linear measurements to modern two- and three-dimensional volumetric approaches. The roles and limitations of the Simpson method, contrast echocardiography, three-dimensional imaging, myocardial deformation analysis, and artificial intelligence are discussed, emphasizing the importance of an integrated and individualized approach.

My Approach to the Echocardiographic Assessment of Left Ventricular Systolic Function

Assessment of Left Ventricular (LV) systolic function is a cornerstone of transthoracic echocardiography and is essential in both clinical practice and cardiovascular research. Left Ventricular Ejection Fraction (LVEF) is widely used for risk stratification, diagnosis, and follow-up of conditions such as heart failure, valvular heart disease, cardiomyopathies, and chemotherapy-related cardiotoxicity.[1-3] Although cardiac magnetic resonance imaging is the gold standard for volumetric quantification, echocardiography is more accessible, noninvasive, low-cost, and applicable in multiple clinical settings. Technological advances and artificial intelligence algorithms have increased accuracy, reproducibility, and the early detection of functional abnormalities,[4] strengthening echocardiography as a first-line imaging modality. Here, we review the main echocardiographic methods used to analyze LV systolic function, with emphasis on practical applications and limitations. Historically, the Teichholz formula, described in the 1970s, estimated ventricular volumes using M-mode or two-dimensional (2D) diameter measurements. Although groundbreaking at the time, it relied heavily on rigid geometric assumptions and is valid only for normal hearts and situations in which high precision is not required. Diameters are measured in the parasternal long-axis view at the level of the chordae tendineae, at end-diastole (LVEDD) and end-systole (LVESD), following guideline recommendations.[5] Small deviations in the ultrasound beam can lead to errors, making standardization essential. This method is no longer routinely used in the United States and Europe, but it still appears in some practices in Brazil, especially in high-volume settings and in patients without structural heart disease. Beginning in the 1990s, the biplane Simpson's method, also known as the modified biplane method of disks, became the reference technique for quantifying ventricular volumes and LVEF.[5] This method reconstructs the LV geometry using images from apical four- and two-chamber views, with adequate endocardial definition. At end-diastole (the largest cavity, identified at the onset of the QRS complex) and end-systole (the smallest cavity), the endocardial border is manually or semi-automatically traced, excluding papillary muscles and trabeculations, which are considered part of the cavity. The software divides the ventricle into multiple thin cylindrical disks to calculate end-diastolic and end-systolic volumes, from which LVEF is automatically derived (Figure 1). The primary technical requirement is to avoid LV foreshortening by ensuring truly orthogonal apical views, preventing volume underestimation. We use this method routinely in patients with regional wall-motion abnormalities, LV dysfunction, and in cases in which clinical decisions depend on precise LVEF quantification, such as in heart failure, cardiomyopathies, valvular heart disease, and selection for cardiac resynchronization therapy.[6] For patients requiring greater accuracy, even when the heart appears structurally normal, such as those receiving or about to receive cardiotoxic chemotherapy, the Simpson method remains the technique of choice. In this context, when available, Three-dimensional (3D) echocardiography is preferred because it reduces variability in volume and EF measurements, which is essential when rigorous monitoring is needed.[7] Some limitations of the biplane method, however, must be acknowledged: its accuracy depends strongly on acoustic window quality; therefore, in cases with suboptimal images, we use Ultrasound Contrast Agents (UCA), microbubbles of gas encapsulated by lipid, protein, or polymer shells and administered intravenously.[8] These microbubbles act as strong acoustic scatterers, increasing signal intensity and improving endocardial border delineation, which allows for more accurate volume and LVEF measurements (Figure 2). It is important to emphasize that UCAs should be reserved for situations with a clear clinical need for enhanced endocardial definition or volumetric quantification, considering their additional costs and potential adverse effects. When the Simpson method cannot be applied due to a limited acoustic window, and UCAs are not available, LVEF may be estimated visually, integrating apical and parasternal views. Visual

Keywords

Echocardiography; Left Ventricular Function; Heart Rate

Mailing Address: Ana Clara Tude Rodrigues •
Instituto de Radiologia (INRAD) do Hospital das Clínicas da Faculdade de Medicina da Universidade de São Paulo (HCFMUSP), Setor de Ecocardiografia. Rua particular, SN. Postal Code: 05403-010, São Paulo, SP – Brazil
E-mail: anaclaratuderodrigues3@gmail.com
Manuscript received November 12, 2025; revised November 12, 2025; accepted November 12, 2025
Editor responsible for the review: Marcelo Tavares

DOI: https://doi.org/10.36660/abcimg.20250078i

Central Illustration: How I Assess Left Ventricular Systolic Function

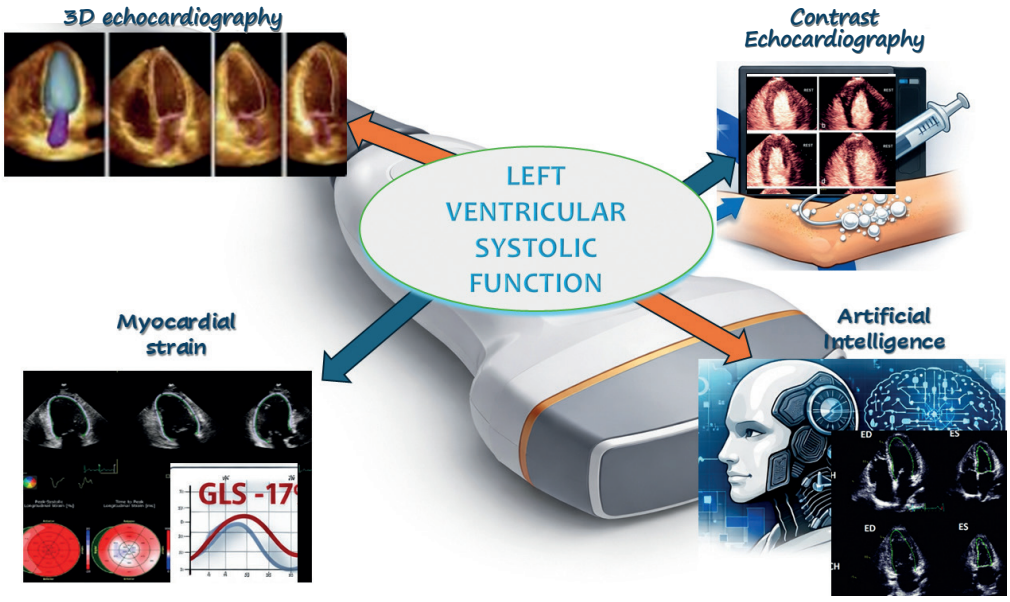

Arq Bras Cardiol: Imagem cardiovasc. 2025;38(4):e20250078

estimation is widely used in clinical practice and even in major clinical trials in which volumetric quantification was not feasible.[9] Another limitation of the Simpson method is the presence of localized contraction abnormalities in the anteroseptal or inferolateral walls. In these cases, when feasible, 3D echocardiography should be prioritized. This technique allows full-volume LV acquisition from multiple planes, eliminating geometric assumptions and providing precise cavity reconstructions (Figure 3). Image quality may still limit adequate volume acquisition, particularly in patients with poor acoustic windows, although recent advances in software and image acquisition have improved processing speed and reliability. Additionally, 3D echocardiography reduces interobserver variability and improves accuracy in volume and EF assessment, making it particularly useful in patients with significant ventricular remodeling.[10] Although inter- and intraobserver variability is lower with the biplane method than with linear measurements, it may still occur, especially in studies with limited technical quality. Finally, compared with cardiac MRI, the Simpson method tends to underestimate absolute volumes, although it maintains good correlation for LVEF. For this reason, 3D echocardiography is generally preferred for more precise volume estimation.[11] Regarding myocardial deformation imaging with two-dimensional speckle tracking, in my practice, I incorporate this analysis whenever LV impairment is suspected but not fully characterized by conventional 2D echocardiography (Figure 4). This includes cases such as unexplained increases in myocardial thickness, use of potentially cardiotoxic drugs,[12] or subtle signs of ventricular dysfunction. For such, we use apical two-, three-, and four-chamber images with adequate endocardial definition, manually or semi-automatically tracing endocardial borders at end-diastole and end-systole to calculate Global Longitudinal Strain (GLS), aiming to acquire at least two consecutive cardiac cycles to reduce variability. Despite being dependent on image quality, GLS is highly sensitive and reproducible, especially with new automated software, and provides a reliable complementary assessment of LV systolic function [1,2]. The need for extensive technical training has become less relevant due to recent technological advances. More recently, artificial intelligence (AI) tools have been incorporated into echocardiographic practice, with algorithms capable of automating 2D, 3D, and strain analyses. These systems enhance standardization, reduce analysis time, and allow the detection of subtle patterns imperceptible to conventional techniques, increasing efficiency and reproducibility. I have used these software tools for cardiac diameter measurement, 2D and 3D volume calculation, and strain assessment;[13,14] however, manual adjustments are still necessary to ensure measurement accuracy. As these technologies continue to evolve, a substantial portion of repetitive echocardiographic tasks will become automated, reducing manual workload.[15] Thus, my current approach to evaluating LV systolic function combines traditional methods with advanced technologies, applied critically and individualized to each patient's clinical context.

Author Contributions

Conception and design of the research: Rodrigues ACT. Writing of the manuscript: Rodrigues ACT. Critical revision of the manuscript for intellectual content: Rodrigues ACT.

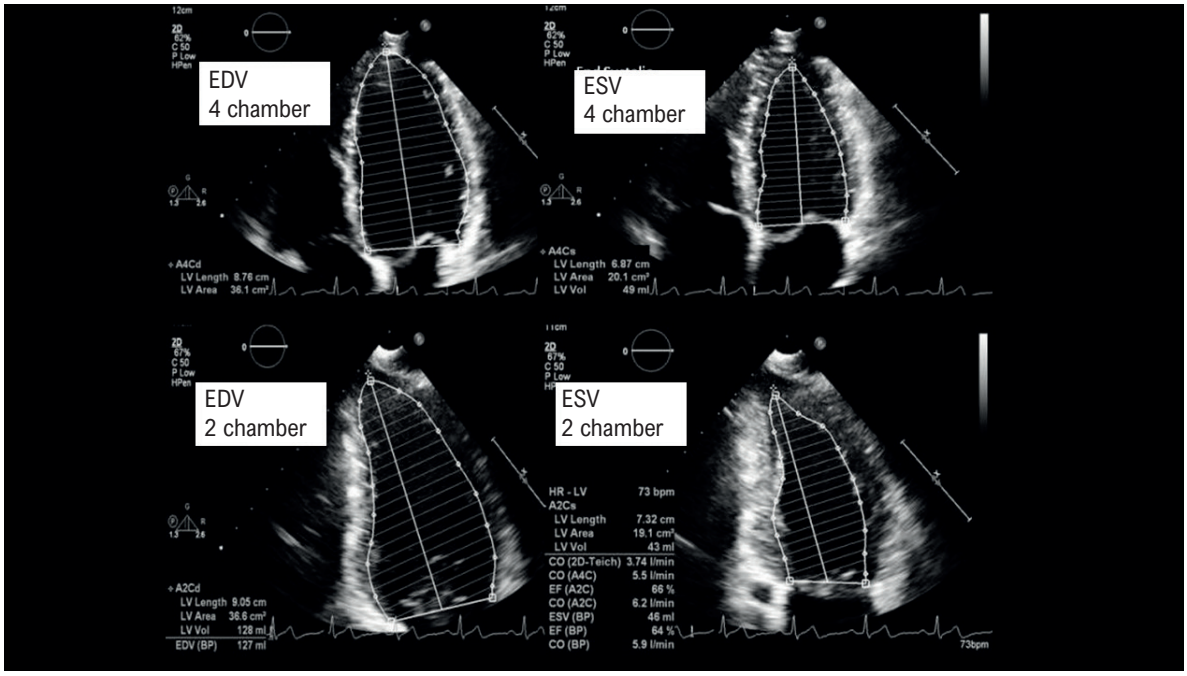

Figure 1 – *Apical 2- and 4-chamber images used to obtain LV volumes and ejection fraction using the biplane Simpson method. EDV: End Diastolic Volume; ESV: End Systolic Volume.*

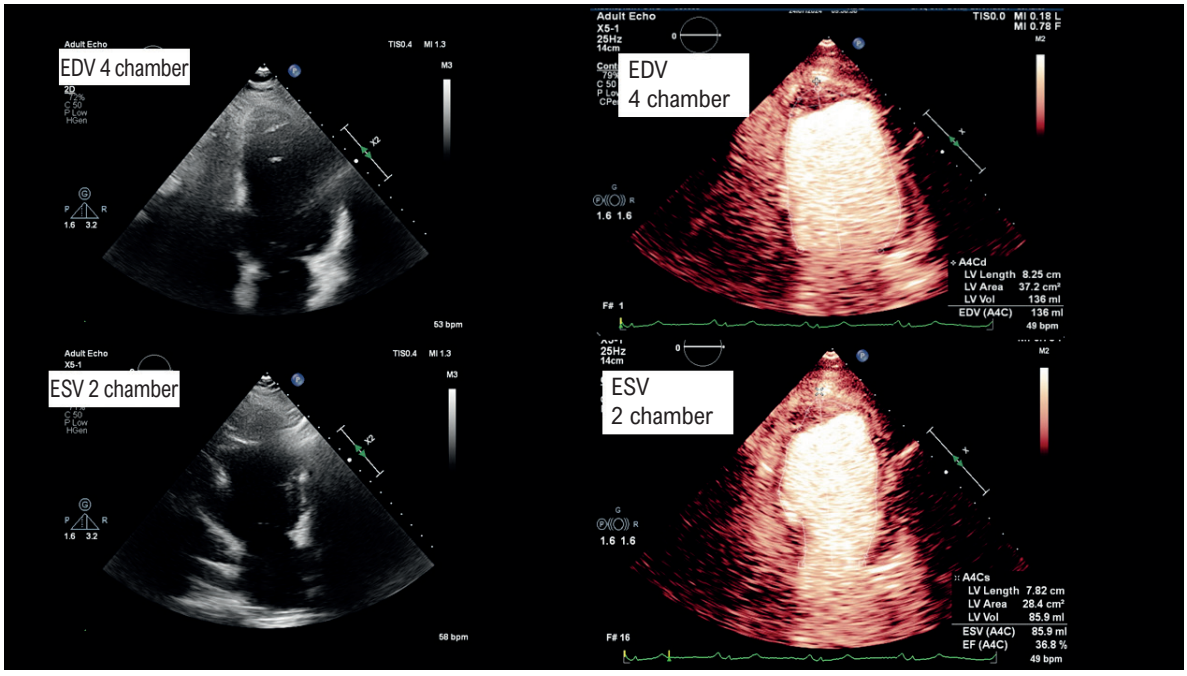

Figure 2 – *Apical 4- and 2-chamber images with limited quality. After administration of the ultrasound contrast agent, there is improved endocardial visualization, enabling accurate delineation and reliable biplane measurements. A mural apical thrombus is also visible. EDV: End Diastolic Volume; ESV: End Systolic Volume.*

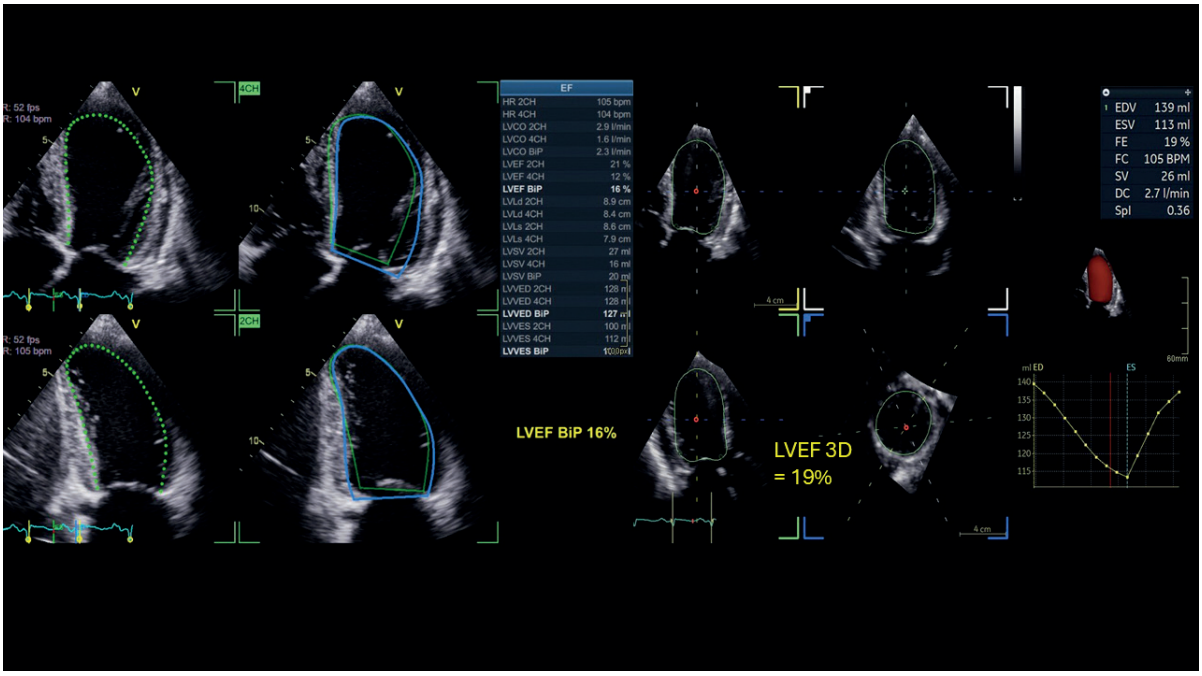

Figure 3 – *Two- and three-dimensional images with LVEF measurements in a patient with peripartum cardiomyopathy and significant systolic dysfunction. Measurements were obtained semi-automatically.*

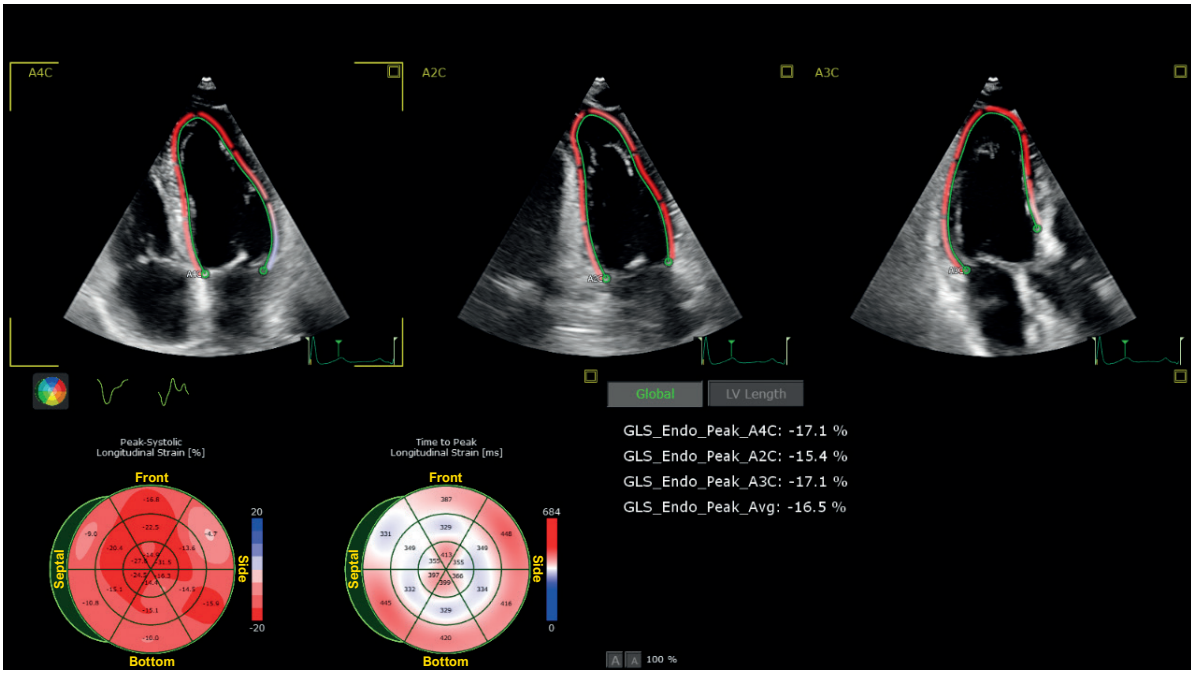

Figure 4 – *Two-dimensional speckle-tracking strain analysis in a patient with suspected hemochromatosis. LVEF was preserved, but GLS was reduced, especially in basal LV segments.*

Potential Conflict of Interest

No potential conflict of interest relevant to this article was reported.

Sources of Funding

There were no external funding sources for this study.

Study Association

This study is not associated with any thesis or dissertation work.

Ethics Approval and Consent to Participate

This article does not contain any studies with human participants or animals performed by any of the authors.

Use of Artificial Intelligence

The authors did not use any artificial intelligence tools in the development of this work.

Availability of Research Data

The underlying content of the research text is contained within the manuscript.

References

1. McDonagh TA, Metra M, Adamo M, Gardner RS, Baumbach A, Böhm M, et al. 2021 ESC Guidelines for the diagnosis and treatment of acute and chronic heart failure: Developed by the Task Force for the diagnosis and treatment of acute and chronic heart failure of the European Society of Cardiology (ESC) With the special contribution of the Heart Failure Association (HFA) of the ESC. Rev Esp Cardiol. 2022;75(6):523. doi: 10.1016/j.rec.2022.05.005.
2. Perry AS, Li S. Optimal Threshold of Left Ventricular Ejection Fraction for Aortic Valve Replacement in Asymptomatic Severe Aortic Stenosis: A Systematic Review and Meta-Analysis. J Am Heart Assoc. 2021;10(7):e020252. doi: 10.1161/JAHA.120.020252.
3. Kirkpatrick JN, Vannan MA, Narula J, Lang RM. Echocardiography in Heart Failure: Applications, Utility, and New Horizons. J Am Coll Cardiol. 2007;50(5):381-96. doi: 10.1016/j.jacc.2007.03.048.
4. Elias P, Jain SS, Poterucha T, Randazzo M, Jimenez FL, Khera R, et al. Artificial Intelligence for Cardiovascular Care-Part 1: Advances: JACC Review Topic of the Week. J Am Coll Cardiol. 2024;83(24):2472-86. doi: 10.1016/j.jacc.2024.03.400.
5. Lang RM, Badano LP, Mor-Avi V, Afilalo J, Armstrong A, Ernande L, et al. Recommendations for Cardiac Chamber Quantification by Echocardiography in Adults: An Update from the American Society of Echocardiography and the European Association of Cardiovascular Imaging. J Am Soc Echocardiogr. 2015;28(1):1-39.e14. doi: 10.1016/j.echo.2014.10.003.
6. Gottdiener JS, Bednarz J, Devereux R, Gardin J, Klein A, Manning WJ, et al. American Society of Echocardiography Recommendations for Use of Echocardiography in Clinical Trials. J Am Soc Echocardiogr. 2004;17(10):1086-119. doi: 10.1016/j.echo.2004.07.013.
7. Thavendiranathan P, Grant AD, Negishi T, Plana JC, Popović ZB, Marwick TH. Reproducibility of Echocardiographic Techniques for Sequential Assessment of Left Ventricular Ejection Fraction and Volumes: Application to Patients Undergoing Cancer Chemotherapy. J Am Coll Cardiol. 2013;61(1):77-84. doi: 10.1016/j.jacc.2012.09.035.
8. Senior R, Becher H, Monaghan M, Agati L, Zamorano J, Vanoverschelde JL, et al. Clinical Practice of Contrast Echocardiography: Recommendation by the European Association of Cardiovascular Imaging (EACVI) 2017. Eur Heart J Cardiovasc Imaging. 2017;18(11):1205-1205af. doi: 10.1093/ehjci/jex182.
9. Pellikka PA, She L, Holly TA, Lin G, Varadarajan P, Pai RG, et al. Variability in Ejection Fraction Measured By Echocardiography, Gated Single-Photon Emission Computed Tomography, and Cardiac Magnetic Resonance in Patients with Coronary Artery Disease and Left Ventricular Dysfunction. JAMA Netw Open. 2018;1(4):e181456. doi: 10.1001/jamanetworkopen.2018.1456.
10. Sheikh M, Fallah SA, Moradi M, Jalali A, Vakili-Basir A, Sahebjam M, et al. Comparing HeartModelAI and Cardiac Magnetic Resonance Imaging for Left Ventricular Volume and Function Evaluation in Patients with Dilated Cardiomyopathy. BMC Cardiovasc Disord. 2024;24(1):670. doi: 10.1186/s12872-024-04355-3.
11. Benameur N, Arous Y, Ben Abdallah N, Kraiem T. Comparison between 3D Echocardiography and Cardiac Magnetic Resonance Imaging (CMRI) in the Measurement of Left Ventricular Volumes and Ejection Fraction. Curr Med Imaging Rev. 2019;15(7):654-60. doi: 10.2174/1573405614666180815115756.
12. Oikonomou EK, Kokkinidis DG, Kampaktsis PN, Amir EA, Marwick TH, Gupta D, et al. Assessment of Prognostic Value of Left Ventricular Global Longitudinal Strain for Early Prediction of Chemotherapy-Induced Cardiotoxicity: A Systematic Review and Meta-Analysis. JAMA Cardiol. 2019;4(10):1007-18. doi: 10.1001/jamacardio.2019.2952.
13. Salte IM, Østvik A, Smistad E, Melichova D, Nguyen TM, Karlsen S, et al. Artificial Intelligence for Automatic Measurement of Left Ventricular Strain in Echocardiography. JACC Cardiovasc Imaging. 2021;14(10):1918-28. doi: 10.1016/j.jcmg.2021.04.018.
14. Zhang Z, Zhu Y, Liu M, Zhang Z, Zhao Y, Yang X, et al. Artificial Intelligence-Enhanced Echocardiography for Systolic Function Assessment. J Clin Med. 2022;11(10):2893. doi: 10.3390/jcm11102893.
15. Zhang J, Gajjala S, Agrawal P, Tison GH, Hallock LA, Beussink-Nelson L, et al. Fully Automated Echocardiogram Interpretation in Clinical Practice. Circulation. 2018;138(16):1623-35. doi: 10.1161/CIRCULATIONAHA.118.034338.

Ischemic Stroke in a Young Adult: a diagnostic challenge. Exploring the association between Patent Foramen Ovale and Chiari Network

Raissa Silva Frota,[1] Mauro de Deus Passos,[1] Simone Nascimento dos Santos,[2] Luciano Moreira Alves,[3] Dilson Palhares Ferreira,[1] Lilian Silva França[1]

Hospital Regional de Sobradinho,[1] Sobradinho, DF – Brazil
ECCOS Diagnóstico Cardiovascular,[2] Brasília, DF – Brazil
Hospital de Urgência de Goiânia,[3] Goiânia, GO – Brazil

Introduction

Globally, strokes are the second leading cause of mortality,[1,2] and are broadly categorized into hemorrhagic and ischemic types.[1,2] In 2019, ischemic stroke accounted for 62.4% of all cases, totaling 7.63 million episodes.[1] Projections indicate a substantial increase in stroke prevalence, from 3.9% in 2020 to an estimated 6.4% by 2050.[3] Despite comprehensive etiological investigations, the underlying cause of cerebrovascular ischemic events remains undefined in 10% to 40% of the cases,[4] known as cryptogenic stroke.

Stroke is often a disabling condition and poses a major threat to the socioeconomic stability of a country, particularly in developing nations. The incidence of ischemic stroke has been increasing, particularly among individuals under 55 years of age.[5] Approximately 10% to 15% of all strokes manifest in young adults aged 18 to 49.[5,6] This trend underscores the critical importance of stroke prevention strategies, even within this younger demographic.[5]

Among the main risk factors for ischemic stroke, such as systemic arterial hypertension and atrial fibrillation, a growing association with patent foramen ovale (PFO) is gaining recognition. Although often considered clinically "innocent," PFO has been implicated in cryptogenic stroke,[7] especially in young adults.[7,8] Furthermore, given that 83% of the patients with a Chiari network also have a PFO,[9] several reported cases suggest that this specific concurrence of PFO and a Chiari network may substantially elevate the risk of ischemic stroke.

Case Report

A previously healthy 25-year-old man, with no history of smoking or illicit drug use, was admitted to the Emergency Room approximately 36 hours after the onset of right hemiparesis. Concomitant symptoms included dysarthria, aphasia, loss of consciousness, and sphincter incontinence. On examination, he exhibited dysarthria along with decreased motor strength in the right hemibody. Cardiopulmonary auscultation revealed no significant findings.

The initial non-contrast head Computed Tomography (CT) revealed no detectable abnormalities. Given the neurological symptomatology, further investigation required a Brain Magnetic Resonance Imaging (MRI) with intravenous contrast. The MRI demonstrated a T2 hyperintensity in the left corona radiata, immediately contiguous to the posterior limb of the ipsilateral internal capsule. This lesion showed no diffusion restriction, post-contrast enhancement, hemorrhage, or surrounding vasogenic edema, consistent with a previous ischemic vascular injury (Figure 1).

Following initial evaluations, a diagnostic workup was performed to determine the underlying etiology of his condition. A transthoracic echocardiogram (TTE) indicated preserved ventricular function. Subsequently, a bubble study with agitated saline, conducted through peripheral venous circulation, unequivocally demonstrated a right-to-left shunt, consistent with a PFO, along with an exuberant Chiari network (Figures 2 and 3). Doppler ultrasound studies of the carotid and vertebral arteries yielded normal results. Confirmation of both the PFO and the exuberant Chiari network was subsequently obtained via transesophageal echocardiogram (TEE). Notably, this study revealed a significant passage of microbubbles across the atrial septum into the left chambers, even at rest. The TEE also provided precise measurements for the PFO: a tunnel length of 10mm, with left and right atrial rims measuring 2mm and 3mm, respectively. The angle between the inferior vena cava and the PFO was also less than 10 degrees.

A chest computed tomography angiography (CTA) was performed to rule out pulmonary thromboembolism, showing normal findings. Additionally, a color Doppler ultrasound of the deep and superficial venous systems of the lower limbs showed no signs of deep vein thrombosis or venous insufficiency.

Further investigations included serological assays for HIV 1 and 2, syphilis, hepatitis B, and hepatitis C, all of which proved to be negative. The patient's lipid profile remained within target ranges, and thyroid function (TSH and free T4) was normal. A comprehensive thrombophilia investigation was also meticulously conducted. This included genetic testing for Factor V Leiden (r506q) and the prothrombin gene (g20210a), as well as the evaluation of homocysteine, anticardiolipin IgM and IgG antibodies, lupus anticoagulant, antithrombin III, functional protein C, and free protein S. All of these tests collectively yielded negative results, effectively ruling out the most common thrombophilias.

Keywords

Ischemic Stroke; Stroke; Patent Foramen Ovale

Mailing Address: Mauro de Deus Passos •
Hospital Regional de Sobradinho. Unidade de Medicina Interna, Q 12, CJ B, LT 38, Postal Code: 73010-120, Sobradinho, DF – Brazil
E-mail: mauropassos@cardiol.br
Manuscript received October 01, 2025; revised October 13, 2025; accepted October 13, 2025
Editor responsible for the review: Marcelo Dantas

DOI: https://doi.org/10.36660/abcimg.20250080i

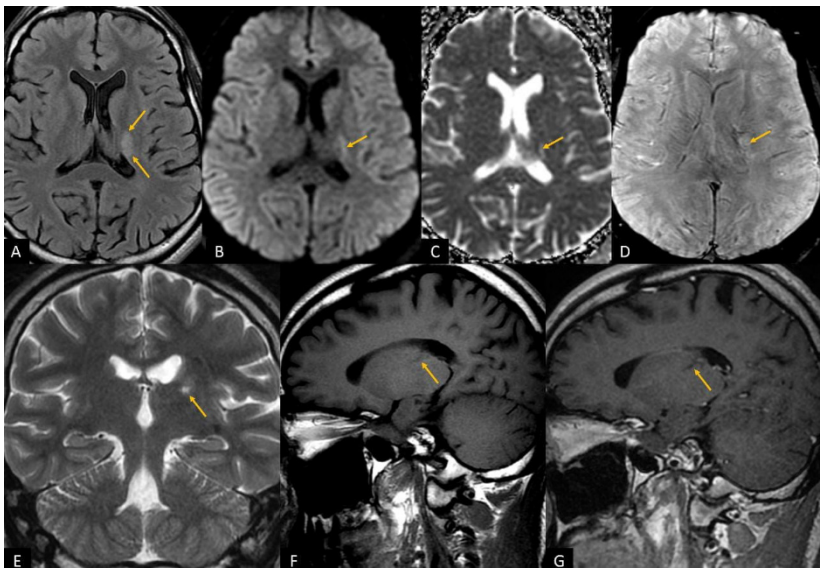

Figure 1 – *Brain MRI Findings. An area of T2-weighted hyperintensity is noted in the left corona radiata, immediately adjacent to the posterior limb of the ipsilateral internal capsule. This lesion shows no diffusion restriction, post-contrast enhancement, hemorrhage, or surrounding vasogenic edema, consistent with prior ischemic vascular injury. (A) FLAIR; (B) Diffusion-weighted imaging (DWI); (C) Apparent diffusion coefficient (ADC) map; (D) Susceptibility-weighted angiography (SWAN) / Gradient recalled echo (GRE) T2*; (E) Coronal T2-weighted image; (F) Sagittal T1-weighted pre-contrast image; (G) Sagittal T1-weighted post-contrast image.*

Percutaneous PFO closure was recommended for the patient and, due to a limited economic situation, he is awaiting the procedure through the public health system. He was discharged with instructions to use Rivaroxaban, 20 mg/day.

Discussion

The foramen ovale plays a fundamental role in maintaining intrauterine life[10,11] and is classified as a subclass of ostium secundum defects.[12] After birth, it typically undergoes functional closure due to changes in systemic and pulmonary pressure differentials. The Koutroulou review reported a PFO prevalence of approximately 24% across all age groups in the general population, based on autopsy and TEE studies.[13] Although often considered an incidental finding, PFO has been associated with cryptogenic stroke[8] and even less common conditions, such as migraine, peripheral embolism, and Alzheimer's dementia.[7]

Ioannidis et al. postulated that PFO in stroke patients might represent an incidental finding, a contributing risk factor, or even a direct causal agent.[14] Proposed mechanisms include paradoxical embolism, in situ thrombus formation, and arrhythmogenesis.[15] Hausmann et al. observed that patients presenting PFO and ischemic arterial events generally exhibit more pronounced right-to-left contrast shunts and larger PFO openings.[16] The SAFAS study indicated that decreased levels of galectin-3 and osteoprotegerin could potentially serve as biomarkers for PFO-related stroke.[17]

In 1897, Austrian pathologist Hans Chiari elucidated the presence of fibrous networks in the right atrium, later named the Chiari Network.[18] Autopsy studies have reported Chiari network prevalences ranging from 1.3% to 4%.[19-24] More contemporary echocardiographic techniques, notably TEE, have identified a 2% prevalence of the Chiari network among 1,436 individuals.[9] The same study revealed associations with PFO and atrial septal aneurysm (ASA) in 83% and 24% of patients with a Chiari network, respectively.[9] The Chiari network likely promotes the persistence of the PFO and may facilitate paradoxical embolism.

Manerikar et al. documented an occipital stroke in a 46-year-old man attributed to the combined presence of a Chiari network and PFO.[25] An additional finding in the case was a mass on the mitral valve consistent with a Lambl's excrescence.[25] Although its echocardiographic diagnosis is typically straightforward, it can occasionally be mistaken for thrombi in the right atrium.[26] The Chiari network itself can serve as a nidus for thrombus formation, potentially leading to a stroke when associated with a PFO through paradoxical emboli that cross from the right to the left atrium and subsequently enter systemic circulation.

The embolic potential of a PFO is primarily attributed to paradoxical embolism through its opening.[15,27] This occurs when a thrombus originating in the venous system

Figure 2 – *Transthoracic Echocardiogram (TTE): Apical 4-chamber view following intravenous infusion of agitated saline solution (microbubbles – blue arrow). (A) First cardiac cycle after opacification of the right chambers and microbubble passage into the left atrium at end-diastole; (B) Microbubbles passing through the opened mitral valve during mid-diastole of the second cycle; (C) Microbubbles within the left ventricle at end-diastole of the second cycle. RV: Right Ventricle; RA: Right Atrium; LV: Left Ventricle; LA: Left Atrium.*

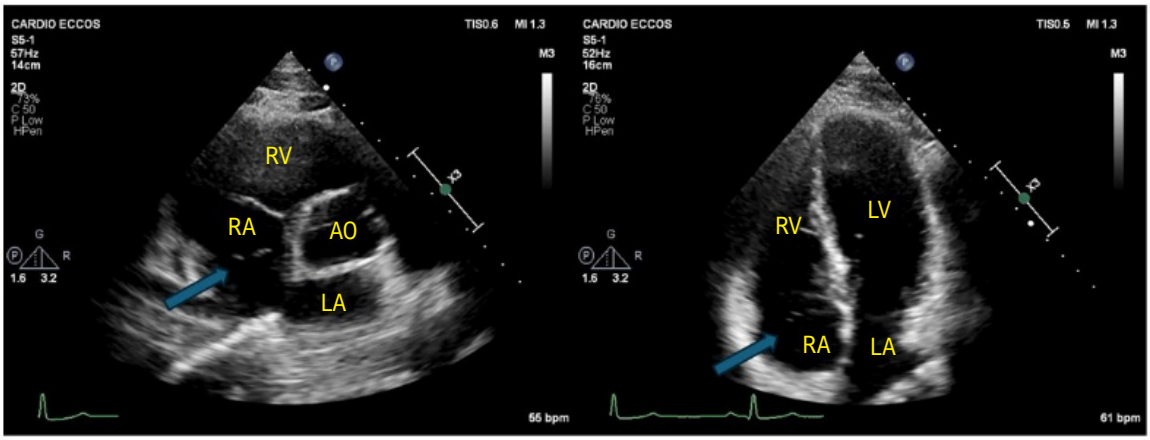

Figura 3 – *Transthoracic Echocardiogram (TTE): The exuberant Chiari network (blue arrow) is shown in (A) short-axis view and (B) apical 4-chamber view. RV: Right Ventricle, RA: Right Atrium, LV: Left Ventricle, LA: Left Atrium, AO: Aorta.*

bypasses pulmonary circulation, passes through the PFO to the left chambers, and subsequently embolizes to the brain, culminating in an ischemic stroke. In patients with a PFO, it is of utmost importance to verify the occurrence of a right-to-left shunt. This is most commonly performed via TTE or, with greater sensitivity, via TEE, both with an infusion of agitated saline. The visualization of microbubble passage from the right to the left atrium confirms the presence of the shunt between these chambers. Another tool is Transcranial Doppler (TCD), which is highly sensitive but cannot differentiate between cardiac and pulmonary shunts. It is the best method to quantify the severity of the shunt, as it is more sensitive than either the TTE or the TEE.[28]

The CLOSE study recommends that after a PFO-associated stroke, secondary prevention is necessary, with options including antiplatelet therapy, anticoagulation, and percutaneous PFO closure, the latter being superior to antithrombotic therapy (antiplatelets or anticoagulants) in preventing new strokes in individuals who have had a cryptogenic stroke.[29] The indication for percutaneous PFO closure is strongest in young patients (up to 60 years), after a cryptogenic ischemic stroke, and especially in the presence of high-risk features, such as an Atrial Septal Aneurysm or a large volume shunt.[30]

Conclusions

Ischemic stroke, particularly when it occurs in young adults, requires an exhaustive etiological investigation. In the present case, the patient's symptoms manifested beyond the window for thrombolysis. The detection of a PFO on both the TTE and the TEE initially suggested a paradoxical embolism, a recognized cause of ischemic stroke. However, the absence of clinical signs or venous Doppler findings indicative of current or previous deep vein thrombosis made this hypothesis less likely, although certainly not excluded.

zOther potential etiologies, such as thrombophilia, were systematically ruled out. The TTE confirmed normal cardiac chamber dimensions and the absence of valvular abnormalities. The 12-lead ECG and 24-hour Holter monitoring were normal, thus ruling out arrhythmias, particularly atrial fibrillation, as the cause of the ischemic stroke.

Therefore, a plausible mechanism for the pathophysiology of the ischemic stroke in this patient (Figure 4), which finds support in the existing literature, involves the in situ formation of a thrombus within the Chiari network, its subsequent passage from the right atrium to the left atrium through the PFO, and the resulting embolization to the carotid system and brain.

Author Contributions

Conception and design of the research: Frota RS, Passos MD, França LS.

Acquisition of data: Frota RS, Passos MD, Santos SN, França LS.

Analysis and interpretation of the data: Frota RS, Passos MD, Santos SN, Alves LM, França LS.

Writing of the manuscript: Frota RS, Passos MD, Santos SN, Alves LM, Ferreira DP, França LS.

Critical revision of the manuscript for intellectual content: Frota RS, Passos MD, Santos SN, Alves LM, Ferreira DP, França LS.

Potential Conflict of Interest

No potential conflict of interest relevant to this article was reported.

Sources of Funding

There were no external funding sources for this study.

Study Association

This article is part of the Final Course Project for the Medical Residency program at ESCS-FEPECS.

Critical revision of the manuscript for intellectual content

This study was approved by the Ethics Committee of the Fundação de Ensino e Pesquisa em Ciências da Saúde – FEPECS/SES/DF under the protocol number 83023524.0.0000.5553. All the procedures in this study were in accordance with the 1975 Helsinki Declaration, updated in 2013. Informed consent was obtained from all participants included in the study.

Use of Artificial Intelligence

The authors did not use any artificial intelligence tools in the development of this work.

Availability of Research Data

The underlying content of the research text is contained within the manuscript.

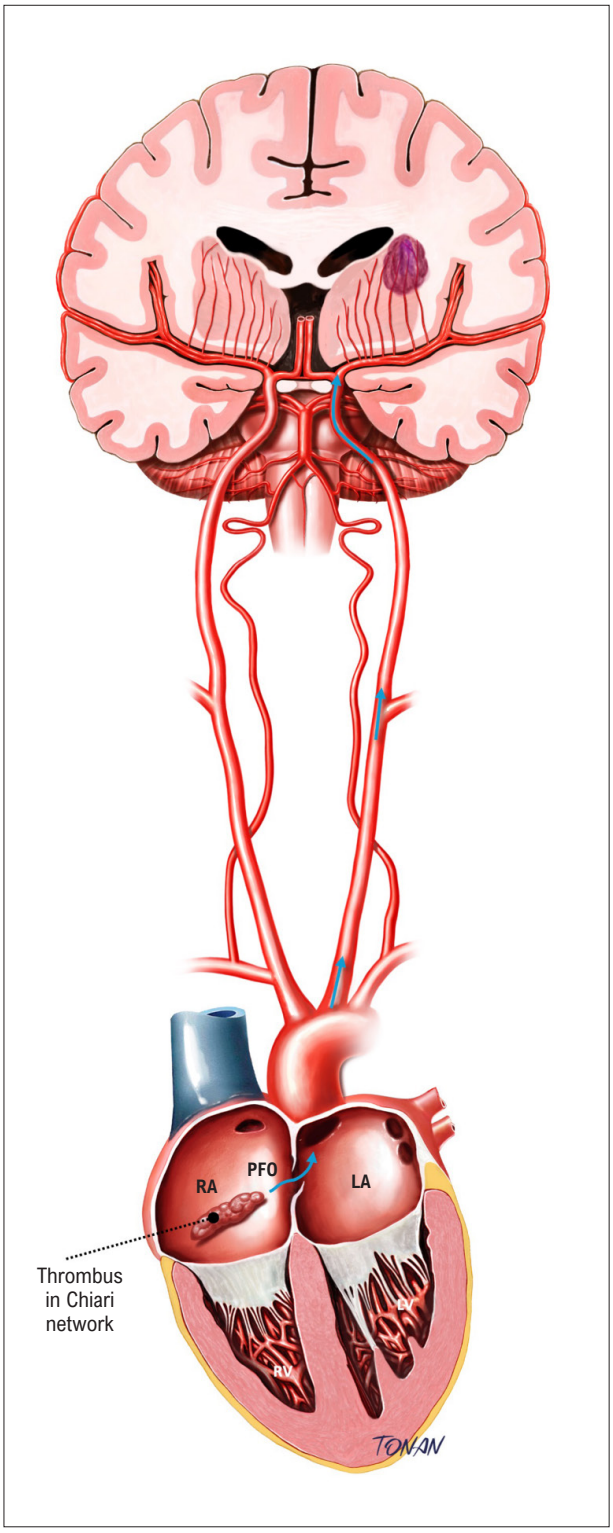

Figure 4 – *Proposed Pathophysiology of Stroke. This illustration elucidates the probable mechanism of the patient's ischemic stroke: the genesis of a thrombus within the Chiari network, its subsequent paradoxical embolization from the right atrium (RA) to the left atrium (LA) through the patent foramen ovale (PFO), and its ultimate transit to the left carotid system and brain, precipitating the ischemic stroke. (Medical illustration by Rodrigo Tonan).*

References

1. GBD 2019 Diseases and Injuries Collaborators. Global Burden of 369 Diseases and Injuries in 204 Countries and Territories, 1990-2019: A Systematic Analysis for the Global Burden of Disease Study 2019. Lancet. 2020;396(10258):1204-22. doi: pubpubpubpppf10.1016/S0140-6736(20)30925-9.
2. Donkor ES. Stroke in the 21st Century: A Snapshot of the Burden, Epidemiology, and Quality of Life. Stroke Res Treat. 2018;2018:3238165. doi: 10.1155/2018/3238165.
3. Maddox KEJ, Elkind MSV, Aparicio HJ, Commodore-Mensah Y, de Ferranti SD, Dowd WN, et al. Forecasting the Burden of Cardiovascular Disease and Stroke in the United States Through 2050-Prevalence of Risk Factors and Disease: A Presidential Advisory from the American Heart Association. Circulation. 2024;150(4):e65-e88. doi: 10.1161/CIR.0000000000001256.
4. Saver JL. Clinical Practice. Cryptogenic Stroke. N Engl J Med. 2016;374(21):2065-74. doi: 10.1056/NEJMcp1503946.
5. Béjot Y, Daubail B, Jacquin A, Durier J, Osseby GV, Rouaud O, et al. Trends in the Incidence of Ischaemic Stroke in Young Adults between 1985 and 2011: The Dijon Stroke Registry. J Neurol Neurosurg Psychiatry. 2014;85(5):509-13. doi: 10.1136/jnnp-2013-306203.
6. Ekker MS, Verhoeven JI, Vaartjes I, Jolink WMT, Klijn CJM, de Leeuw FE. Association of Stroke Among Adults Aged 18 to 49 Years with Long-Term Mortality. JAMA. 2019;321(21):2113-23. doi: 10.1001/jama.2019.6560.
7. Aggeli C, Verveniotis A, Andrikopoulou E, Vavuranakis E, Toutouzas K, Tousoulis D. Echocardiographic Features of PFOs and Paradoxical Embolism: A Complicated Puzzle. Int J Cardiovasc Imaging. 2018;34(12):1849-61. doi: 10.1007/s10554-018-1406-1.
8. Miranda B, Fonseca AC, Ferro JM. Patent Foramen Ovale and Stroke. J Neurol. 2018;265(8):1943-9. doi: 10.1007/s00415-018-8865-0.
9. Schneider B, Hofmann T, Justen MH, Meinertz T. Chiari's Network: Normal Anatomic Variant or Risk Factor for Arterial Embolic Events? J Am Coll Cardiol. 1995;26(1):203-10. doi: 10.1016/0735-1097(95)00144-o.
10. Friedman AH, Fahey JT. The Transition from Fetal to Neonatal Circulation: Normal Responses and Implications for Infants with Heart Disease. Semin Perinatol. 1993;17(2):106-21.
11. Kiserud T, Acharya G. The Fetal Circulation. Prenat Diagn. 2004;24(13):1049-59. doi: 10.1002/pd.1062.
12. Menillo AM, Alahmadi MH, Pearson-Shaver AL. Atrial Septal Defect. Treasure Island: StatPearls Publishing; 2025.
13. Koutroulou I, Tsivgoulis G, Tsalikakis D, Karacostas D, Grigoriadis N, Karapanayiotides T. Epidemiology of Patent Foramen Ovale in General Population and in Stroke Patients: A Narrative Review. Front Neurol. 2020;11:281. doi: 10.3389/fneur.2020.00281.
14. Ioannidis SG, Mitsias PD. Patent Foramen Ovale in Cryptogenic Ischemic Stroke: Direct Cause, Risk Factor, or Incidental Finding? Front Neurol. 2020;11:567. doi: 10.3389/fneur.2020.00567.
15. Caso V, Turc G, Abdul-Rahim AH, Castro P, Hussain S, Lal A, et al. European Stroke Organisation (ESO) Guidelines on the Diagnosis and Management of Patent Foramen Ovale (PFO) after Stroke. Eur Stroke J. 2024;9(4):800-34. doi: 10.1177/23969873241247978.
16. Hausmann D, Mügge A, Daniel WG. Identification of Patent Foramen Ovale Permitting Paradoxic Embolism. J Am Coll Cardiol. 1995;26(4):1030-8. doi: 10.1016/0735-1097(95)00288-9.
17. Pommier T, Lafont A, Didier R, Garnier L, Duloquin G, Meloux A, et al. Factors Associated with Patent Foramen Ovale-Related Stroke: SAFAS Study. Rev Neurol. 2024;180(1-2):33-41. doi: 10.1016/j.neurol.2023.05.007.
18. Chiari H. Ueber netzbildungen im recten Vorhofe des Herzens. Beitr Path Anat. 1897;22:1-10.
19. Helwig FC. The Frequency of Anomalous Reticula in the Right Atrium of the Human Heart "Chiari Network": Report of Eight Cases. Am J Pathol. 1932;8(1):73-80.7.
20. Yater WM. Variations and Anomalies of the Venous Valves of the Right Atrium of the Human Heart. Arch Pathol. 1929;7:418-41.
21. Yater WM. The Paradox of Chiari's Network: Review and Report of a Case of Chiari's Network Ensnaring a Large Cmbolus. Am Heart J. 1936;11(5):542-53. doi: 10.1016/S0002-8703(36)90472-6.
22. Gresham GA. Networks in the Right Side of the Heart. Br Heart J. 1957;19(3):381-6. doi: 10.1136/hrt.19.3.381.
23. Bankl H, Kretschmer G. Residues of Embryonic Structures in Human Cardiac Atria. A Contribution to their Significance in Heart Catheterization. Beitr Pathol Anat. 1968;138(1):1-35.
24. Agmon Y, Khandheria BK, Meissner I, Gentile F, Whisnant JP, Sicks JD, et al. Frequency of Atrial Septal Aneurysms in Patients with Cerebral Ischemic Events. Circulation. 1999;99(15):1942-4. doi: 10.1161/01.cir.99.15.1942.
25. Manerikar A, Malaisrie SC. Chiari Network and Patent Foramen Ovale Associated with Stroke. JTCVS Tech. 2021;11:45-7. doi: 10.1016/j.xjtc.2021.11.006.
26. Renani SA, Badalabadi RM, Abbasi Z, Gharebaghi M. Huge Chiari Network in the Right Atrium Diagnosed as Thrombosis - Case Report and a Brief Review. J Cardiovasc Echogr. 2022;32(2):126-8. doi: 10.4103/jcecho.jcecho_81_21.
27. Di Tullio MR, Homma S. Patent Foramen Ovale and Stroke: What Should be Done? Curr Opin Hematol. 2009;16(5):391-6. doi: 10.1097/MOH.0b013e32832d47dd.
28. Mahmoud AN, Elgendy IY, Agarwal N, Tobis JM, Mojadidi MK. Identification and Quantification of Patent Foramen Ovale-Mediated Shunts: Echocardiography and Transcranial Doppler. Interv Cardiol Clin. 2017;6(4):495-504. doi: 10.1016/j.iccl.2017.05.002.
29. Turc G, Calvet D, Guérin P, Sroussi M, Chatellier G, Mas JL, et al. Closure, Anticoagulation, or Antiplatelet Therapy for Cryptogenic Stroke with Patent Foramen Ovale: Systematic Review of Randomized Trials, Sequential Meta-Analysis, and New Insights from the CLOSE Study. J Am Heart Assoc. 2018;7(12):e008356. doi: 10.1161/JAHA.117.008356.
30. Gonnah AR, Bharadwaj MS, Nassar H, Abdelaziz HK, Roberts DH. Patent Foramen Ovale: Diagnostic Evaluation and the Role of Device Closure. Clin Med. 2022;22(5):441-8. doi: 10.7861/clinmed.2022-0040.

Dorsalis Pedis Artery Aneurysm: an Ultrasound Diagnosis

Ana Claudia Gomes Pereira Petisco,[1,2] Larissa Chaves Nunes Carvalho,[1] Mohamed Hassan Saleh,[1] Fabio Henrique Rossi,[1] Marcela da Silva Dourado,[1] Juliana Chen,[1] Heraldo Antonio Barbato,[1] Andrea de Andrade Vilela[1]

Instituto Dante Pazzanese de Cardiologia,[1] São Paulo, SP – Brazil

Clínica Procoração Cardiologia Preventiva – Ecocardiografia,[2] São Paulo, SP – Brazil

Dorsalis Pedis Artery Aneurysms (DPAAs) are rare, and few cases have been described in the literature. Pseudoaneurysms are believed to be more common than true aneurysms, but little is known about their clinical behavior.[1] The present study shows a case report of a patient with a DPAA, diagnosed by vascular ultrasound (VUS) and surgically treated at our facility.

We treated a 59-year-old female patient, who was a saleswoman. She was asymptomatic until one year ago, when she noticed the appearance of a pulsatile mass on the dorsum of her right foot, which was occasionally painful, especially when wearing closed-toe shoes. She reported trauma five years prior to the onset of symptoms, caused by an iron bar falling on her feet.

Medical History: hypertension, diabetes mellitus, and dyslipidemia.

At the time of treatment, she was continuously taking simvastatin, metformin, and losartan. Physical examination was normal, except for the presence of a pulsatile mass on the dorsum of the right foot, varicose veins, and ochre dermatitis on both lower limbs. BP: 120X85 mmHg; HR=76 bpm.

Laboratory tests, an electrocardiogram, chest X-ray, and transthoracic echocardiogram were performed, all of which were normal.

The VUS of the arteries of the right lower limb showed an image suggestive of a fusiform aneurysm of the right DPAA, with thrombi measuring approximately 1.9 cm x 0.7 cm. Flow was present and multiphasic. Other arteries of the right lower limb showed flow to be present and multiphasic, without stenosis or other dilations (Figure 1).

An arteriography of the lower right limb demonstrated saccular dilation of the DPAA, near the metatarsal branches, with a maximum diameter of 1.0 cm. Arteriography suggested the diagnosis of a pseudoaneurysm (Figure 2).

Keywords

Dorsalis pedis artery aneurysm; Doppler ultrasonography; Vascular ultrasonography; Surgery; Dorsalis pedis artery

Mailing Address: Ana Claudia Gomes Pereira Petisco •
Instituto Dante Pazzanese de Cardiologia – Ecocardiografia. Rua Dr. Dante Pazzanese, 500. Postal Code: 04012-909, São Paulo, SP – Brasil
E-mail: anapetisco@outlook.com
Manuscript received August 27, 2025; revised September 17, 2025; accepted September 17, 2025
Editor responsible for the review: Marcelo Tavares

DOI: https://doi.org/10.36660/abcimg.20250066i

The patient underwent open surgery, and the intraoperative findings, upon opening the aneurysm sac, showed no evidence of a pseudoaneurysm orifice; however, evidence of a true aneurysm was observed.

An end-to-end graft with an inverted great saphenous vein was performed, preserving the arterial flow.

The patient was discharged the following day after a control ultrasound demonstrated preserved, multiphasic flow in the dorsal artery of the right foot (Figure 3).

Discussion

The DPAA (pedal artery) was first described in 1907.[2] Since then, other authors have reported this rare type of aneurysm, but its clinical manifestations are still relatively unknown.[1] With only 24 cases reported in the literature until 2017, according to Aragão et al.,[1] the DPAA aneurysm is more common among men (63%) with a mean age of 55.4%.[3] In general, it appears as a pulsatile mass, which may lead to microembolization, hemorrhage, rupture, and nerve compression.[4] Physical examination usually reveals a pulsatile mass that can cause pain, paresthesia, and discomfort when walking or wearing shoes, complaints similar to the case reported in our study.[5]

The pathophysiology of these aneurysms is still uncertain, but it appears to be related to two types of mechanisms: an intrinsic mechanism, related to weakness in the vessel wall structure, such as collagen diseases, Marfan and Ehlers-Danlos syndromes, syphilis, diabetes, infections, trauma, atherosclerosis, and fibrodysplasia; and an extrinsic mechanism, caused by mechanical stress on the arterial wall, such as trauma.[3-6] However, according to the literature, many DPAAs are pseudoaneurysms and occur after trauma or iatrogenic injuries secondary to orthopedic or vascular procedures.[1] Although trauma is a cause of DPAAs, patients are often unable to remember the acute event, and symptoms arise when they experience a compression of local structures or specific events, including embolism or rupture.[5] There have also been cases of repeated, low-impact trauma that have led to aneurysmal degeneration, such as tight shoes in patients with congenitally markedly high arches.[5]

True aneurysms appear with all three layers of the arterial wall, while pseudoaneurysms refer to hematomas with flow resulting from a rupture of the vessel wall.[6,7] In our case, contrast angiography diagnosed the dilation as a pseudoaneurysm, but the VUS characteristics were those of a true DPAA with mural thrombus, which proved to be consistent with the surgical finding, which also presented as a true DPAA. Other authors have described a similar

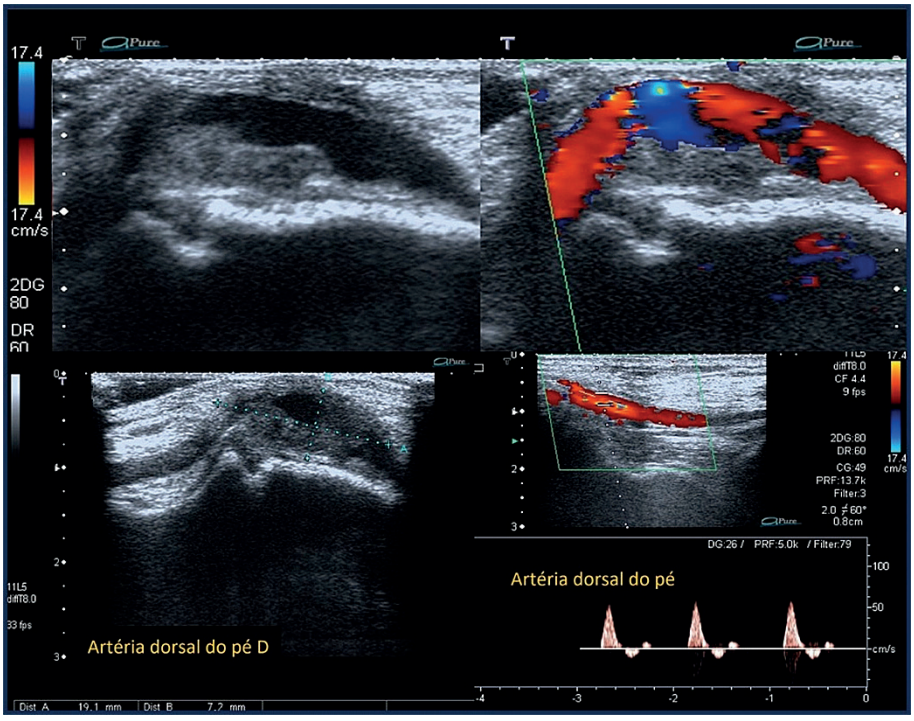

Figure 1 – *Dorsalis Pedis Artery Aneurysms (DPAA) of the foot. A and B: Two-dimensional and color Doppler ultrasound images demonstrate arterial patency and the presence of thrombi; C: aneurysm measurements; D: Multiphasic flow before dilation on spectral Doppler.*

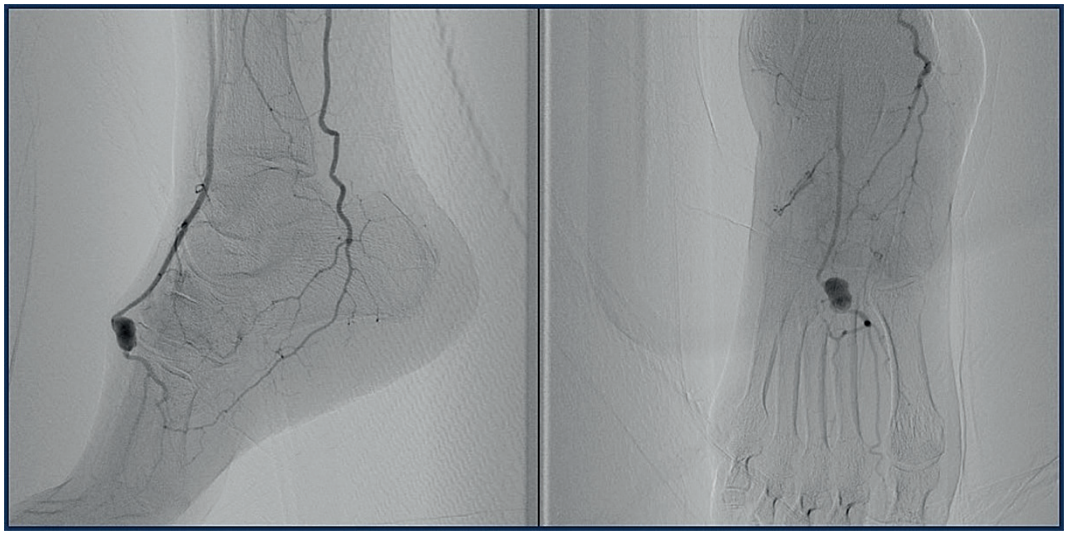

Figure 2 – *A and B: arteriography demonstrating saccular dilation of the dorsalis pedis artery.*

situation, and in some cases, only histopathological examination can differentiate between pseudoaneurysms and true DPAAs.[5,6,8]

Diagnosis must be made promptly to avoid complications, such as thrombosis, distal embolism, hemorrhage, and rupture.[1] In a review by Kato et al.,[3] 4% of infrapopliteal

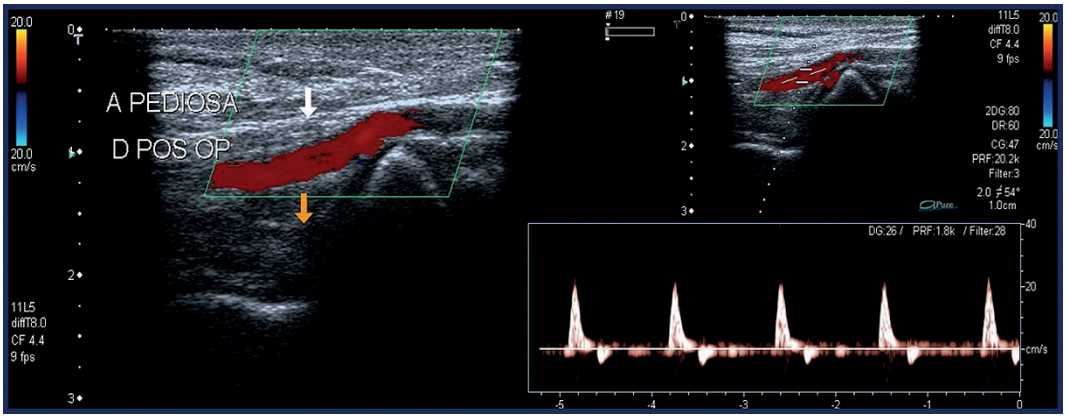

Figure 3 – *Postoperative control ultrasound. A: absence of aneurysm and arterial patency with preserved flow on color Doppler; B: multiphasic flow in the dorsalis pedis artery via spectral Doppler.*

aneurysms progress to rupture and 12.5% to thrombosis. VUS should be the first diagnostic test performed due to its high sensitivity and specificity in detecting aneurysms and pseudoaneurysms, as well as its noninvasive nature and lack of iodinated contrast.[7] However, other tests, such as computed tomography, conventional angiography, or magnetic resonance imaging, may also be performed for further diagnostic investigation or in doubtful cases.[9] The diagnostic investigation is usually similar in patients with pseudoaneurysms and true DPAAs.[9] Our patient initially underwent vascular ultrasonography, which diagnosed the DPAA, and conventional arteriography was subsequently performed to demonstrate the arterial arch and better evaluate other vascular structures.

Treatment of a DPAA should be tailored to the individual case, with the options being endovascular or open surgical treatment.[9] Open surgical methods include simple ligation with or without resection, reconstruction of the artery with primary anastomosis, or interposition of a vein graft.[4,6,9,10] In the present case, an end-to-end graft with an inverted great saphenous vein and preservation of arterial flow were performed. The patient is currently asymptomatic and is being treated through outpatient follow-up.

Author Contributions

Conception and design of the research: Petisco ACGP, Saleh MH. Acquisition of data: Petisco ACGP, Carvalho LCN, Rossi FH, Dourado MS, Barbato HA, Chen J. Analysis and interpretation of the data: Petisco ACGP, Carvalho LCN, Saleh MH, Dourado MS, Barbato HA, Chen J. Writing of the manuscript: Petisco ACGP, Carvalho LCN, Saleh MH, Dourado MS. Critical revision of the manuscript for intellectual content: Petisco ACGP, Saleh MH, Rossi FH, Vilela AA.

Potential Conflict of Interest

No potential conflict of interest relevant to this article was reported.

Sources of Funding

There were no external funding sources for this study.

Study Association

This study is not associated with any thesis or dissertation work.

Ethics Approval and Consent to Participate

This study was approved by the Ethics Committee of the Instituto Dante Pazzanese de Cardiologia under protocol number CAAE: 94268925.3.0000.5462, opinion 8.052.126. All procedures involved in this study are in accordance with the Declaration of Helsinki of 1975, updated in 2013.

Use of Artificial Intelligence

The authors did not use any artificial intelligence tools in the development of this work.

Availability of Research Data

The underlying content of the research text is contained within the manuscript.

References

1. Aragão JA, Neves OMG, Miranda FGG, Leão WB, Aragão FMS, Aragão ICS. True Aneurysm of the Dorsal Artery of the Foot: Case Report and Review of the Literature. Ann Vasc Surg. 2017;44:414.e1-414.e4. doi: 10.1016/j.avsg.2017.04.011.
2. Cuff A. Spontaneous Aneurysm of the Dorsalis Pedis Artery. Br Med J. 1907;2(2427):16. doi: 10.1136/bmj.2.2427.16.
3. Kato T, Takagi H, Sekino S, Manabe H, Matsuno Y, Furuhashi K, et al. Dorsalis Pedis Artery True Aneurysm Due to Atherosclerosis: Case Report and Literature Review. J Vasc Surg. 2004;40(5):1044-8. doi: 10.1016/j.jvs.2004.08.052.
4. Kwon MJ, Ra JH, Said J, Tamim PM. Open Surgical Repair of True Saccular Aneurysm of Dorsalis Pedis Artery Using a Reversed Great Saphenous Vein Bypass Graft. J Vasc Surg Cases Innov Tech. 2023;10(1):101378. doi: 10.1016/j.jvscit.2023.101378.
5. Nolan FC, Bourke M, Kenny A, Moloney T. Dorsalis Pedis Artery Aneurysm. BMJ Case Rep. 2020;13(2):e231969. doi: 10.1136/bcr-2019-231969.
6. Grzela T, Piotrowicz R, Leksowski K. Should the Histological Examination Be Used in the Diagnosis of Aneurysms of the Dorsalis Pedis Artery? A Case Report and Review of the Literature. Ann Vasc Surg. 2019;54:336.e1-336.e4. doi: 10.1016/j.avsg.2018.06.023.
7. Santos JHB, Santana BVRC, Brandão CMF, Lima CVBQ, Rego FN Neto, Araujo HJB, et al. Pseudoaneurysm of the Dorsalis Pedis Artery: A Case Report. Res Soc Dev. 2021;10(17):e69101724157. doi: 10.33448/rsd-v10i17.24157.
8. Bausells MI, Raymundo SRO, Silva AAM, Casagrande MR, Miquelin DG, Reis LF. Aneurysm of the Dorsalis Pedis Artery: Case Report and Literature Review. J Vasc Bras. 2003;2(1):26-8.
9. Erkut B, Ates A. Post-Traumatic Dorsalis Pedis Pseudo-Aneurysm Caused by Crush Injury. EJVES Short Rep. 2019;44:29-32. doi: 10.1016/j.ejvssr.2019.07.003.
10. Ferreira UG, Aragão JA, Lenik AA, Aragão ICS, Aragão FMS, Leão WB, et al. True Dorsalis Pedis Artery Aneurysm: Case Report. J Vasc Bras. 2018;17(2):152-5. doi: 10.1590/1677-5449.012817.

Hypocalcemia and Reversible Cardiomyopathy Assessed by Magnetic Resonance Imaging

Bruno Lenzi,[1] *Gustavo Tortajada,*[1] *Victoria Rabaza,*[1] *Ernesto Cairoli,*[1] *Gabriel Parma*[1]
Hospital Evangelico,[1] *Montevidéu – Uruguay*

Introduction

Calcium is a fundamental component of biological systems and plays a key role in excitation-contraction coupling in cardiac myocytes. Calcium entry triggers a mechanism known as calcium-induced calcium release, in which calcium released from the sarcoplasmic reticulum is modulated by the influx of calcium from the extracellular space. Muscle contraction subsequently occurs through the interaction between calcium and the troponin-tropomyosin complex. In the heart, intracellular calcium is the primary regulator of contractile force (inotropism).[1]

Hypocalcemia-induced cardiomyopathy is a rare condition with few reports in the scientific literature. We present a clinical case associated with hypoparathyroidism, one of the main causes of chronic hypocalcemia.[2] This case report includes a novel element: the use of cardiac Magnetic Resonance Imaging (cMRI), which, to our knowledge, has not been previously described in the literature.

Case report

A 74-year-old female patient with a history of thyroid cancer underwent total thyroidectomy 10 years ago, resulting in hypoparathyroidism as a consequence of the procedure. Other relevant medical history includes type 2 diabetes and hypertension. Cardiac function was evaluated eight months prior to the current consultation using transthoracic Doppler echocardiography, which reported a left ventricular ejection fraction (LVEF) of 55%. In the three months leading up to the consultation, the patient discontinued her pharmacological treatment with calcium, cholecalciferol, and calcitriol.

The patient complained at the emergency department with exertional dyspnea, asthenia and adynamia. Bilateral edema of the lower limbs and moist rales in the lung fields. She denies history of chest pain, palpitations, infections or exposure to cardiotoxic agents. Chvostek and Trousseau signs were absent.

Keywords

Cardiomyopathies; Hypocalcemia; Case Reports

Mailing Address: Bruno Lenzi •
Hospital Evangelico. Bvar. Batlle y Ordóñez 2759. Postal Code: 11600, Montevideo – Uruguay
E-mail: brunol22222@gmail.com
Manuscript received June 7, 2025; revised August 14, 2025; accepted September 30, 2025
Editor responsible for the review: Maria Otto

DOI: https://doi.org/10.36660/abcimg.20250048i

A 12-lead electrocardiogram (ECG) was performed (Figure 1), showing sinus rhythm at 80 beats per minute, narrow QRS complexes, diffuse T wave inversions, and a prolonged isoelectric ST segment, with a corrected QT interval (QTc) of 700 ms.

Initial blood tests revealed a serum calcium level of 4 mg/dL (reference range: 8.5–10.2 mg/dL) and an ionized calcium level of 0.61 mmol/L (reference range: 1.1–1.3 mmol/L). NT-proBNP was elevated at 2000 pg/mL (normal <300 pg/mL), while troponins were undetectable (<40 ng/dL). Renal function tests, standard electrolyte panel, complete blood count, and thyroid profile were all within normal limits.

Subsequently, a TTE was performed (Figure 2), showing a left ventricle with normal dimensions, diffuse hypokinesia, a LVEF of 28% (measured by the Biplane Simpson method), and severe secondary mitral regurgitation.

Intravenous and oral calcium supplementation was initiated. Intravenous furosemide was also started, along with bisoprolol (2.5 mg daily), ramipril (2.5 mg daily), and spironolactone (12.5 mg daily). Within seventy-two hours of starting treatment, the patient showed clear clinical improvement. Follow-up blood tests revealed a serum calcium level of 9.5 mg/dL and an ionized calcium level of 1.23 mmol/L. A repeat ECG showed positive T waves and a corrected QT interval (QTc) of 480 ms (Figure 3).

A new TTE revealed a LVEF of 35% and mild mitral insufficiency. All TTEs were performed by the same technician and using the same equipment.

Three days later, a cMRI was performed (Figure 4), showing global hypokinesia of the left ventricle with, a LVEF of 45% and mild mitral insufficiency. T1 mapping was 1061 ms and T2 mapping was 49 ms. Late gadolinium enhancement was observed at the intramyocardial level in the inferior, inferoseptal and inferolateral basal segments, consistent with a non-ischemic pattern. The late enhancement mass measured 4g representing 3.4% of the left ventricular mass.

The patient was discharged on calcium, calcitriol, and vitamin D supplementation, along with treatment for systolic dysfunction. Four weeks later, a TTE was performed, showing a LVEF of 60% (Figure 5).

Discussion

The link between calcium and myocardial contractility was established more than 150 years ago by Dr. Sidney Ringer.[3] During the 20th century, the relationship between serum calcium levels and ventricular function was experimentally demonstrated, revealing a linear relationship between calcium levels and inotropism.[4]

CONTENTS

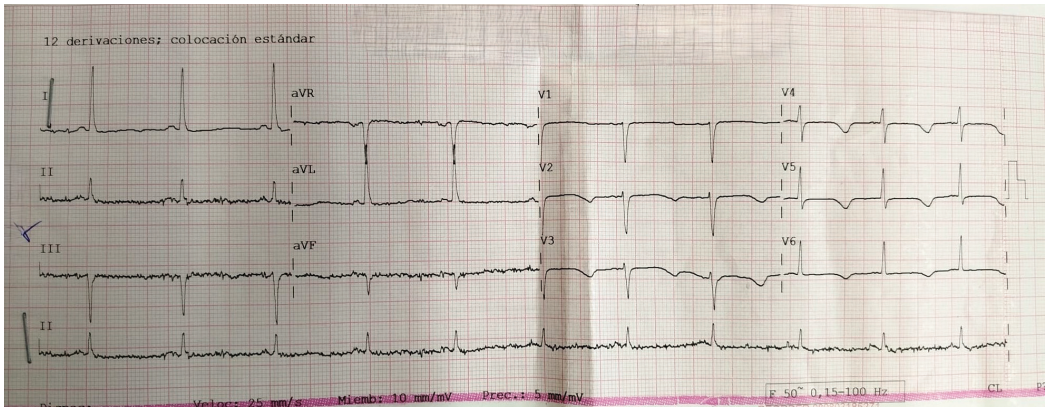

Figure 1 – *Echocardigram showing sinus rhythm, narrow QRS complexes, diffuse inverted T waves and a QTc of 700 ms.*

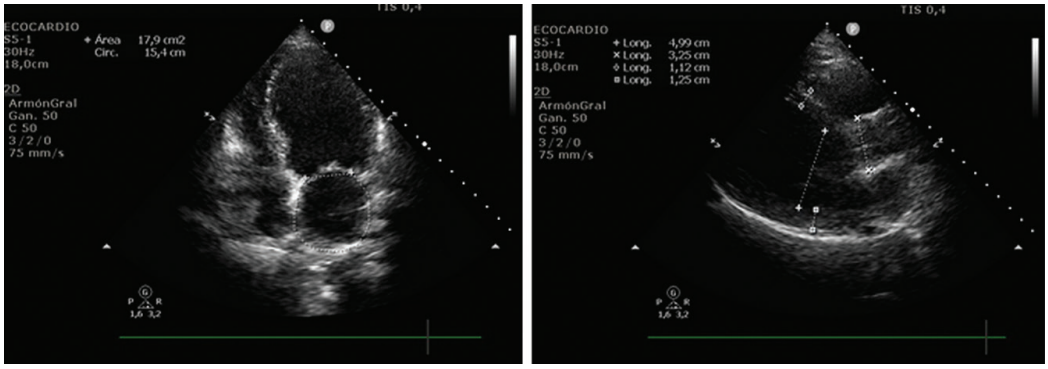

Figure 2 – *Transthoracic echocardiogram showing diffuse hypokinesia of the left ventricle and a left ventricular ejection fraction (LVEF) of 28%.*

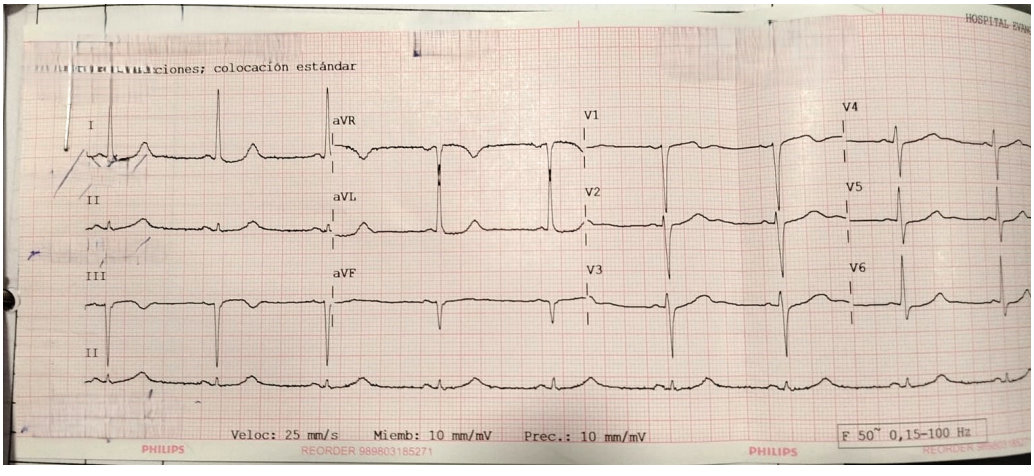

Figure 3 – *Echocardiogram showing positive T waves with a corrected QT interval of 480 ms.*

Case Report

Hypocalcemia is a rare etiology of cardiomyopathy, with few reports in the literature. The only systematic review published to date includes 47 patients from case series and reports, most of them secondary to hypoparathyroidism,[5] which is the main cause of chronic hypocalcemia.[6]

Most case reports highlight three features that characterize this condition as a distinct subtype of cardiomyopathy: a) a limited response to standard heart failure therapy, b) an association with chronic hypoparathyroidism, and c) its reversibility upon normalization of serum calcium levels.[5]

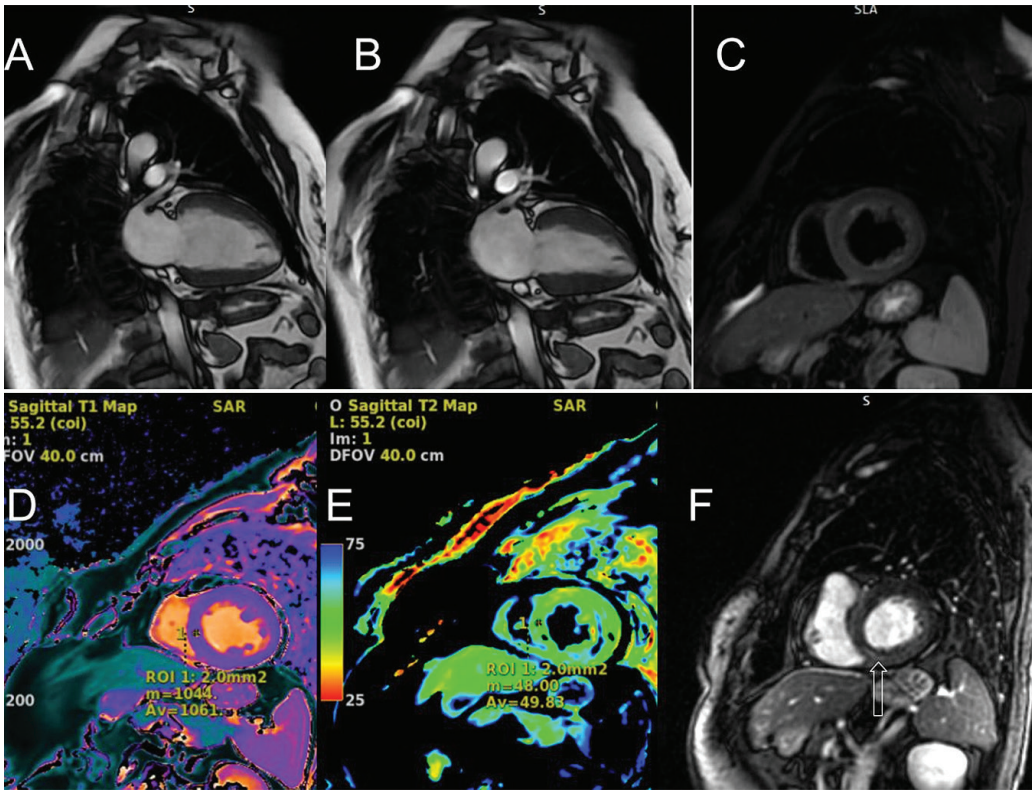

Figure 4 – *ardiac-MRI. Panels A and B show diastole and systole, respectively, in a two-chamber projection (FFPP). Panel C displays a T2-enhanced sequence. Panels D and E show the T1 and T2 mapping, respectively. Panel F displays a late gadolinium enhancement sequence (PSIR); the arrow indicates the site of enhancement.*

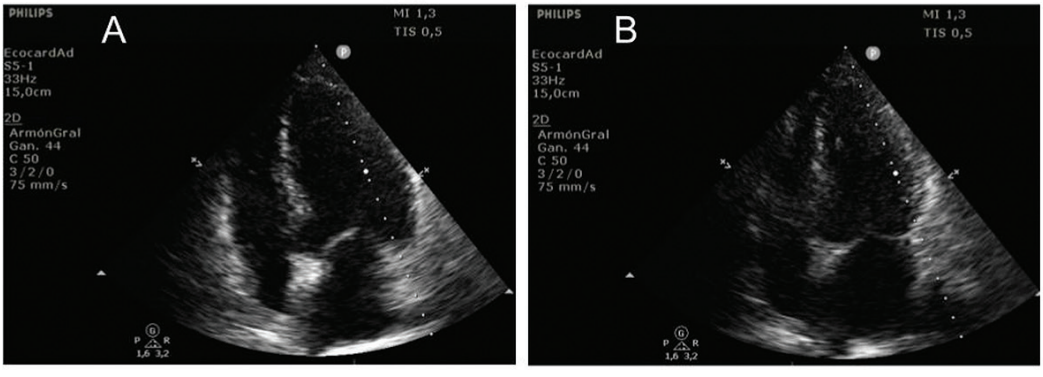

Figure 5 – *Transthoracic echocardiogram performed four weeks after discharge. Panel A shows the left ventricle in diastole, and Panel B in systole; the left ventricular ejection fraction (LVEF) was calculated at 60%.*

Regarding the pathophysiology of this condition, the leading theory suggests that reduced calcium influx through L-type channels impairs the sarcoplasmic reticulum's ability to elevate intracellular calcium levels via the calcium-induced calcium release mechanism. This disruption negatively affects actin–myosin cross-bridge formation, thereby reducing cardiac inotropism.[7-9]

Phase 2 of the cardiac action potential corresponds to the ST segment and T wave on the ECG. The ST segment reflects a balance between inward calcium currents and outward potassium currents. In hypocalcemia, the QTc interval is prolonged due to an extended isoelectric ST segment (plateau), which distinguishes it from other causes of QT prolongation. This phenomenon occurs because the termination of transmembrane calcium current relies on calcium flow through L-type channels via a mechanism known as calcium-mediated inactivation. Consequently, reduced calcium flow prolongs the duration of this current, leading to an extended ST segment.[10]

Our patient presented with transient systolic dysfunction, which showed rapid clinical and echocardiographic improvement following calcium administration. This supports the diagnosis of myocardial dysfunction secondary to severe hypocalcemia.

Cardiac MRI represents a novel diagnostic element in this context. The T2 mapping and T2-weighted sequences showed no evidence of edema, helping to rule out differential diagnoses such as acute myocarditis. The normal T1 values suggest minimal impact on overall myocardial composition. However, the observed fibrosis pattern evokes the possibility of a harmful agent or toxin affecting the myocardium. Could hypocalcemia trigger a degree of cellular dysfunction leading to myocyte necrosis and fibrosis?

Based on the rapid recovery of ventricular function following calcium replacement, as observed in this case and others, it is expected that this condition does not induce fibrosis or significant structural alterations. Instead, it likely involves a substrate of reversible myocardiopathic dysfunction linked to impaired actin–myosin interaction. In this context, the abnormalities seen on cardiac MRI may reflect an intercurrent condition such as chronic-phase myocarditis, hypertensive or diabetic cardiomyopathy, or a genetically determined cardiomyopathy, which could have amplified the myocardial depressant effects of hypocalcemia.

In conclusion, this case highlights a rare clinical entity that can be suspected based on clinical history and electrocardiographic findings. It was characterized through cardiac MRI and is associated with an excellent prognosis.

Author Contributions

Conception and design of the research: Lenzi B, Tortajada G, Rabaza V, Cairolli E, Parma G. Acquisition of data: Lenzi B. Analysis and interpretation of the data: Lenzi B, Tortajada G, Cairolli E. Writing of the manuscript: Lenzi B, Rabaza V. Critical revision of the manuscript for intellectual content: Tortajada G, Cairolli E, Parma G.

Potential Conflict of Interest

No potential conflict of interest relevant to this article was reported.

Sources of Funding

There were no external funding sources for this study.

Study Association

This study is not associated with any thesis or dissertation work.

Ethics Approval and Consent to Participate

This study was approved by the Ethics Committee of the Mutualista Hospital Evangélico under protocol number 110. All procedures involved in this study are in accordance with the Declaration of Helsinki of 1975, as revised in 2013. Informed consent was obtained from all participants included in the study.

Use of Artificial Intelligence

The authors did not use any artificial intelligence tools in the development of this work.

Availability of Research Data

The underlying content of the research text is contained within the manuscript.

References

1. Boron WF, Boulpaep EL. Medical physiology. 3rd ed. Philadelphia: Elsevier; 2016.
2. Bove-Fenderson E, Mannstadt M. Hypocalcemic Disorders. Best Pract Res Clin Endocrinol Metab. 2018;32(5):639-56. doi: 10.1016/j.beem.2018.05.006.
3. Ringer S. Concerning the Influence Exerted by Each of the Constituents of the Blood on the Contraction of the Ventricle. J Physiol. 1882;3(5-6):380-93. doi: 10.1113/jphysiol.1882.sp000111.
4. Lang RM, Fellner SK, Neumann A, Bushinsky DA, Borow KM. Left Ventricular Contractility Varies Directly with Blood Ionized Calcium. Ann Intern Med. 1988;108(4):524-9. doi: 10.7326/0003-4819-108-4-524.
5. Newman DB, Fidahussein SS, Kashiwagi DT, Kennel KA, Kashani KB, Wang Z, et al. Reversible Cardiac Dysfunction Associated with Hypocalcemia: A Systematic Review and Meta-Analysis of Individual Patient Data. Heart Fail Rev. 2014;19(2):199-205. doi: 10.1007/s10741-013-9371-1.
6. Bjornsdottir S, Ing S, Mitchell DM, Sikjaer T, Underbjerg L, Hassan-Smith Z, et al. Epidemiology and Financial Burden of Adult Chronic

Hypoparathyroidism. J Bone Miner Res. 2022;37(12):2602-14. doi: 10.1002/jbmr.4675.

7. Bansal B, Bansal M, Bajpai P, Garewal HK. Hypocalcemic Cardiomyopathy-Different Mechanisms in Adult and Pediatric Cases. J Clin Endocrinol Metab. 2014;99(8):2627-32. doi: 10.1210/jc.2013-3352.

8. Santos TS, Carvalho AC. Hypocalcemic Cardiomyopathy - A Rare and Reversible Entity. Am J Emerg Med. 2022;51:426.e1-426.e3. doi: 10.1016/j.ajem.2021.06.060.

9. Lozano PJM, Junyent JMG. Hypocalcaemia: An Unusual and Potentially Reversible Cause of Dilated Cardiomyopathy. Med Clin. 2011;136(3):133-4. doi: 10.1016/j.medcli.2009.11.010.

10. Kramer DB, Zimetbaum PJ. Long-QT Syndrome. Cardiol Rev. 2011;19(5):217-25. doi: 10.1097/CRD.0b013e3182203504.

Acute Thrombosis During Ductus Arteriosus Stenting Successfully Treated with Balloon Angioplasty and In Situ Alteplase Infusion: Case Report

Jonathan Guimarães Lombardi,[1] Paulo Correia Calamita,[1] Mayra Rosana Palmeira Barreto,[1,2] Luiza Silveira Neves Ficht,[2] Giulliano Gardenghi[3,4]

Hospital Estadual de Urgências Governador Otávio Lage de Siqueira,[1] Goiânia, GO – Brazil
CRD Medicina Diagnóstica,[2] Goiânia, GO – Brazil
Hospital Encore,[3] Aparecida de Goiânia, GO – Brazil
Clínica de Anestesia de Goiânia,[4] Goiânia, GO – Brazil

Introduction

Tricuspid atresia with pulmonary atresia is a rare congenital heart defect, representing about 1% to 3% of all congenital heart diseases.[1] Tricuspid atresia is subdivided into type I (normal position of the great arteries) and type II (transposition of the great arteries), with type 1A characterized by the presence of associated pulmonary atresia or stenosis.[2] Pulmonary blood flow in these patients is dependent on the patency of the ductus arteriosus, making its maintenance essential in the neonatal period.

The treatment of tricuspid atresia follows a staged surgical approach, aiming for a Fontan circulation as the final goal. In the neonatal period, the focus is to ensure adequate pulmonary blood flow through hemodynamic or surgical interventions, including systemic-pulmonary shunts or ductal interventions.[3]

This case report describes a newborn with type 1A tricuspid atresia who underwent a hemodynamic intervention with stent implantation in the ductus arteriosus, discussing technical aspects of the procedure, complications, and clinical evolution.

Case report

A term male newborn weighing 2,920 g was transferred at 6 days of life to a cardiac intensive care unit. The patient was hemodynamically stable, with oxygen saturation of 85% in room air, and was receiving a continuous intravenous infusion of prostaglandin at 0.01 mcg/kg/min. Transthoracic echocardiography demonstrated tricuspid valve atresia, pulmonary valve atresia, a hypoplastic right ventricle, the aorta arising from the left ventricle, and a tortuous ductus arteriosus (type 1A tricuspid atresia) (Figure 1). Chest computed tomography angiography showed a tortuous ductus arteriosus and stenosis at the origin of the left pulmonary artery (Figure 2). The patient also had a multicystic dysplastic left kidney. After multidisciplinary discussion, ductal stenting was chosen as a palliative procedure in the neonatal period.

Interventional procedure

Due to the angle between the aortic end of the ductus arteriosus and the aortic arch, the right carotid artery was chosen as the access route. To improve catheter and guidewire manipulation and ergonomics, the patient was positioned in reverse orientation on the hemodynamic table (Figure 3).

The right carotid artery was punctured under ultrasound guidance, and a 5F slender transradial introducer was placed. Intravenous heparin (100 IU/kg) and prophylactic cefazolin (50 mg/kg) were administered. Left heart catheterization and cineangiography confirmed the tortuous ductal anatomy and the stenosis at the origin of the left pulmonary artery (proximal to the ductal insertion). A 0.014″ Balance Heavy Weight (BHW) guidewire was placed in the left pulmonary artery with microcatheter support. A Mini Trek 2 × 8 mm balloon catheter was positioned in the ductal trajectory for radiopaque landmark-based measurements. At this point, the patient developed decreased end-tidal carbon dioxide ($ETCO_2$) and oxygen saturation, with significant ductal spasm and reduced effective pulmonary flow. Continuous adrenaline infusion was started. The BHW guidewire was replaced with an exchange-length 0.014″ wire. With guidewire support, an Inspiron 4 × 19 mm stent was implanted in the ductus arteriosus (Figure 4).

The patient showed transient improvement in saturation and $ETCO_2$, but a few minutes later developed significant hypoxemia, decreased $ETCO_2$, and bradycardia. Acute stent thrombosis was identified, and in situ alteplase was administered as a 0.05 mg/kg bolus, followed by continuous infusion at 0.5 mg/kg/h. Sequential balloon angioplasty of the entire stent with a Trek 4 × 12 mm balloon catheter was performed. These measures restored

Keywords

Congenital Heart Defects; Tricuspid Atresia; Ductus Arteriosus; Percutaneous Coronary Intervention; Thrombosis

Mailing Address: Giulliano Gardenghi •
Hospital Encore. Rua Gurupi, Qd.25, Lt.06/08. Postal code: 74905-350. Setor Vila Brasília, Aparecida de Goiânia, GO - Brazil
E-mail: coordenacao.cientifica@ceafi.edu.br
Manuscript received October 12, 2025, revised manuscript November 17, 2025, accepted December 17, 2025
Editor responsible for the review: Márcio Brito

DOI: https://doi.org/10.36660/abcimg.20250084i

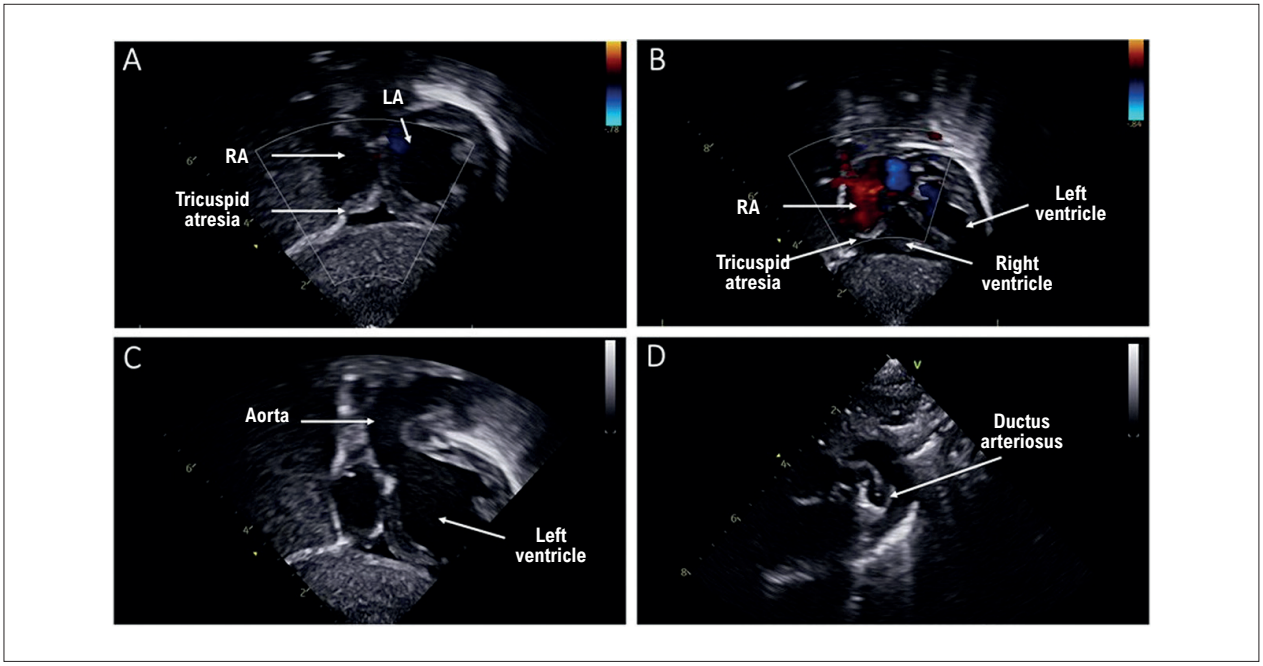

Figure 1 – *Transthoracic echocardiography. A and B) Patent foramen ovale and atretic tricuspid valve. C) Left ventricle connected to the aorta. D) Tortuous patent ductus arteriosus. LA: left atrium; RA: right atrium.*

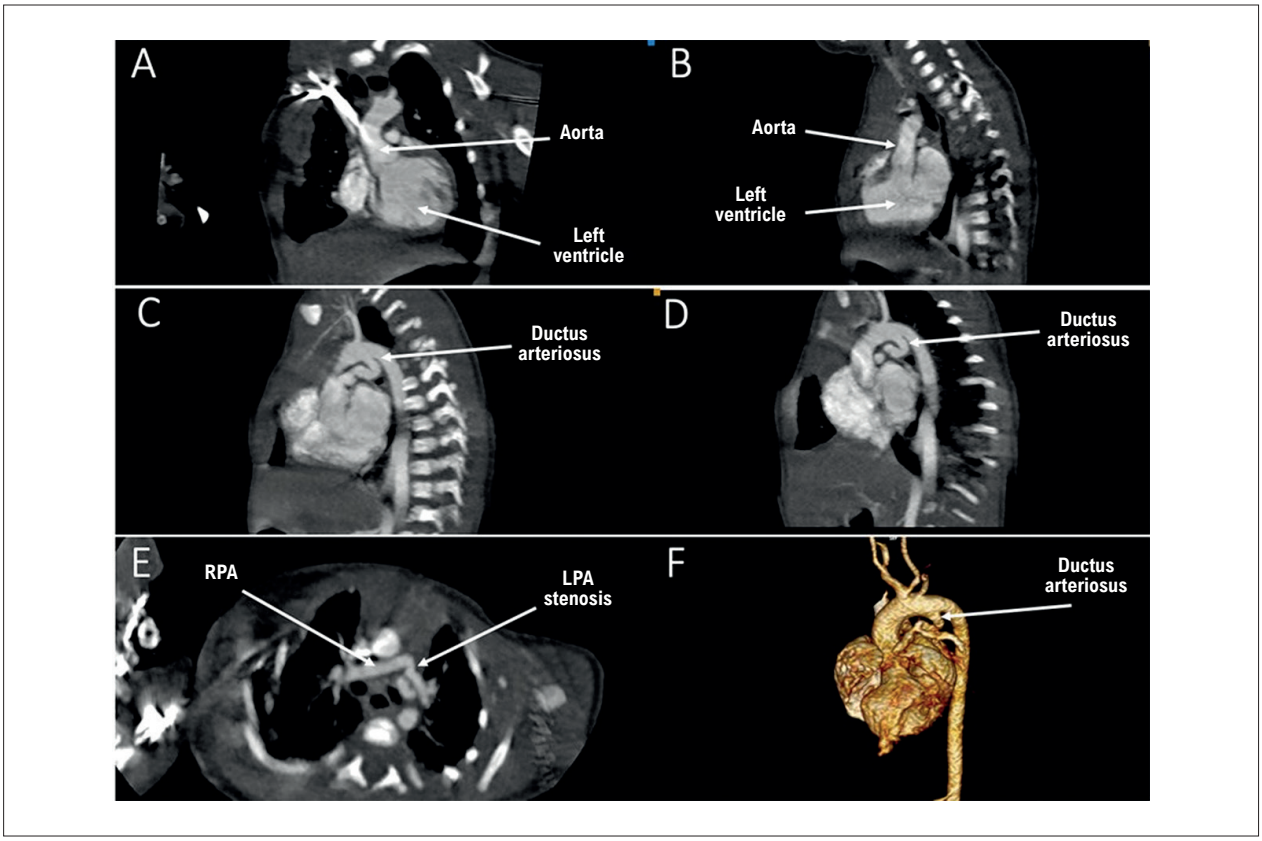

Figure 2 – *Aortic computed tomography angiography. A and B) Left ventricle connected to the aorta. C and D) Markedly tortuous patent ductus arteriosus. E) Stenosis at the origin of the left pulmonary artery. E) Three-dimensional reconstruction showing the anatomy of the ductus arteriosus. LPA: left pulmonary artery; RPA: right pulmonary artery.*

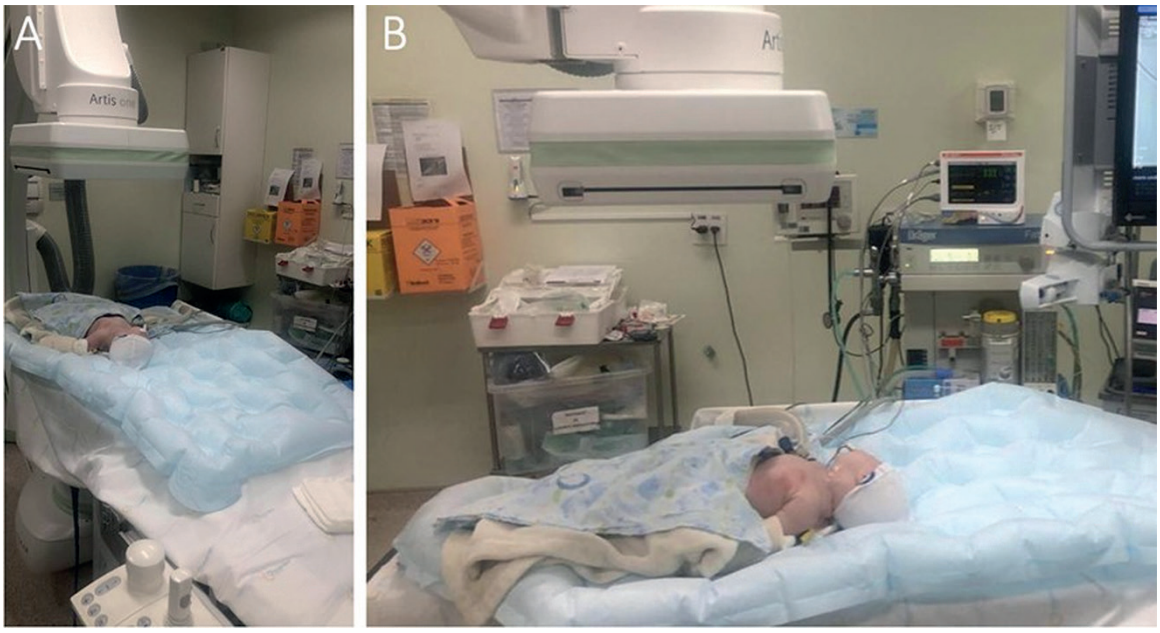

Figure 3 – *A and B) Image showing the patient positioned in reverse orientation on the catheterization table (with the cranial portion away from the radiation source).*

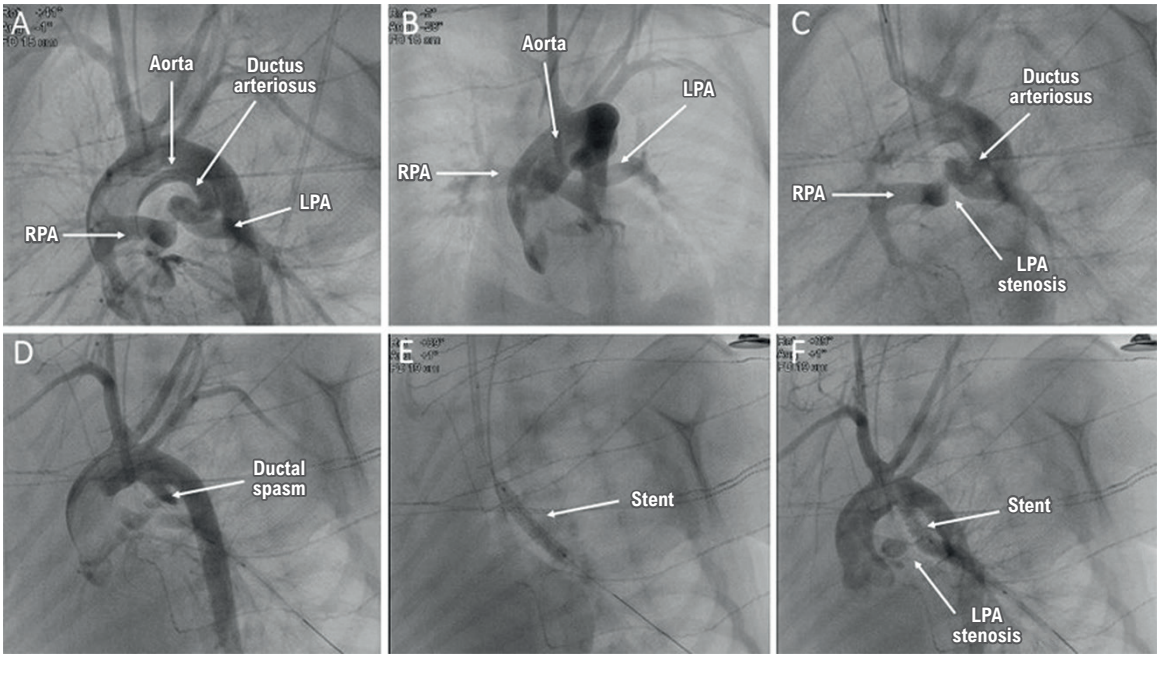

Figure 4 – *Percutaneous intervention. A, B, and C) Angiograms obtained via carotid access showing a tortuous ductus arteriosus and stenosis at the origin of the left pulmonary artery. D) With the support of a 0.014" BHW guidewire positioned in the left pulmonary artery, a Mini Trek 2 × 8 mm balloon catheter was placed along the ductal trajectory; at this moment, ductal spasm was observed. E) An Inspiron 4 × 19 mm stent was implanted in the ductus arteriosus. F) Angiogram showing preserved flow through the ductal stent but with worsening stenosis at the origin of the left pulmonary artery. LPA: left pulmonary artery; RPA: right pulmonary artery.*

ductal flow and partially improved heart rate, oxygen saturation, and $ETCO_2$.

Stenosis at the origin of the left pulmonary artery significantly restricted flow to the pulmonary trunk and right pulmonary artery. Proximal optimization technique (POT) was used with a 4 × 8 mm balloon (inflated to burst pressure). With the support of a JR 4F catheter, a 0.014″ guidewire was placed in the right pulmonary artery through the lateral mesh of the prior stent. Balloon angioplasty of the right pulmonary artery origin was then performed with a Trek 3 × 12 mm balloon (opening the lateral mesh of the previous stent) (Figure 5). After balloon angioplasty, the guidewire was withdrawn from the right pulmonary artery, but the stenosis at the origin of the left pulmonary artery persisted.

The 0.014″ guidewire was then repositioned in the right pulmonary artery, and an Inspiron 3.5 × 9 mm stent was implanted through the lateral mesh of the previous stent, directed toward the origin of the left pulmonary artery and the pulmonary trunk (Figure 6). The introducer was removed, and manual hemostatic compression and compressive occlusive dressing were applied.

The patient was transferred to the intensive care unit on mechanical ventilation and continuous intravenous adrenaline (0.1 mcg/kg/min). Alteplase continued for another 3 hours but discontinued due to bleeding at the puncture and central venous access sites. Grade I left intracranial hemorrhage was detected on post-procedure transfontanellar ultrasound, which normalized on follow-up 3 months later. The patient had infectious complications such as pneumonia and sepsis with positive blood cultures for *Pseudomonas aeruginosa*, treated with broad-spectrum antibiotics. He also experienced extubation failure and prolonged mechanical ventilation (total of 49 days). Hospitalization was prolonged, with discharge 3 months after the procedure. Transthoracic echocardiography showed patent stents with adequate flow through the ductus arteriosus and pulmonary branches. Clinically, the patient remains hemodynamically stable, with oxygen saturation of 84% in room air, and is being followed for planned Glenn surgery.

Discussion

Tricuspid atresia with pulmonary atresia is one of the most complex challenges in interventional pediatric cardiology, especially because of the absolute dependence on ductal flow for pulmonary perfusion in the neonatal period.[4,5] This case illustrates the multiple layers of anatomic and technical complexity involved in the management of these patients, highlighting both the therapeutic possibilities and the inherent limitations and complications of interventional procedures in high-risk neonates.

Ductal stenting has emerged as a viable and often preferable alternative to surgical shunts in selected neonates,

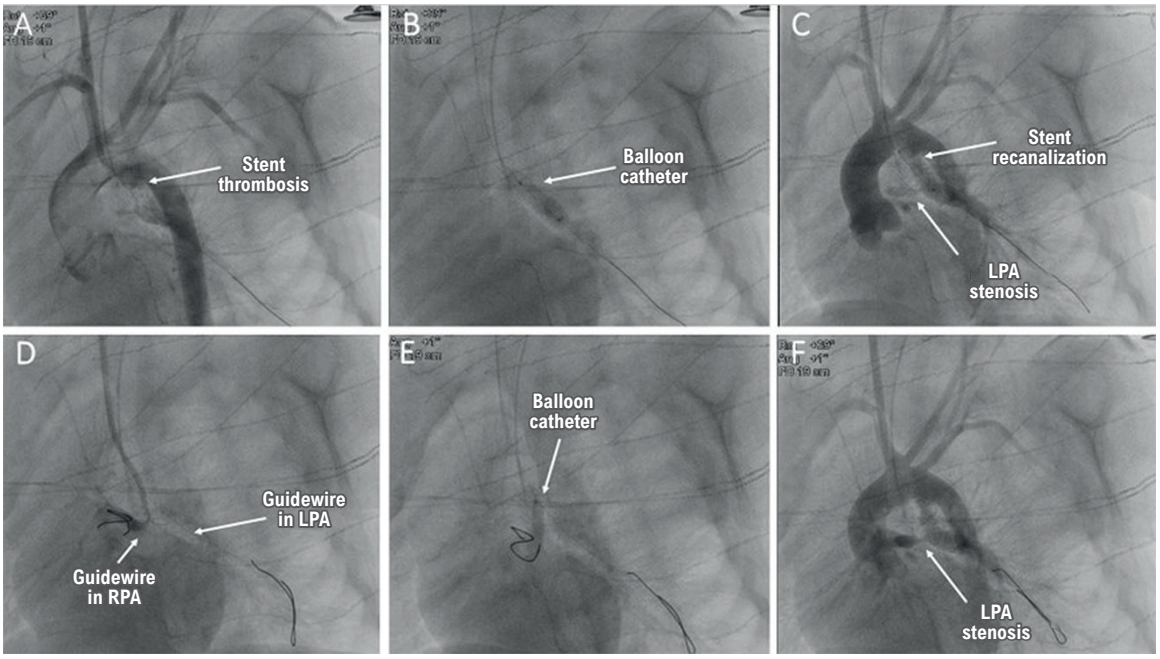

Figure 5 – *Percutaneous intervention. A) Angiography showing acute thrombosis of the ductal stent. B) Angioplasty with a 4 × 12 mm Trek balloon catheter along the entire length of the stent. C) Angiography demonstrating effective recanalization of the stent. D) Guidewire positioned in the right pulmonary artery through the lateral struts of the stent. E) Angioplasty with a 3 × 12 mm Trek balloon catheter (opening the lateral struts of the previous stent). F) Guidewire withdrawn from the right pulmonary artery, showing persistence of stenosis at the origin of the left pulmonary artery. RPA: right pulmonary artery; LPA: left pulmonary artery.*

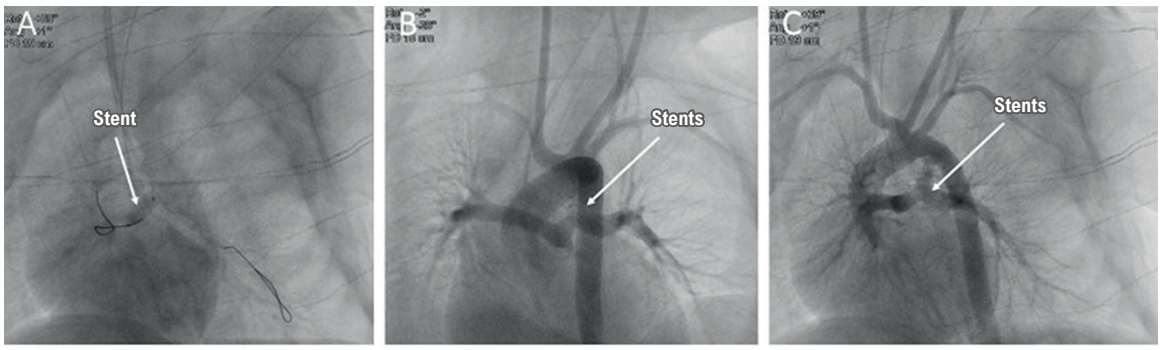

Figure 6 – *Percutaneous intervention. A) Implantation of an Inspiron 3.5 × 9 mm stent through the lateral mesh of the previous stent. B and C) Angiograms showing adequate flow through the stent assembly from the ductus arteriosus to both pulmonary arteries.*

offering significant advantages in terms of perioperative morbidity and mortality.[6,7] Recent comparative studies have shown similar survival rates between the two therapeutic modalities, but with a lower incidence of immediate complications in the percutaneous intervention group.[8,9] However, appropriate patient selection remains critical, considering factors such as neonatal weight, ductal anatomy, associated pulmonary stenoses, and pre-procedure hemodynamic stability.[10,11]

The angle formed between the aortic end of the ductus arteriosus and the aortic arch, as seen in this case, is an anatomical limitation that requires significant technical adaptations, including changes in patient positioning and careful selection of the vascular access route.[12-14] The extreme ductal tortuosity[15] combined with the short length of the pulmonary branches in a newborn complicates coronary guidewire navigation and the support it provides for stent delivery. The use of specific materials such as a microcatheter and more than one 0.014″ guidewire positioned simultaneously makes the procedure feasible. Pre-existing pulmonary branch stenosis prior to stent implantation is a risk factor for worsening stenosis and total occlusion of a pulmonary branch.[16] Techniques such as positioning a 0.014″ guidewire in each pulmonary branch during stent implantation can increase procedural safety by maintaining patency of the stenotic pulmonary branch and facilitating the opening of the stent's lateral mesh. In this case, this technique was not possible because the patient developed acute clinical deterioration during guidewire manipulation within the ductus, causing ductal spasm.

The occurrence of acute stent thrombosis is one of the most feared complications in neonatal procedures, with an incidence of 2% to 3%. Predisposing factors include elevated hematocrit, prolonged procedure time, endothelial trauma during manipulation, and activation of the coagulation cascade secondary to the prosthetic material. Immediate treatment with local fibrinolytics, as demonstrated in this case with alteplase, has been effective, allowing successful recanalization with low risk of systemic bleeding. Sequential mechanical angioplasty of the stent also restores adequate flow quickly and sustainably.[10,17]

The technique of stent implantation through the lateral mesh of a previously placed stent ("stent-in-stent") used to address stenosis at the origin of the left pulmonary artery represents a significant technical innovation in pediatric interventional cardiology. The literature documents growing experience with this technique in various anatomical situations, demonstrating medium-term safety and efficacy.[18,19]

The complications observed in this case, including grade I intracranial hemorrhage and hospital-acquired infections, reflect the fragility of neonates undergoing complex and prolonged interventional procedures. Intracranial hemorrhage, possibly related to the use of fibrinolytics, is a known but relatively rare complication, requiring strict neurological monitoring in the post-procedural period.[20,21] The development of nosocomial infections in critically ill patients on prolonged mechanical ventilation is an additional challenge in post-intervention management, demanding rigorous prevention and early treatment protocols. The favorable medium-term outcome, with maintained stent patency and hemodynamic stability, supports the efficacy of the chosen therapeutic strategy and the use of this approach as an effective bridge to subsequent surgical staging in selected patients.[22,23]

Conclusion

This case demonstrates the feasibility and efficacy of hemodynamic intervention in neonates with type 1A tricuspid atresia. Ductal stenting allowed for adequate pulmonary blood flow and clinical stabilization. The observed complications, including acute stent thrombosis, worsening of left pulmonary artery origin stenosis after ductal stenting, and hemodynamic instability, reflect the complexity of neonatal procedures and the need for rapid and effective medical (fibrinolytic) and interventional (balloon angioplasty of the thrombosed stent, POT technique, balloon and stent angioplasty through the lateral stent mesh) strategies. The favorable medium-term outcome, with preserved pulmonary flow and ventricular function, supports the use of this technique as a bridge to future surgical staging in selected patients.

Author Contributions

Conception and design of the research and writing of the manuscript: Lombardi JG, Gardenghi G; acquisition of data: Lombardi JG, Calamita PC, Barreto MRP, Ficht LSN, Gardenghi G; analysis and interpretation of the data: Lombardi JG, Calamita PC, Barreto MRP; critical revision of the manuscript for intellectual content: Calamita PC, Barreto MRP, Ficht LSN, Gardenghi G.

Potential Conflict of Interest

No potential conflict of interest relevant to this article was reported.

Sources of Funding

There were no external fundingsources for this study.

Study Association

This study is not associated with any thesis or dissertation work.

Ethics Approval and Consent to Participate

This study was approved by the Ethics Committee of the CEP do Hospital de Urgëncias de Goiás under the protocol number 85497418.2.0000.0033. All the procedures in this study were in accordance with the 1975 Helsinki Declaration, updated in 2013. Informed consent was obtained from all participants included in the study.

Use of Artificial Intelligence

The authors did not use any artificial intelligence tools in the development of this work.

Availability of Research Data

The data cannot be made publicly available due to legal considerations related to Brazil's General Data Protection Law, as the data could allow the identification of the patient in the case in question.

References

1. Minocha PK, Horenstein MS, Phoon C. Tricuspid Atresia. Treasure Island: StatPearls Publishing; 2024.
2. Karamlou T, Ashburn DA, Caldarone CA, Blackstone EH, Jonas RA, Jacobs ML, et al. Matching Procedure to Morphology Improves Outcomes in Neonates with Tricuspid Atresia. J Thorac Cardiovasc Surg. 2005;130(6):1503-10. doi: 10.1016/j.jtcvs.2005.07.024.
3. Downing TE, Boucek DM, Glatz AC, Qureshi AM, Zampi JD, Petit CJ, et al. Stenting the Ductus Arteriosus in Neonates with Ductal-Dependent Pulmonary Blood Flow: Technical and Anatomic Considerations. Pediatr Cardiol. 2025. doi: 10.1007/s00246-025-03834-4.
4. Schranz D, Michel-Behnke I, Heyer R, Vogel M, Bauer J, Valeske K, et al. Stent Implantation of the Arterial Duct in Newborns with a Truly Duct-Dependent Pulmonary Circulation: A Single-Center Experience with Emphasis on Aspects of the Interventional Technique. J Interv Cardiol. 2010;23(6):581-8. doi: 10.1111/j.1540-8183.2010.00576.x.
5. Mini N, Schneider MBE, Asfour B, Mikus M, Zartner PA. Duct Stenting vs. Modified Blalock-Taussig Shunt: New Insights Learned from High-Risk Patients with Duct-Dependent Pulmonary Circulation. Front Cardiovasc Med. 2022;9:933959. doi: 10.3389/fcvm.2022.933959.
6. Bentham JR, Zava NK, Harrison WJ, Shauq A, Kalantre A, Derrick G, et al. Duct Stenting versus Modified Blalock-Taussig Shunt in Neonates with Duct-Dependent Pulmonary Blood Flow: Associations with Clinical Outcomes in a Multicenter National Study. Circulation. 2018;137(6):581-8. doi: 10.1161/CIRCULATIONAHA.117.028972.
7. Glatz AC, Petit CJ, Goldstein BH, Kelleman MS, McCracken CE, McDonnell A, et al. Comparison between Patent Ductus Arteriosus Stent and Modified Blalock-Taussig Shunt as Palliation for Infants with Ductal-Dependent Pulmonary Blood Flow: Insights from the Congenital Catheterization Research Collaborative. Circulation. 2018;137(6):589-601. doi: 10.1161/CIRCULATIONAHA.117.029987.
8. Boucek DM, Qureshi AM, Goldstein BH, Petit CJ, Glatz AC. Blalock-Taussig Shunt versus Patent Ductus Arteriosus Stent as First Palliation for Ductal-Dependent Pulmonary Circulation Lesions: A Review of the Literature. Congenit Heart Dis. 2019;14(1):105-9. doi: 10.1111/chd.12707.
9. Li D, Zhou X, Li M. Arterial Duct Stent versus Surgical Shunt for Patients with Duct-Dependent Pulmonary Circulation: A Meta-Analysis. BMC Cardiovasc Disord. 2021;21(1):9. doi: 10.1186/s12872-020-01817-2.
10. Alwi M. Stenting the Ductus Arteriosus: Case Selection, Technique and Possible Complications. Ann Pediatr Cardiol. 2008;1(1):38-45. doi: 10.4103/0974-2069.41054.
11. Bahaidarah S, Al-Ata J, Alkhushi N, Azhar A, Zaher Z, Alnahdi B, et al. Outcome of Ductus Arteriosus Stenting Including Vertical Tubular and Convoluted Tortuous Ducts with Emphasis on Technical Considerations. Egypt Heart J. 2021;73(1):83. doi: 10.1186/s43044-021-00210-4.
12. Choudhry S, Balzer D, Murphy J, Nicolas R, Shahanavaz S. Percutaneous Carotid Artery Access in Infants < 3 Months of Age. Catheter Cardiovasc Interv. 2016;87(4):757-61. doi: 10.1002/ccd.26310.
13. Bauser-Heaton H, Qureshi AM, Goldstein BH, Glatz AC, Nicholson GT, Meadows JJ, et al. Use of Carotid and Axillary Artery Approach for Stenting the Patent Ductus Arteriosus in Infants with Ductal-Dependent Pulmonary Blood Flow: A Multicenter Study from the Congenital Catheterization Research Collaborative. Catheter Cardiovasc Interv. 2020;95(4):726-33. doi: 10.1002/ccd.28631.
14. Bauser-Heaton H, Qureshi AM, Goldstein BH, Glatz AC, Petit CJ. Use of Novel "Flip Technique" Aids in Percutaneous Carotid Artery Approach in Neonates. JACC Cardiovasc Interv. 2019;12(16):1630-1. doi: 10.1016/j.jcin.2019.04.053.
15. Qureshi AM, Goldstein BH, Glatz AC, Agrawal H, Aggarwal V, Ligon RA, et al. Classification Scheme for Ductal Morphology in Cyanotic Patients with Ductal Dependent Pulmonary Blood Flow and Association with Outcomes of Patent Ductus Arteriosus Stenting. Catheter Cardiovasc Interv. 2019;93(5):933-43. doi: 10.1002/ccd.28125.
16. Koneti NR, Bakhru S, Dhulipudi B, Rajan S, Sreeram N. Stent Strut Dilation in Branch Pulmonary Artery Stenosis Following Stenting of Arterial Duct in Duct-Dependent Pulmonary Circulation. Pediatr Cardiol. 2025;46(1):53-60. doi: 10.1007/s00246-023-03319-2.
17. Bauser-Heaton H, Price K, Weber R, El-Said H. Stenting of the Patent Ductus Arteriosus: A Meta-Analysis and Literature Review. J Soc Cardiovasc Angiogr Interv. 2022;1(6):100392. doi: 10.1016/j.jscai.2022.100392.
18. Wu H, Li M, Lin C. Influence of Balloon Location during Proximal Optimization Technique (POT): A Finite Element Analysis. J Biomech. 2021;127:110703. doi: 10.1016/j.jbiomech.2021.110703.
19. Darremont O, Leymarie JL, Lefèvre T, Albiero R, Mortier P, Louvard Y. Technical Aspects of the Provisional Side Branch Stenting Strategy. EuroIntervention. 2015;11(Suppl V):V86-90. doi: 10.4244/EIJV11SVA19.

20. Wang M, Hays T, Balasa V, Bagatell R, Gruppo R, Grabowski EF, et al. Low-Dose Tissue Plasminogen Activator Thrombolysis in Children. J Pediatr Hematol Oncol. 2003;25(5):379-86. doi: 10.1097/00043426-200305000-00006.

21. Will A. Neonatal Haemostasis and the Management of Neonatal Thrombosis. Br J Haematol. 2015;169(3):324-32. doi: 10.1111/bjh.13301.

22. Jayaram N, Spertus JA, Kennedy KF, Vincent R, Martin GR, Curtis JP, et al. Modeling Major Adverse Outcomes of Pediatric and Adult Patients with Congenital Heart Disease Undergoing Cardiac Catheterization: Observations from the NCDR IMPACT Registry (National Cardiovascular Data Registry Improving Pediatric and Adult Congenital Treatment). Circulation. 2017;136(21):2009-19. doi: 10.1161/CIRCULATIONAHA.117.027714.

23. Wang X, Li S, Huo D, Zhu Z, Wang W, He H, et al. Nosocomial Infections after Pediatric Congenital Heart Disease Surgery: Data from National Center for Cardiovascular Diseases in China. Infect Drug Resist. 2024;17:1615-23. doi: 10.2147/IDR.S457991.

Intramyocardial Cardiac Tumor: A Case Report

Luisa Latado,[1] *Fabio Figueiredo Costa,*[1] *Carlos Frederico Lopes Benevides,*[1] *Jorge Andion Torreão,*[2] *Adna Keyne Lima,*[3] *Adelina Sanches de Melo,*[4] *Adriana Lopes Latado*[1]

Universidade Federal da Bahia,[1] *Salvador, BA – Brazil*
Hospital Cardio Pulmonar, IDOR, Instituto D'or de Pesquisa e Ensino,[2] *Salvador, BA – Brazil*
Delfin Medicina Diagnóstica,[3] *Salvador, BA – Brazil*
Hospital Santa Izabel,[4] *Salvador, BA – Brazil*

Introduction

Primary cardiac tumors are rare entities, approximately 75% of which are benign, with myxoma as the most common type.[1,2] Only about 15% of primary cardiac tumors are malignant, predominantly sarcomas.[2] In contrast, metastatic cardiac involvement is relatively frequent and has been identified in up to 9% of patients who died from cancer.[3]

Clinical manifestations are more closely related to tumor location than to histopathological classification. They may result from embolic phenomena, intracardiac obstruction with signs of heart failure (HF), valvular involvement, myocardial invasion with alterations in contractile function and electrical conduction, and pericardial involvement with the risk of effusion and cardiac tamponade, among other presentations.[4]

The diagnostic approach is primarily based on imaging methods. Echocardiography is the initial examination of choice and may be complemented by computed tomography (CT) or cardiac magnetic resonance (CMR).[5] Positron emission tomography–CT (PET-CT) is useful for assessing the metabolic activity of the lesion, assisting in the differentiation between benign and malignant tumors, identifying metastatic cardiac involvement,[6] and defining the most appropriate site for biopsy when distant lesions are present.[7] Cardiac catheterization allows evaluation of the tumor's vascular supply.[7] In selected situations, image-guided endomyocardial biopsy based on preoperative imaging findings may contribute to therapeutic decision-making.[8]

Treatment depends fundamentally on tumor type. Surgical resection is indicated in most cases of myxomas and sarcomas. Myxomas have a low risk of recurrence after complete resection, whereas cardiac sarcomas are more frequently associated with tumor recurrence.[9,10] In the context of metastatic cardiac involvement, surgical resection is reserved for carefully selected cases.[8]

Keywords

Case Reports; Heart Neoplasms; Cardiovascular Diseases

Mailing Address: Luisa Latado •
Universidade Federal da Bahia, Faculdade de Medicina da Bahia. Avenida Reitor Miguel Calmon, s/n. Postal Code: 40110-100. Salvador, BA – Brazil
E-mail: luisa.latado@gmail.com
Manuscript received June 8, 2025, revised manuscript November 6, 2025, accepted November 16, 2025
Editor responsible for the review: Isabela Costa

DOI: https://doi.org/10.36660/abcimg.20250051i

Because of the rarity of these conditions and the diagnostic challenges often involved, clinical case reports of cardiac tumors are relevant because they highlight the role and impact of a multimodal cardiovascular imaging approach in differential diagnosis and clinical decision-making. Accordingly, this article aims to report the case of a patient with a primary intramyocardial cardiac tumor.

Case report

A 57-year-old woman, self-identified as mixed race, born and residing in the state of Bahia, Brazil, began cardiology follow-up in 2017 due to poorly characterized precordial chest pain and dyspnea on moderate exertion. Her medical history included systemic arterial hypertension, diabetes mellitus, and dyslipidemia, with no family history of neoplasms. She was on regular treatment with acetylsalicylic acid, hydrochlorothiazide, losartan, amlodipine, spironolactone, atenolol, metformin, and simvastatin. Previous laboratory tests showed isolated elevation of low-density lipoprotein cholesterol.

Electrocardiography showed sinus rhythm with nonspecific ventricular repolarization abnormalities in the inferior wall of the left ventricle. Chest radiography revealed no significant abnormalities. 24-hour Holter monitoring demonstrated sinus rhythm with preserved atrioventricular and intraventricular conduction and no relevant arrhythmias.

Initial transthoracic echocardiography revealed a left ventricular ejection fraction (LVEF) of 42% by the Simpson method, associated with inferodorsolateral akinesia and apical dyskinesia. In view of these findings, medical therapy for HF was optimized, and cardiac catheterization with hemodynamic assessment and coronary angiography was performed to exclude coronary artery disease and guide therapeutic management. The examination showed no evidence of obstructive coronary atherosclerotic disease. Serological tests for Chagas disease, viral infections, and the venereal disease research laboratory test were negative, as was the autoimmune antibody panel.

CMR and CT of the chest and abdomen were subsequently requested. CT scans showed no lymphadenopathy or findings suggestive of infiltrative or neoplastic disease. CMR performed in December 2021 demonstrated a hypointense lesion located in the mid-basal inferolateral segment of the left ventricle, measuring 5.6 × 2.7 × 2.3 cm, associated with marked edema and late gadolinium enhancement, suggestive of a tumoral lesion. The CMR findings were

compatible with a benign lesion, with fibroma considered the leading diagnostic hypothesis. Given the patient's clinical stability and an apparently unfavorable risk–benefit ratio for invasive intervention, a strategy of periodic clinical and imaging follow-up was adopted.

In May 2022, repeat CMR demonstrated growth of the intramyocardial lesion, which measured 6.0 × 5.4 × 3.2 cm (Figure 1). Evaluation by the Oncology team recommended PET-CT with fluorine-18 fluorodeoxyglucose (^{18}F-FDG) and repeat whole-body CT imaging. PET-CT performed in June 2022 showed a hypodense lesion in the inferolateral wall of the left ventricle without significant metabolic activity, of indeterminate nature, and unable to exclude fibrosis or a neoplastic process with low ^{18}F-FDG avidity (Figure 2). No suspicious extracardiac lesions were identified on CT, and serum tumor markers were within normal limits.

After further multidisciplinary discussion, the most likely diagnosis was considered to be a fibrous lesion, such as fibroma or elastoma, or alternatively a low-grade mesenchymal tumor, based on imaging findings and the indolent clinical course. Image-guided endomyocardial biopsy, which could provide a definitive diagnosis, was deemed to carry a high risk of complications by the surgical team. Therefore, a shared decision was made to continue outpatient follow-up with periodic CMR.

Subsequent CMR examinations were performed in 2022 and 2023, with the most recent study demonstrating stability of the intramyocardial mass. To date, the patient remains oligosymptomatic and continues to receive optimized medical therapy for HF.

Discussion

Based on nonspecific cardiologic complaints, the patient described in this case was diagnosed with an intramyocardial tumoral lesion. Unlike intracavitary lesions, which carry a higher risk of embolization, intramural lesions of the left ventricle tend to manifest with conduction disturbances, left ventricular dysfunction, and/or syncope.[8,11]

Initially, the patient presented with transthoracic echocardiography showing mildly decreased LVEF and akinesia in the inferodorsolateral region of the left ventricle, corresponding to the site where the tumoral lesion was later identified. Further investigation included chest CT and CMR, imaging modalities with superior soft tissue resolution that allow detailed assessment of the mediastinum and exclusion of extracardiac involvement. CT, which is more widely available than CMR, enables not only evaluation of tumor location, morphology, and margins but also identification of calcifications, a relevant feature in the differential diagnosis of cardiac neoplasms.[5,11,12]

Among the diagnostic hypotheses considered, benign cardiac tumors appeared more likely. Fibromas consist of aggregates of fibroblasts surrounded by collagen and are typically intramyocardial, most often located in the interventricular septum or the free wall of the left ventricle, without a tendency for spontaneous regression.[11,12] Although more common in the pediatric population and histologically benign, they may be associated with ventricular arrhythmias, sudden death due to involvement of the conduction system, and dyspnea resulting from ventricular cavity compression. On CMR, fibromas typically show signal intensity isointense to myocardium on T1-weighted images and hypointense and homogeneous on T2-weighted images, with minimal or absent late gadolinium enhancement. On CT, more than half of cases demonstrate areas of calcification.[12]

Fibroelastomas are rare tumors, predominantly located on the endocardial surface of the aortic and mitral valves in 80%-90% of cases, and are usually smaller than 1 cm. Although often asymptomatic, they may cause embolic events, including sudden death due to coronary embolism. On CMR, they appear as well-defined nodular lesions with signal intensity similar to that of the endocardium and may exhibit late gadolinium enhancement due to gadolinium accumulation.[13,14]

Myxomas are the most frequent primary cardiac tumors. They typically form intracavitary masses, most commonly located in the left atrium and attached to the fossa ovalis by a pedicle. They may also occur in the right atrium, particularly in children, in the atrial free wall, or on the mitral valve leaflets, although less frequently.[11] On echocardiography, myxomas usually appear as mobile, pedunculated masses attached to the endocardium. Transesophageal echocardiography may be required for better definition of the implantation site and assessment of possible extension into the pulmonary or caval veins. On CT, myxomas present as low-attenuation intracavitary masses with a smooth or slightly villous surface, with calcification observed in approximately 14% of cases. On CMR, they often display a heterogeneous appearance on T1- and T2-weighted images, reflecting their variable composition, which may include myxoid, hemorrhagic, ossified, and necrotic components.[11,15]

Lipoma is the second most common benign primary cardiac neoplasm, accounting for approximately 8%-12% of cases, and occurs predominantly in middle-aged and older adults. About half originate from the subendocardial layer, while the remainder arise from the subepicardial or myocardial layers, with growth toward the pericardial sac. Although usually asymptomatic, they may cause arrhythmias or valvular dysfunction. On echocardiography, lipomas appear as well-defined, immobile masses with a broad base and no pedicle. CT demonstrates homogeneous masses with characteristic fat attenuation, whereas on CMR they exhibit homogeneous high signal intensity on T1-weighted images, hyperintensity on T2-weighted images, and signal suppression on fat-saturation sequences.[11,16]

Other benign cardiac tumors, such as rhabdomyomas and paragangliomas, are rarer or present clinical and imaging characteristics distinct from those observed in the present case.[11]

When imaging findings suggest diffuse and nonresectable tumors, image-guided endomyocardial biopsy may contribute to therapeutic decision-making.[8] In the present case, the surgical team considered lesion excision

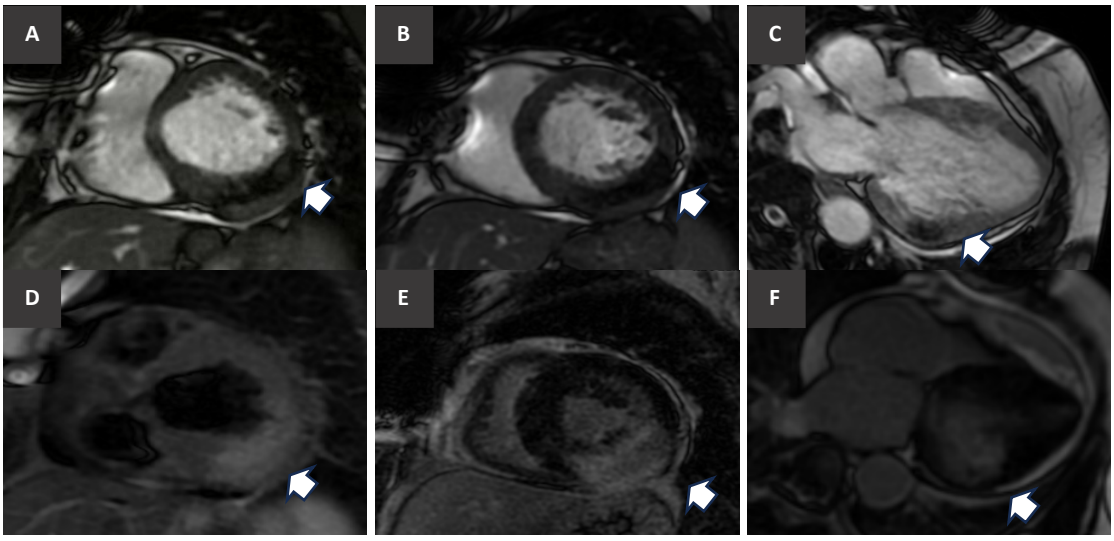

Figure 1 – *Intramyocardial lesion identified by cardiac magnetic resonance in 2022. An intramyocardial mass located in the inferior and mid-basal inferolateral walls of the left ventricle, with imaging features consistent with a low-vascularization tumor and predominantly fibrous tissue. A) Basal short-axis gradient-echo sequence showing a hypointense signal within the lesion; B) mid short-axis gradient-echo sequence demonstrating persistent hypointensity; C) three-chamber gradient-echo view depicting a hypointense lesion; D) T2-weighted sequence with fat suppression (short tau inversion recovery), demonstrating hyperintense signal; E) short-axis late gadolinium enhancement sequence showing marked delayed contrast uptake; F) four-chamber late gadolinium enhancement sequence confirming intense delayed enhancement of the lesion.*

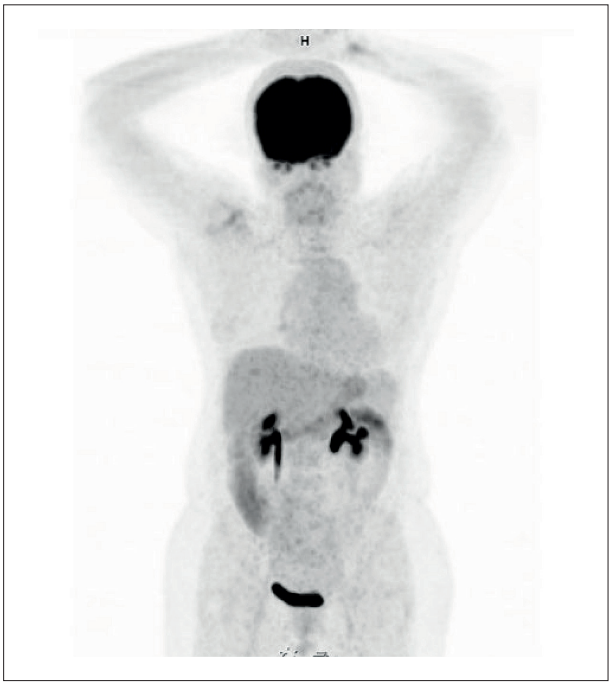

Figure 2 – *Positron emission tomography–computed tomography with fluorine-18 fluorodeoxyglucose (3D maximum intensity projection). Maximum intensity projection image demonstrating physiological distribution of the radiotracer, with no evidence of abnormal uptake in the cardiac region, as indicated by the arrow.*

technically challenging due to the absence of a well-defined cleavage plane on imaging studies. Endomyocardial biopsy was also not performed because of the tumor location, the associated higher risk of complications, and the possibility of obtaining nonrepresentative tissue samples. The combined use of imaging modalities such as CMR, PET-CT, and chest CT provides complementary information for diagnosis, therapeutic planning, and prognostic assessment, as each modality has specific limitations but, when integrated, increases diagnostic confidence.[7]

When feasible, surgical resection of cardiac tumors is recommended. However, in asymptomatic or small lesions, serial follow-up with imaging modalities may be an appropriate alternative.[7] In the present case, given the intramyocardial location, the probable benign etiology, the lack of a clear cleavage plane on imaging, and the patient's oligosymptomatic status, a strategy of outpatient clinical follow-up with periodic imaging was chosen.

Conclusion

This report describes the case of a patient with an intramyocardial cardiac tumor located in the left ventricle, who remained oligosymptomatic and was managed with a conservative approach and clinical follow-up. This case contributes to the understanding of this rare condition and highlights the inherent diagnostic and therapeutic limitations, emphasizing the importance of a multimodal imaging approach in the management of such patients.

Author Contributions

Conception and design of the research and writing of the manuscript: Latado L, Costa FF, Latado AL; acquisition of data: Latado L, Torreão JÁ, Melo AS, Latado AL, Lima AK; analysis and interpretation of the data: Latado L, Benevides CFL, Latado AL; critical revision of the manuscript for intellectual content: Latado L, Costa FF, Benevides CFL, Torreão JÁ, Melo AS, Latado AL, Lima AK.

Potential Conflict of Interest

No potential conflict of interest relevant to this article was reported.

Sources of Funding

There were no external funding sources for this study.

Study Association

This study is not associated with any thesis or dissertation work.

Ethics Approval and Consent to Participate

This study was approved by the Ethics Committee of the Universidade Federal da Bahia under the protocol number 6304046. All the procedures in this study were in accordance with the 1975 Helsinki Declaration, updated in 2013. Informed consent was obtained from all participants included in the study.

Use of Artificial Intelligence

The authors did not use any artificial intelligence tools in the development of this work.

Availability of Research Data

The underlying content of the research text is contained within the manuscript.

References

1. Brasil. Ministério da Saúde. Doenças Cardiovasculares - Principal Causa de Morte no Mundo pode ser Prevenida [Internet]. Brasília: Ministério da Saúde; 2022 [cited 2025 dez 23]. Available from: https://www.gov.br/pt-br/noticias/saude-e-vigilancia-sanitaria/2022/09/doencas-cardiovasculares-principal-causa-de-morte-no-mundo-pode-ser-prevenida.
2. Tazelaar HD, Locke TJ, McGregor CG. Pathology of Surgically Excised Primary Cardiac Tumors. Mayo Clin Proc. 1992;67(10):957-65. doi: 10.1016/s0025-6196(12)60926-4.
3. Silvestri F, Bussani R, Pavletic N, Mannone T. Metastases of the Heart and Pericardium. G Ital Cardiol. 1997;27(12):1252-5.
4. Salm TJV. Unusual Primary Tumors of the Heart. Semin Thorac Cardiovasc Surg. 2000;12(2):89-100. doi: 10.1053/ct.2000.5080.
5. Araoz PA, Mulvagh SL, Tazelaar HD, Julsrud PR, Breen JF. CT and MR Imaging of Benign Primary Cardiac Neoplasms with Echocardiographic Correlation. Radiographics. 2000;20(5):1303-19. doi: 10.1148/radiographics.20.5.g00se121303.
6. García JR, Simo M, Huguet M, Ysamat M, Lomeña F. Usefulness of 18-Fluorodeoxyglucose Positron Emission Tomography in the Evaluation of Tumor Cardiac Thrombus from Renal Cell Carcinoma. Clin Transl Oncol. 2006;8(2):124-8. doi: 10.1007/s12094-006-0169-7.
7. Brandão SCS, Sobrinho JMDR, Leão EDLM, Carreira LCTF, Brito ASX. My Approach to Evaluation of Cardiac Masses Using FDG PET/CT. Arq Bras Cardiol: Imagem Cardiovasc. 2024;37(2):e20240040. doi: 10.36660/abcimg.20240040i.
8. Vander Salm TJ. Cardiac tumors [Internet]. Waltham: UpToDate; 2023 [cited 2025 Dec 23]. Available from: https://www.uptodate.com/contents/cardiac-tumors.
9. Keeling IM, Oberwalder P, Anelli-Monti M, Schuchlenz H, Demel U, Tilz GP, et al. Cardiac Myxomas: 24 Years of Experience in 49 Patients. Eur J Cardiothorac Surg. 2002;22(6):971-7. doi: 10.1016/s1010-7940(02)00592-4.
10. Ramlawi B, Leja MJ, Abu Saleh WK, Al Jabbari O, Benjamin R, Ravi V, et al. Surgical Treatment of Primary Cardiac Sarcomas: Review of a Single-Institution Experience. Ann Thorac Surg. 2016;101(2):698-702. doi: 10.1016/j.athoracsur.2015.07.087.
11. Tyebally S, Chen D, Bhattacharyya S, Mughrabi A, Hussain Z, Manisty C, et al. Cardiac Tumors: JACC CardioOncology State-of-the-Art Review. JACC CardioOncol. 2020;2(2):293-311. doi: 10.1016/j.jaccao.2020.05.009.
12. Burke AP, Rosado-de-Christenson M, Templeton PA, Virmani R. Cardiac Fibroma: Clinicopathologic Correlates and Surgical Treatment. J Thorac Cardiovasc Surg. 1994;108(5):862-70.
13. Hoey ET, Mankad K, Puppala S, Gopalan D, Sivananthan MU. MRI and CT Appearances of Cardiac Tumours in Adults. Clin Radiol. 2009;64(12):1214-30. doi: 10.1016/j.crad.2009.09.002.
14. Angeli F, Bodega F, Bergamaschi L, Armillotta M, Amicone S, Canton L, et al. Multimodality Imaging in the Diagnostic Work-Up of Patients with Cardiac Masses: JACC: CardioOncology State-of-the-Art Review. JACC CardioOncol. 2024;6(6):847-62. doi: 10.1016/j.jaccao.2024.09.006.
15. Grebenc ML, Rosado-de-Christenson ML, Green CE, Burke AP, Galvin JR. Cardiac Myxoma: Imaging Features in 83 Patients. Radiographics. 2002;22(3):673-89. doi: 10.1148/radiographics.22.3.g02ma02673.
16. Sparrow PJ, Kurian JB, Jones TR, Sivananthan MU. MR Imaging of Cardiac Tumors. Radiographics. 2005;25(5):1255-76. doi: 10.1148/rg.255045721.

Left Atrial Septal Pouch Thrombosis Detected Before Electrical Cardioversion: a Rare Source of Embolism

Andre Barcellos Amon,[1] *Mariana De Castro Lopes,*[1] *Marina Petersen Saadi,*[1] *Willian R. Menegazzo,*[1] *Angela Barreto Santiago Santos*[1,2]

Hospital de Clínicas de Porto Alegre,[1] *Porto Alegre, RS – Brazil*
Universidade Federal do Rio Grande do Sul,[2] *Porto Alegre, RS – Brazil*

A 59-year-old male patient with a history of systemic arterial hypertension was admitted to the emergency department with a seven-day history of chest pain and palpitations. On examination, he was hypotensive (93/70 mmHg) and tachycardic (150 bpm). A prominent systolic–diastolic murmur was heard along the right upper sternal border.

The initial investigation included electrocardiography (ECG) and Transthoracic Echocardiography (TTE). The ECG revealed atrial flutter, and the TTE showed biventricular dilation [Left Ventricular (LV) end-diastolic/end-systolic diameters: 60/51 mm; right ventricular (RV) basal diameter: 54 mm] and severe systolic dysfunction (LV ejection fraction: 19%; RV fractional area change: 16%). Additionally, a bicuspid aortic valve with mixed disease was identified: low-flow, low-gradient aortic stenosis (peak velocity: 3.1 m/s; peak/mean gradients: 39/23 mmHg; velocity ratio: 0.15; valve area: 0.7 cm^2, stroke volume index: 17 ml/m^2) and severe aortic regurgitation (pressure half-time: 170 ms; holodiastolic reversal in the descending aorta, end-diastolic velocity: 24 cm/s).

Parenteral anticoagulation was initiated, and a Transesophageal Echocardiogram (TEE) was performed before planned cardioversion. The TEE demonstrated a tubular interatrial septum forming a Left Atrial Septal Pouch (LASP). Within the LASP, a homogeneous echodense mass consistent with thrombus was detected (Figure 1), while no thrombus was present in the Left Atrial Appendage. Agitated saline was injected in a peripheral vein, and no interatrial communication was observed (Figure 2). Consequently, cardioversion was deferred, and systemic anticoagulation was continued.

During hospitalization, the patient underwent surgical aortic valve replacement with a mechanical prosthesis. It was decided not to perform surgical removal of the thrombus, and anticoagulation therapy was maintained. After two weeks of anticoagulation, follow-up transesophageal echocardiography demonstrated complete resolution of the thrombus in the Left Atrial Appendage (Figure 3). Subsequently, successful electrical cardioversion was performed.

Keywords

Transesophageal Echocardiography; Thrombosis; Atrial Septum.

Mailing Address: Andre Barcellos Amon •
Hospital de Clínicas de Porto Alegre. Rua Ramiro Barcelos, 2350. Postal code: 90035-903. Porto Alegre, RS - Brazil
E-mail: andreamon@hotmail.com.br
Manuscript received September 28, 2025; revised October 27, 2025; accepted November 12, 2025
Editor responsible for the review: Maria Otto

DOI: https://doi.org/10.36660/abcimg.20250075i

This case highlights the clinical relevance of LASP, an anatomic variant resulting from incomplete fusion of the septum primum and secundum, which potentially carries a thrombogenic risk—particularly in the presence of additional prothrombotic conditions such as blood stasis from atrial arrhythmias and/or left ventricular dysfunction.[1] LASP is found in up to 38% of the general population.[2] Its role as an embolic source, however, remains controversial, as studies have reported conflicting associations with stroke.[1] Thrombus formation within LASP is exceedingly rare.[3] To our knowledge, this is the first reported case of an LASP thrombus detected prior to electrical cardioversion. This observation underscores the importance of careful echocardiographic assessment of the interatrial septum, in addition to the left atrial appendage, not only in patients with prior stroke but also in those with atrial arrhythmias who are being considered for rhythm control strategies.

Author Contributions

Conception and design of the research and acquisition of data: Amon AB, Saadi MP; analysis and interpretation of the data and Writing of the manuscript: Amon AB; critical revision of the manuscript for intellectual content: Amon AB, Lopes MC, Saadi MP, Menegazzo WR, Santos ABS.

Potential Conflict of Interest

No potential conflict of interest relevant to this article was reported.

Sources of Funding

There were no external funding sources for this study.

Study Association

This study is not associated with any thesis or dissertation work.

Ethical Approval and Informed Consent

All participants gave their consent before being included in the study.

Use of Artificial Intelligence

The authors did not use any artificial intelligence tools in the development of this work.

Availability of Research Data

The underlying content of the research text is contained within the manuscript.

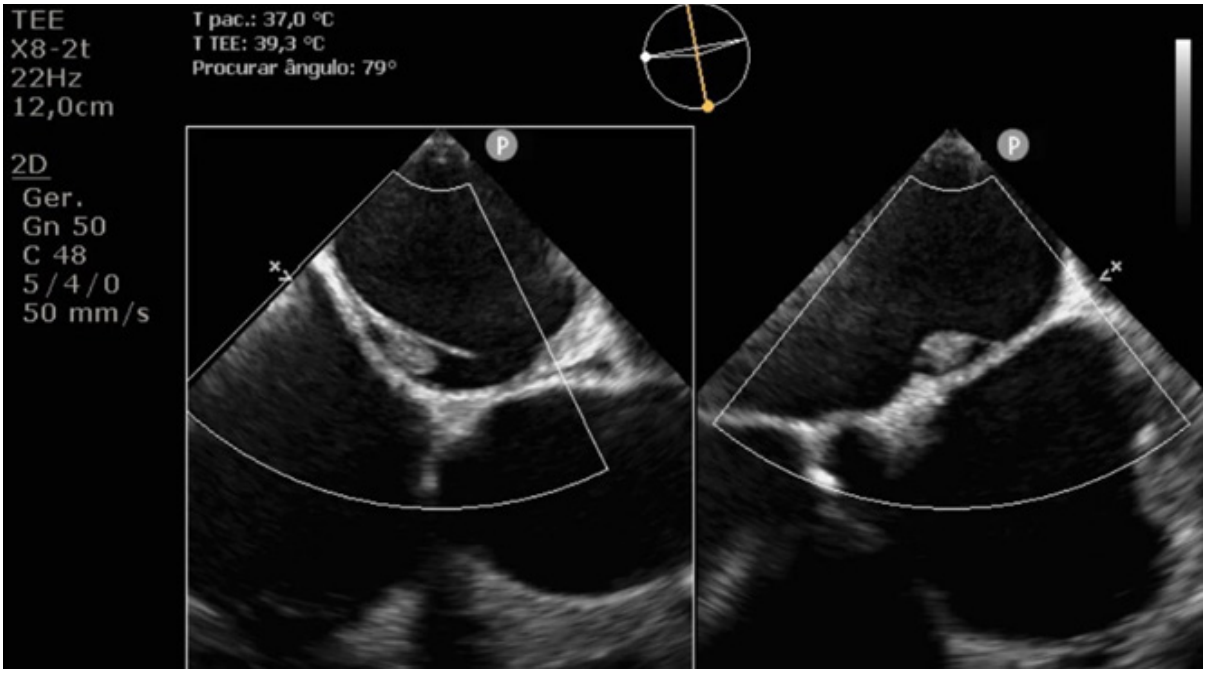

Figure 1 – *Mid-esophageal biplane TEE demonstrates a left atrial septal pouch (LASP) with an intraluminal thrombus measuring up to 1.3 cm in its longest axis. TEE: transesophageal echocardiography; LASP: left atrial septal pouch.*

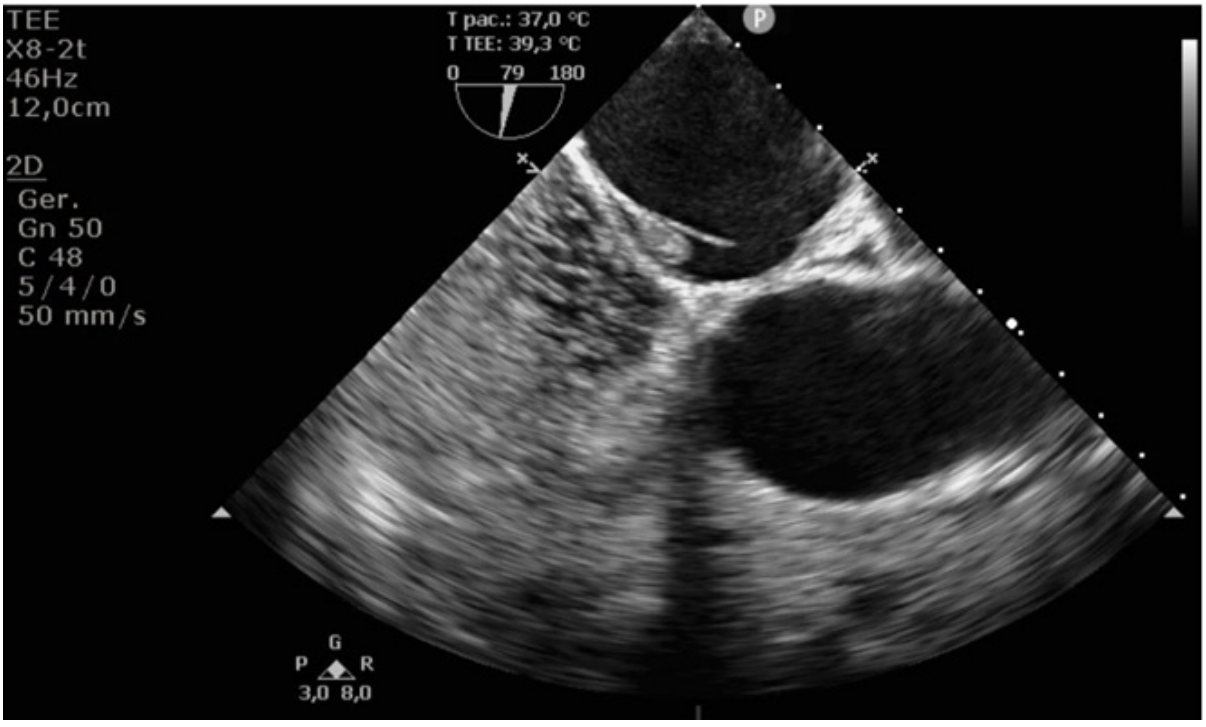

Figure 2 – *Peripheral agitated saline injection demonstrates opacification of the right cardiac chambers without evidence of interatrial communication.*

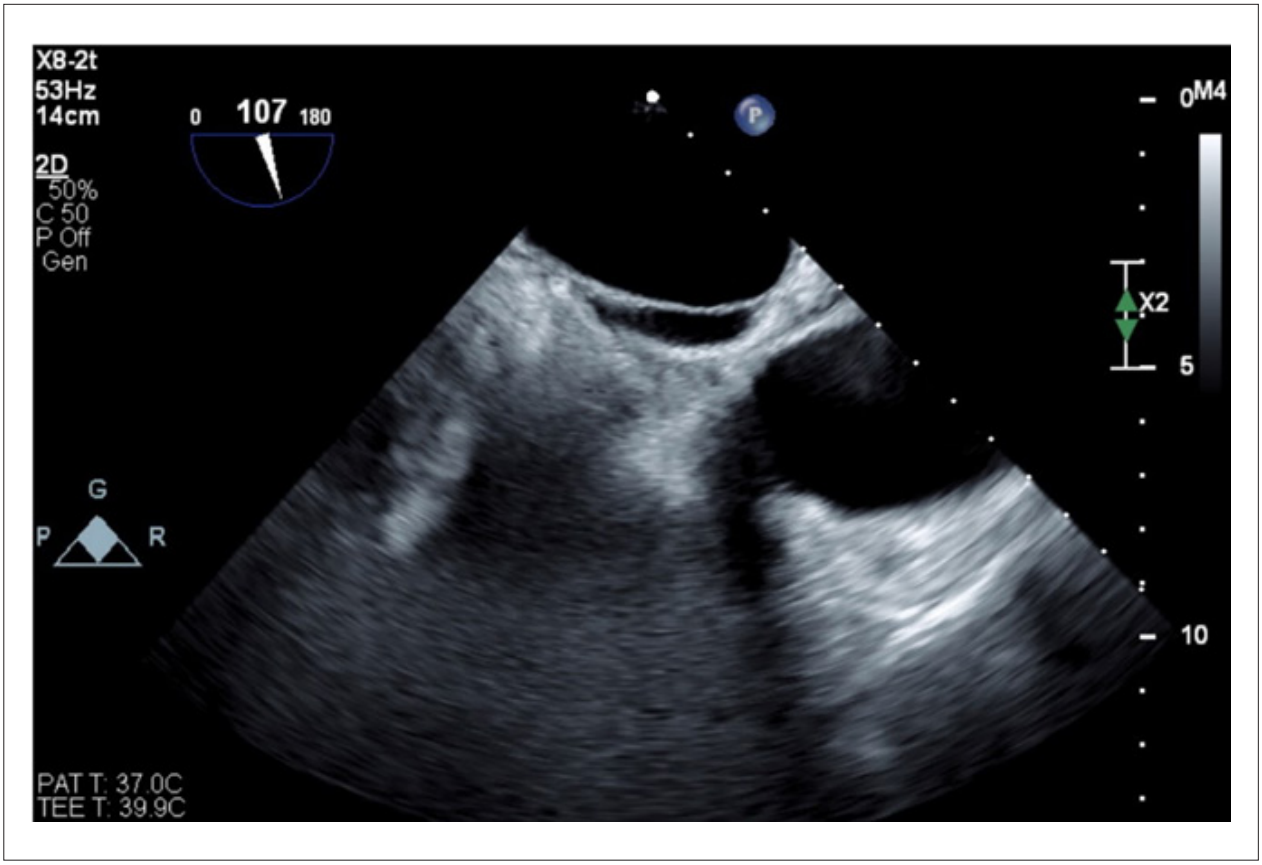

Figure 3 – *Follow-up TEE two weeks after anticoagulation with resolution of LASP thrombus. TEE: transesophageal echocardiography; LASP: left atrial septal pouch.*

References

1. Farooqi P, Yaqobi A, Khail BM, Medina JAN, Ullah ZO, Saeed A, et al. Left Atrial Septal Pouch (LASP) and Cryptogenic Stroke: A Narrative Review. Cureus. 2024;16(7):e64245. doi: 10.7759/cureus.64245.
2. Michałowska I, Dudzińska K, Kowalik I, Kwiatek P, Piotrowski R, Kułakowski P, et al. Left Atrial Septal Pouch-Is it Really a New Risk Factor for Ischemic Stroke?: Subanalysis of the ASSAM Study. J Thorac Imaging. 2022;37(3):168-72. doi: 10.1097/RTI.0000000000000582.
3. Bhave A, Patel A, Patel R, Barmore W, Siddu M, Switzer J, et al. Left Atrial Septal Pouch Thrombus: An Unusual Cause of an Embolic Stroke. Clin Case Rep. 2024;12(9):e9279. doi: 10.1002/ccr3.9279.